THE COPPER CLADDING OF STEEL BY THE SUBMERGED ARC WELDING METHOD

by

PETER SEXTON

S.B., Metallurgy, Massachusetts Institute of Technology, 1965

Submitted in Partial Fulfilment of the

Requirements for the degree of

DOCTOR OF PHILOSOPHY

at the

University of Aston in Birmingham

May 1974

Signature of Author
Department of Metallurgy

Peter Sexton

Signature of Thesis Supervisor

J.W. Brame.

ABSTRACT

The literature available on submerged arc welding of copper and copper alloys, submerged arc welding with strip electrodes, and related areas has been reviewed in depth.

Copper cladding of mild steel substrates by deposition from strip electrodes using the submerged arc welding process has been successful. A wide range of parameters, and several fluxes have been investigated. The range of deposit compositions is 66.4% Cu to 95.7% Cu.

The weld beads have been metallographically examined using optical and electron microscopy.

Equating weld beads to a thermodynamical equivalent of iron has proven to be an accurate and simplified means of handling quantitative data for multicomponent welds.

Empirical equations derived using theoretical considerations characterize the weld bead dimensions as functions of the welding parameters and hence composition. The melting rate for strip electrodes is dependent upon the current-voltage product. Weld nugget size is increased by increased thermal transfer efficiencies resulting from stirring which is current dependent.

The presence of Fe_2O_3 in a flux has been demonstrated to diminish electrode melting rate and drastically increase penetration, making flux choice the prime consideration in cladding operations.

A theoretical model for welding with strip electrodes and the submerged arc process is presented.

TABLE OF CONTENTS

FIGURES

TABLES

ACKNOWLEDGMENTS

The author wishes to express his sincere gratitude: to Mr. L.W. Crane and Professor W.O. Alexander for their supervision, guidance, and enthusiasm throughout the course of this work; to Dr. J.L. Aston for his assistance on experimental design and analysis of results; to International Copper Research Association for the financial support of this research; to Dr. L.McD. Schetky of INCRA for his critical assessments during the course of investigation; and to Texas Instruments Incorporated for their award of a TI Research Assistanceship.

A particular word of thanks to Ing. V.Orszagh and the rest of the staff at Vyskumny Ustav Zvracksky, Bratislava, Czechoslovakia, for sharing their considerable experience of submerged arc welding copper.

Lastly, recognition is due to Mr. S.G.Vince and the other members of the Technical Staff at the University who contributed their time and knowledge toward the success of this project.

1. INTRODUCTION[1]

1.1. Initial Considerations for Constructing with Duplex Materials

There are many industrial situations where a low alloy structural steel does not provide the surface properties required to give adequate service life. Obvious examples of these occur in chemical and food processing plant, and in marine environments. Most of the applications require corrosion resistance on one side only, i.e. the inside of a vessel or pipe which is to contain a corrosive fluid, for example, or the outer surface of a boat hull where antifouling properties are valuable. Thus the use of a steel construction, lined or faced with another material with the required surface properties, has always been an interesting proposition. The advantages of using a duplex material of this type may be broadly summarized as follows:

1.1.1. Economic

It is the economic gain in using a duplex system which includes a substantial proportion of a cheap "base" metal which is most apparent. For example, corrosion resistant alloys commonly used in industry cost on a weight basis, from five to twenty times as much as a structual low alloy steel. Thus except for "thin walled" applications, there is a substantial overall saving in costs, even when the extra fabrication costs incurred by the use of duplex material are taken into account. Naturally, however, the route by which the construction is achieved is very important, and this will be dealt with later on.

1.1.2. Constructional

In some cases the duplex material is substantially stronger than the corrosion resistant alloy which is part of it, thus giving a design advantage. This applies particularly to copper and its alloys when

combined with steel. The strength advantage becomes more pronounced if the service temperature is elevated. Since the density of mild steel is 10% less than copper, there is an additional improvement in strength to weight ratio when using the duplex material. Again, there are generally considerable welding problems involved in a solid wall construction with copper and copper alloys. By constructing in steel and weld overlaying with the required copper alloy, joint welding problems will be reduced. This is assuming, of course, that there are no serious problems involved in the weld overlaying, which may well prove to be the case.

1.1.3. Market

The more expensive the corrosion resistant alloy, the more competitive the use of clad plate becomes. Thus, in applications where a particular alloy is losing ground on the basis of cost, its use may become reestablished by the introduction of clad plate. Similarly, it should be possible to extend the market for an alloy by promoting the duplex wall approach. It is better to maintain a market with reduced consumption than to lose the market altogether. There are occasions where enforced conservation is applied to a particular metal, either by a company or by a government. The use of clad material would ease this situation.

1.2. Constructional Approach

Taking the construction of a vessel requiring a corrosion resistant inner surface as an example, there are three possible routes, namely:

a. homogeneous plate, i.e. solid wall;

b. preclad plate, e.g. roll bonded;

c. overlaying a steel construction.

Where stainless steel is needed on the working face, all three routes are industrially feasible and in general use. Copper and its alloys, however, are rarely used at present as a clad layer in large vessels and containers. The choice of route for a particular construction is often affected by unpredictable factors such as supply of raw materials; these aspects will be discussed later. However, there are some broad rules which seem to apply in most cases. Thus for thin walled constructions, say less than 20 mm, homogeneous plate is used on the basis of cost and convenience. Above this thickness, preclad plate is the favored route. There is a limit to the maximum thickness available in roll bonded material, which in the U.K. is about 65 mm,[2] so that above this thickness a weld overlay method becomes necessary. It should be noted, however, that thicker roll bonded material is available from other sources such as France and Japan. Preclad plate prepared by explosive welding[3] is becoming more readily available, but how it will affect the basic situation is difficult to predict at this stage. Certainly, this process is very attractive for cladding small preshaped areas, such as tube plates, in a wide range of thicknesses. Although it is accepted that in industry, as mentioned earlier, the route is not necessarily determined by direct technical and economic considerations, these aspects should be reviewed in order to maintain clarity.

The technical aspects of preclad and weld overlaid material are briefly compared in Table 1. Thus the basic features of preclad plate are relatively clear; the weld overlaying technique is analyzed in detail in section 2.1.1.

TABLE 1. COMPARISON OF PRECLAD AND OVERLAID PLATE

Item	Preclad	Weld overlaid
Integrity of interface	Roll bonded: only 95% guaranteed bonded area. Explosive: metallic bond, but not 100% guaranteed bond area, and possibility of very thin brittle layer at interface.	True metallic bond. Possibility of substantial brittle interface layer, slag inclusions, porosity, and intergranular or other mode of penetration into base material.
Geometry	Even thickness of clad layer. Generally smooth surface, possibly some irregularities on explosively bonded material. Can work to a minimum thickness of cladding, of the order of 3 mm.	Variable thickness of deposit. Uneven surface on deposit, may need dressing. Some discontinuity where individual beads overlap. Basemetal distortion during deposition is a problem. Minimum deposit thickness about 5 mm.
Composition of working face	No problem	Careful control of deposition required due to dilution* and chemical reactions. Multilayer deposit commonly applied for better control over dilution.

* Dilution - the ratio of melted base metal to weld nugget area. (Am/An, see Figure 1.)

1.3. Commercial Considerations

Construction from preclad plate is expensive for the following reasons:

a. Roll bonded plate is made to order, and the demand is intermittent.

b. Few sources exist for heavy gauge roll bonded plate.

c. Explosive cladding is in an early stage of commercialization.

d. Welding of preclad plate creates special problems.

e. Scrap has little value, particularly in the case of copper alloy, steel combinations.

In the U.K., availability of preclad plate is not reliable, and it is not uncommon for the decision to use a weld overlaying route to be influenced by this situation. It appears that the consumables for stainless steel weld overlaying are generally more readily obtained than preclad plate. One problem with overlaying, of course, is the need for additional welding equipment if the construction is large. It is unlikely that a fabricator would have sufficient orders to keep the "excess" welding equipment in continuous use. The fact remains, however, that the weld overlaying route is economically very attractive. A recent cost exercise based on a clad "model" pressure vessel of 9 meters length, 3 meters diameter and 60 mm wall thickness, yielded the following results:

Using stainless steel clad mild steel, the costing was marginally in favor of the preclad plate construction; for copper clad mild steel the weld cladding technique was determined to be decisively more economical that construction with preclad plate.[4]

2. LITERATURE REVIEW

2.1. Submerged Arc Welding Process

Submerged arc welding is an arc welding process wherein coalescence is produced by heating via an arc or arcs between a bare metal electrode or electrodes and the workpiece beneath a fusible granular material which shields the arc and weld pool. Filler metal is obtained from the continuously fed consumable electrode or from supplementary rod, strip, or powder, which is introduced into the arc. The fusible shielding material is known as the flux, melt, or welding composition.

Thus, in submerged arc welding the passage of current between electrode and workpiece is entirely within a volume of molten flux; above the molten flux is a volume of flux which is unfused and in the granular state. Figure 2 graphically represents the submerged arc welding process. Passage of current is not visible. The electrode does not contact the workpiece since otherwise a short circuit would be created. Adams[6] has concluded from voltage and amperage requirements that there is sufficient power density in submerged arc welding to vaporize part of the hidden flux cover and form an ionized gas pocket, with the pocket probably acting as a plasma to concentrate the arc. Rubin,[7] however, has recently shown that the empirical data substantiates a theoretical model that is rate controlled by resistance rather than an ionized plasma. In Figure 2 the pocket or cavity is not represented because of the unknown nature of its size and shape.

Fluxes are manufactured in a particle size which allows them to be utilized by manual or automatic positioning of the required volume in advance of the electrode. The compositions of the fluxes are such that evolution of gases is minimal at temperatures up to that of the welding zone gases. The submerged nature of the operation eliminates gas pick

up from the atmosphere, smoke, arc flash, and spatter which are problems often associated with the other "open" arc welding processes. Thermal efficiency is also very high, with heat transfer efficiencies of 50% to 65%.[8]

2.1.1. Modified submerged arc processes

The basic submerged arc process is characterized by a high deposition rate and deep penetration. The characteristics afford excellent joining of assemblies but are undesirable when cladding with dissimilar metal electrodes due to the resultant high dilution effects. Deposits of acceptable composition can in some instances be achieved by welding at very low speeds and deposition rates to minimize dilution, but this method is not economical. These undesirable characteristics may be overcome in the case of stainless steel by using overalloyed electrodes to compensate for iron dilution from the substrate.[9]

The sections immediately following describe modifications to the submerged arc process to reestablish the high deposition rate with a minimum dilution and penetration.

2.1.1.1. Series (independent) arc process

Vainerman[10] has demonstrated that the depth of arc penetration in the submerged arc process is always greatest when the base metal is in the circuit. The penetration can be minimized by using "indirect" arcing from a tungsten electrode to the consumable electrode above the surface of the base plate, as illustrated in Figure 3.

The resultant bond is, understandably, similar to that achieved in brazing.[12]

The major advantages of the series arc technique are:

a. Provision to control penetration into base metal, resulting in minimum dilution.

b. Dilution below 10 per cent allowing cladding at normal travel speeds.

c. Heat energy largely consumed in electrode melting, resulting in high deposition rate.

d. Minimum transport of heat to base metal, providing means of cladding thin cross sections or materials where minimum base metal heating is desired.

e. Maximum carbon retention, resulting in high hardness for certain surfacing applications.

The major disadvantage to series arc cladding is that base metal dilution is critically dependent upon the distance between the electrode and the base metal. Slight increases in this distance may result in lack of fusion, whereas a slight decrease increases pentration and makes it impossible to attain the desired chemistry.

As early as 1950 Frost[13] used the series arc technique to clad copper and copper alloys. The limiting feature of his investigation was that the best flux he formulated still resulted in a dimpled and pockmarked deposit surface.

Vainerman[10] claims that one pass using twin independent arcs results in copper and copper alloy overlays on steel with less than 1 per cent iron in the deposit.

2.1.1.2. Submerged arc process cold wire addition

The submerged arc cold wire system, Figure 4, is essentially the basic single wire single arc equipment supplemented by an additional

wire feed unit. Welding is practised much like conventional submerged arc welding; the cold wire is positioned to enter the leading edge of the weld pool thus preempting any difficulties associated with trying to penetrate a solidifying slag pool. Cold wire filler additions increase deposition rate and decrease dilution, but because the arc is the sole source of energy the filler metal is melted by using excess arc energy. This limits the total amount of control over the process by limiting the amount of filler used and restricting parameters to those melting 100% of the filler wire.

2.1.1.3. Submerged arc process hot wire addition

The submerged arc hot wire system is essentially two independent sets of equipment, Figure 5. Each has its power supply, wire feed, torch assembly, and electronic controls. One unit is set to arc; the other provides filler metal at or near the melting point by utilizing resistance (I^2R) heating without an arc. The parameters for each of the arc wire and the hot wire addition are independently adjusted to attain the desired composition and dimensions. A hot wire may be added to any single wire, multiwire or (conceivably) strip submerged arc welding set up.[14]

The geometry of the set up is similar to a cold wire addition with the end of the contactor 38 mm to 50 mm from the leading edge of the weld pool.[14] The hot wire can independently supply large amounts of weld metal without increasing penetration.

2.1.1.4. Submerged arc process metal powder additions to the flux

The metal powder addition submerged arc cladding process employs a submerged arc set up using a consumable electrode and a system for combining metal powders with the flux in sufficient quantities to

produce a weld bead of the desired composition. This is done either by compensating for base metal dilution, [9,15-17] or by formulating an entirely different composition from the base metal or electrode, e.g. aluminum bronze powder containing flux. Ershov[18] has recently reported using two copper wire electrodes, one aluminum wire electrode and a ceramic flux containing 10% nickel powder. The third weld pass gave a composition within the limits of a 10% Al - 4% Fe - 4% Ni bronze alloy.

Limitations for this process are that:

a. Metal powder additions must be formulated for the metal transfer characteristics for one set of parameters.

b. Homogeneity of the dispersion of metal powder additions may be difficult to maintain, as flux consumption is generally a strong function of voltage.[16,19]

A subtle modification of this process is called "bulk welding" and partially overcomes the aforementioned limitations. In bulk welding the metal powders are metered to the surface of the plate, ahead of the flux, so that the additions are adjusted to have a functional dependence on the electrode feed rate. Arnoldy[20] makes the following claims for "bulk welding":

a. Lower temperature of deposit resulting in higher quality and lower stress levels in deposit and substrate.

b. Control of dilution.

c. Higher deposition rates at a given power.

d. Resultant alloys deriving from utilization of

less expensive materials.

e. Greatly decreased use of flux.

f. Fine grain size in deposits.

The availability of a wide range of metal powders makes "bulk welding" attractive for cladding.[21]

2.1.1.5. The strip electrode submerged arc process

The strip electrode techniques utilize a flat, rectangular strip instead of a conventional wire electrode, Figures 6 and 7. Lower dilution is generally observed with strip electrodes than with wire electrodes. This is reported to be because of the fact that the anode or cathode spot (depending on welding polarity) on the plate is not concentrated, since the arc travels back and forth across the strip seeking the path of least resistance. The strip electrode is fed from a coil through contacts for current pick up, then through the bed of flux towards the workpiece. The arc is struck between the workpiece and the electrode. The relative motion between the welding head and workpiece is such that the width dimension of the strip is usually perpendicular to the direction of travel. Flux is continuously provided on the surface of the workpiece in front of the advancing welding head.[22]

Early efforts at strip cladding were aimed at eliminating the demanding tolerances of electrode positioning with the series arc technique.[23]

In theory, strip electrodes may be of any wrought metal or alloy processed to the desired dimensions. A "powder tape" electrode has been developed by Bakshi et al.[24] which conceivably can be used to extend the composition beyond the normally available wrought composition.

The technology for cladding with strip electrodes is particularly well established for stainless steel electrodes onto carbon steel substrates.[9,15,16,19,25-33] This differs substantially from cladding with nonferrous strip electrodes inasmuch as electrode and base metal may be viewed conceptually as two different compositions on the same phase diagram. The proper choice of strip electrode composition results in an alloy intermediate between the base metal composition and the electrode composition yielding the desired alloy weld bead. The major consideration in ferrous cladding is accurate control of minor constituents (often carbon [9,33]) to maintain the desired chemistry, whereas, the major consideration in nonferrous cladding is minimization of dilution in order to control the major constituents. To avoid using overalloyed strips, considerable attention has been given to alloy addition via the flux.[9,15,16] Utilizing the latitude in parametric choice available effecting the desired composition in stainless steel cladding, investigators may indeed choose to maintain very close controls over weld bead geometry.

The nonferrous electrode compositions reported in the literature are limited to nickel base alloys with the following exceptions:

a. The investigation of Wilson[23] yielding a marginally successful copper cladding, and the unsuccessful attempts of Taylor[22] and Griffiths[34] to clad with aluminum bronze and cupronickel electrodes respectively.

b. The use of copper and copper alloy electrodes by Russian investigators[35,36] for multipass welding; weld quality and dimensions inadequately reported.

Successful single pass welding yielding intended compositions in the overlay has been reported by Marshall[9,15] for stainless steel electrodes.

2.1.1.6. Dual strip (barrier layer) submerged arc process

The dual strip process is a modification of the strip electrode submerged arc process. A barrier layer of strip is placed on the base metal directly beneath the proposed area of the weld bead,[1,28-30] Figure 8. By correctly determining the barrier strip dimensions, a substantial fraction of the energy that melts the base metal can be used to melt the barrier layer which has the same composition as the strip electrode, and this should effect the desired composition in a single pass. The limiting constraint on this is that the maximum barrier strip dimension is one that allows fusion at all locations of the weld bead.

Krasulin[37] has shown that, on the basis of wettability and flow properties, the prerequisite for fusion is the dissolution of the surface layer of metal oxide, and that its thickness is the criterion for minimum fusion penetration of parent metal. In view of this, the optimum welding conditions for minimum dilution are such that the difference between the minimum penetration and the average penetration approaches zero and thus the maximum barrier layer can be used.

Thomas[28] claims the following advantages for dual strip cladding:

a. Deposition rates of 11 g s^{-1} and higher are attainable.

b. Dilution is controlled to obtain composition within required specifications.

c. Bead width allows fewer tie-ins with previous beads.

d. Fewer defects occur than with mechanically oscillating wire electrode cladding.

e. Flexibility exists in choosing electrode compositions to obtain the desired overlay chemistry.

f. Fluxes with alloy powders permit further adjustments to the overlay composition.

Nelson[21] cites the following possible disadvantages:

a. Cladding may be difficult on an unsymmetrical surface or surfaces of small diameter. (This is disputed by Almqvist and Egeman[31] who show a cross section of a weld over two plates tied together with a large protruding weld bead. The cladding is level).

b. It is necessary to obtain filler metals and fluxes developed exclusively for cladding with the dual strip electrode process.

It is the opinion of the author that the latter comment is equally true for all of the modifications of the submerged arc process already described.

2.1.2. Physics of submerged arc welding with strip electrodes

Eichhorn and Lohrmann[38] have used X-ray flash photography and substitution of shielding gas for flux to examine the behavior of the arc and material transfer. The results provide an understanding of the submerged arc welding process with strip electrodes. X-ray flash photography showed that the substitution of shielding gas for flux was adequate for the study of mechanisms of metal transfer and arc behavior, but that the times characteristic of the various

phenomena are different for the two shielding media. Kretschmann[39] has confirmed these results using the same techniques and in addition using a glass window in the flux to view directly into the region at the edge of the weld pool. Both of the investigations used austenitic stainless steel electrodes of 25 mm, 50 mm, and 60 mm width, all of thickness 0.5 mm.

The following sections on arc behavior and material transfer are entirely attributable to Eichhorn and Lohrmann[38] and Kretschmann[39] whose work is in broad agreement.

2.1.2.1. Arc behavior with strip electrodes

With strip electrodes the anode and cathode spots wander irregularly at both the strip end and workpiece surface. This complex behavior is determined by electrical, magnetic, gas dynamic, and chemical factors as well as dimensions of the strip electrode. With the same thermal and geometric conditions, the arc attempts to burn at the point where the distance between the strip electrode and workpiece is a minimum, and where resistance is least. The arc burns preferentially at locations of higher charge density and electrical field concentration, due to the small radius of curvature resulting from incipient droplets or the strip edge. The temperature gradient along the strip electrode and irregular ionization level results in irregular migration of the arc. Sudden changes of position occur after a sustained period of dwell, approaching 0.1s. The arc behavior results in irregular numbers and sizes of droplets transferred to the workpiece, which causes uneven fusion penetration. Magnetic arc blow can have a particularly detrimental effect on bead formation

in strip electrode welding. During the long periods of arc dwell with greater localized fusion penetration into the workpiece there is accordingly greater localized melting at the end of the arc on the strip electrode. The latter effect is exaggerated on thin strip, where considerable vaporization of the material can occur due to the high electrical power density.[38,39]

For higher arc voltages, which are achieved by increasing the average distance between the electrode and the weld pool, thus also increasing arc length, arc movement is more sluggish.[38,39]

The occurrence simultaneously of two or more arcs for periods of 0.001 s to 0.15 s has been definitely proven by photographic methods. The multiple arcs may or may not have a common starting point on the workpiece; on the ~~workpiece~~ electrode they usually start on a droplet or strip edge. Due to magnetic attraction forces between two mobile conductors carrying like charged current, the parallel arcs attract and merge. Secondary attraction forces can cause the droplets to move along the edge of the melting strip and merge. These double or multiple arcs when observed do not alter the voltage or current patterns, since the parallel branching of the current causes higher resistances through lower temperatures in the individual arcs.[38,39]

2.1.2.2. Material transfer using strip electrodes

With strip electrodes, the material is mainly transferred to the weld pool as droplets 2 to 4 mm in diameter. In exceptional cases droplets as large as 9 mm have been observed. Under welding conditions with current on the order of 650 amperes for strips 50 to 60 mm wide, 80% of the material transfer is via droplets greater than

2 mm in diameter. Droplet formation time varies from 0.03 s to 0.69 s according to size and formation mode. The formation time increases with increase in strip width and increase in arc voltage and is greater for negative polarity. At greater current densities droplets form more rapidly. The large droplets are usually formed by the merging of smaller drops. This is prevented at lower temperatures if they are coated with slag because of the slag viscosity. On the 50 and 60 mm wide strips up to nine droplets have been observed simultaneously. The drop detaches from the strip electrode end under a combination of forces due to gravity, electromagnetism, surface tension, and gas eruption. Sometimes this is supplemented by forces created by sudden movement of the arcs and the cavity. The drops travel to the weld pool through the cavity, along the cavity wall, and less frequently through the liquid slag adjacent to the cavity. Because of a slag coating, droplets may float for a time on the weld pool until they are absorbed by it. On rare occasions short circuits have been observed during the transfer of a large drop.[38,39]

As current density increases, the rate at which droplets transfer increases but the average size of the droplets decreases. This applies to both polarities, as well as to both ferritic and austenitic steels. As voltage increases, the rate at which droplets transfer decreases but the average size of the droplets increases. At currents over 700 amperes for 50 to 60 mm strips the percentage of droplets less than 1.5 mm in diameter increases as current density increases.[38,39]

2.2. Submerged Arc Welding of Copper and Copper alloys

The demands for overlaying using strip electrodes are more difficult than for overlaying with wire electrodes, which again is more demanding than simple submerged arc welding of similar metals. Therefore in developing the following review, if a multiple application exists it is treated as for the most difficult case.

2.2.1. Simple* submerged arc welding of copper and copper alloys

Very little submerged arc welding of copper or copper alloys has been attempted in western countries with perhaps the exception of cupronickel alloys. An attempt was made to develop a flux composition for submerged arc welding of Evedur†[13]; field performance proved to be inadequate.

To the best knowledge of the British Copper Development Association there is one firm believed to have successfully developed a process for joining aluminum bronze by submerged arc welding.[40]

Successful submerged arc welding of copper and copper alloys dates back to at least 1952 in the Soviet Union[41] and is extensively reported in Soviet journals.[42-52] Attempts at pursuing a literature search of the Soviet material much beyond 1953 becomes progressively more difficult because the earlier material is not abstracted in English and complete English, French or German translations do not exist. For these reasons, and recognizing that the most pertinent work is in all probability covered since that time, a search of earlier literature was deemed to be basically of historical interest and not pursued.

*Simple in this context refers to welding with a workpiece and electrodes of the same material as opposed to welding with a workpiece and electrode of dissimilar materials.

†Nominal composition 95.80% Cu, 3.10% Si, 1.10% Mn

The Welding Institute in Bratislava, Czechoslovakia has contributed significantly to the general understanding of submerged arc welding of copper.[53,54]

2.2.2. Surfacing and joining copper to steel with wire electrode submerged arc welding

With the emergence in the Soviet Union of the submerged arc process to weld copper, investigators also devised ways to use the process to join copper to steel,[46-48] and to clad with copper and copper alloys onto steel substrates.[10,17,18,45,48].

Early attempts in the U.S.A. at cladding copper and copper alloys were abandoned[13] because single pass routines resulted in overlays with excessive base metal dilution and multipass routines left subsequent overlays dimpled and pockmarked.

Whether or not these problems have been overcome in the Soviet Union is entirely unclear from the literature. In the majority of the papers aforementioned, no remarks are made as to the surface quality or absence of macroscopic internal defects.

There is indirect evidence that porosity must exist in at least some weld overlays, since Ilyushenko and Sedov[17] suggest flux additives to minimize porosity in bronze deposits, and it is not to be expected that they are solving a nonexistent problem. Teitel et al[44] report porosity in simple submerged arc copper welds and later literature does not indicate the solution to this problem. (The centralized nature of research in the Soviet Union ensures a substantial continuity in pursuing a particular problem which tends to be reported in a particular journal. There would also appear to be less withholding of proprietary information because of the

nationalized nature of enterprises. Thus the previous remarks can be made with greater confidence than if this work had been done in the West).

Renewed interest in overlays of copper and copper alloys has prompted several projects at the Ohio State University, U.S.A.[21,55,56]

No references can be found for successfully accomplishing the desired weld composition using a single pass welding regime for copper or its alloys; up to 6 passes are used in practice.[18,27,36] Kitler[45] reports a minimum iron composition of 5% using copper wire electrodes, and Vainerman[10] only 10%.

2.2.3. Cladding with strip electrode submerged arc welding

The earliest reported attempt at surfacing by welding with copper strip electrode is by Wilson[23] who used electrodes of deoxidized copper strip 19 mm x 0.8 mm and claims dilutions of as little as 4 to 5%; however, the surfaces were dimpled and pockmarked, and multiple pass welding impossible.

Shekhter[36] reports depositing aluminum bronze onto steel slide blocks for electric rail equipment using both strip and wire electrodes each requiring 6 passes to achieve the required composition. Shadrin et al.,[35] further develop the technology using 60mm x 0.5mm for aluminum bronze strip.

Recent attempts in the U.K. at developing methods for cladding using cupronickel[34] and aluminium bronze[22] have made considerable advances in understanding the process, but have run into serious obstacles. The weld beads were cracked or porous; when cracking was eliminated porosity occurred and vice versa.

2.3. Flux and Slag Technology

2.3.1. General flux and slag technology

The American Welding Society defines a flux as a "Material used to prevent, dissolve or facilitate removal of oxides and other undesirable substances."[5] According to Jackson,[57] however, fluxes may also have the purpose of protecting the weld from the atmosphere and/or acting as a deoxidizer or arc stabilizer. Empirical results have proven that flux composition has a definite effect on the composition and physical characteristics of a weld.

Jackson has defined a slag as "the fused product formed by the action of a flux with the impurities in a weld metal".[57] A slag should have the following properties:

a. It is formed from the flux and remains fluid at a temperature below the fusion point of the metal.

b. It has a lower specific gravity than the weld metal, in order to float on the molten weld metal.

c. It adequately shields the molten weld from the atmosphere.

d. It has a slag-metal interface and viscosity that influences the desired weld bead shape.

e. It has an acid-base ratio facilitating transfer of the desired alloying elements.

f. It is readily detached from the weld after cooling.

The number of constituents present in fluxes is generally large, as is the number of alternative constituents available. Each of the major ingredients usually has some specific purpose or purposes while

the minor ingredients may be present for the sole reason of economy of raw materials since the raw materials are usually naturally occurring ceramic minerals. These are subject to composition ranges, since a minimum of processing is commonplace after mining due to economic considerations.

The formulation of fluxes is largely empirical; initial attention is given to the known concepts with the ultimate refinements arrived at by trial and error iterations. There are no rigid rules for formulating fluxes.

Unlike the coatings used on covered electrodes, the compositions of which are complicated by production considerations, submerged arc welding fluxes can be based on simple mineral compounds selected from ternary or quaternary oxide systems. The fluxes commonly used are based on either the manganous oxide-silica or the lime-silica system, each of which may be combined with various proportions of alumina, magnesia, zirconia, or titania to form complex oxide fluxes.[57] Phase diagrams[58] for some of the simple combinations are useful guides in flux formulation. The viscosities of the welding slags are in the order of 0.2 to 0.7 kg $m^{-1}s^{-i}$ at 1400° C. The 20 kg $m^{-1}s^{-1}$ temperature of welding slags is typically of the order of 1100 to 1200° C. A welding slag must completely cover the weld pool to shield it from atmospheric gases, but the viscosity must be low enough to permit gases to be evolved from the molten metal and to provide a smooth slag-metal interface. At room temperatures the granules of submerged arc fluxes are actually insulators; the electrical resistance decreases with an increase in temperature and the particles become conductive at the temperature in the welding zone.[57]

Unlike the coatings used on covered electrodes, submerged arc welding fluxes contain few additions aimed at changing the electrical properties of the composition. With covered electrodes, a large portion of the coating is composed of compounds that break down in the heat of the arc to provide shielding gas. In addition, compounds with low work functions, such as sodium oxide and potassium oxide, are added to facilitate arc initiation and sustention. Other additions may be made to control penetration and melting rate, to enable the chosen polarity of operation to be used.

2.3.2. Production of submerged arc welding fluxes

Submerged arc welding fluxes may be produced in any of three ways: fully fused, bonded, or agglomerated. The fusing method requires the use of an electric furnace, necessitating a larger capital equipment expenditure than does the relatively simple procedure of producing bonded or agglomerated fluxes in an inclined, heated kiln. Aside from the differences in production equipment expenditure, there are certain inherent advantages associated with each method, [57] as outlined in the following sections.

2.3.2.1. Fused fluxes

To produce a fused flux, the ingredients are dry mixed and then melted in an electric furnace. The ingredients are melted by high frequency induction heating (if in a graphite vessel), or by indirect heating in a conventionally fired furnace (if in a refractory vessel)[59] Once molten, the flux can easily absorb powder additions if desired. Following melting and last minute additions, the melt may either be water shotted or poured on chill plates to cool, before subsequent crushing and sizing. Typical melting and pouring temperatures are of

the order of 1500 to 1700° C. With proper chilling, a glassy product is produced. The crushed product is passed over a series of screens for sizing, the size decreasing as the current range for which the composition is to be employed is increased. After screening to set upper and lower limits on the particle size, the product is ready for packaging.[57]

The advantages of fused fluxes are:

a. Extremely good chemical homogeneity.

b. The capability to remove fines without changing the composition of the flux.

c. A nonhygroscopic product which simplifies storage problems and obviates the need for drying before use.

d. The ability to reuse flux without altering flux composition or particle size.

e. The suitability for higher welding speeds. (This is because the particle size affords for easy handling in the flux distribution system and the particle size may be matched to the higher current range associated with increased speeds).

The primary disadvantage of fused compositions is the inability to add deoxidizers and ferroalloys without segregation if added as a powder in the final stages, as well as prohibitive losses during processing due to the high temperatures involved in fusing the constituents.[57]

2.3.2.2. Bonded and agglomerated fluxes

With bonded fluxes, the constituents are ground to a very fine particle size ($\leq$ 0.05 mm), then sprayed with a bonding agent such as sodium or potassium silicate. There is a tendency for the powder to

form into moist balls; this is enhanced by tumbling. Tumbling is terminated when the balls reach the desired particle size. The balls are then dried at a low temperature in a kiln with a controlled and usually reducing atmosphere.

The primary advantages of bonded fluxes are that:

a. The low temperatures involved in the bonding process permit the extensive use of metallic deoxidizers and ferroalloys.

b. The lower bulk density permits the use of a thicker layer of flux in the weld zone.

c. The fused slag is readily detached.

However, there are disadvantages:

a. Fines cannot be removed for fear of altering the flux composition.

b. Bonded fluxes may have a tendency to absorb moisture.

The agglomerated fluxes are produced in a similar way to the bonded fluxes except that a ceramic binder is used which must be cured at temperatures in excess of 1400° C. The high temperature required limits the use of deoxidizers and ferroalloys as with fused fluxes.[57]

The sizing of a submerged arc welding composition is important because the amount and size of the particles determine the current level for which a flux may be used. For higher currents, the percentage of small particles must be increased and the minimum particle size decreases. Bonded fluxes are generally available in only one grade with a wide variation of size within the grade; thus the maximum currents are generally limited to the 800 to 1100 ampere range.[57]

2.3.3. Submerged arc welding fluxes for copper and copper alloys

As with literature on submerged arc welding of copper and copper alloys, the majority of literature citing the application or development of welding fluxes for copper and copper alloys is in the journals of the U.S.S.R. and Czechoslovakia.

With the exception of one flux for simple submerged arc welding of aluminum bronze marketed in the U.K. from late 1973, inquiries yielded no information as to available fluxes for submerged arc welding of copper or copper alloys; these inquiries identified only one firm using the subarc process on these materials and this was in the development stage. The status in the U.S.A. of submerged arc welding fluxes for copper and copper alloys is similar to the U.K. with INCRA not being able to identify any users of this process until January 1974.[60]

2.3.3.1. Fluxes for simple submerged arc welding of copper and copper alloys

The Union Carbide Corp. in the early 1950's made a preliminary investigation of the use of fluxes in the submerged arc welding of copper alloys; the investigation yielded a flux which gave adequate results on simple welds, but the resultant welds were dimpled and pocked and were typified by deep penetration.[13] The flux was inadequate for deposition of a second pass; this and the deep penetration made it unsuitable for cladding. A subsequent investigation[23] found a flux comprised of 25-50% AB Unionmelt and the remainder Unionmelt Type 50, both commercially available fluxes, produced by Union Carbide for subarc welding of steel. This flux showed promise for use with copper electrodes. Literature studies show that most fluxes proposed for use with copper and copper alloys

were originally developed for steel or are combinations or modifications of steel welding fluxes.

Korenyuk[42,44] reports successful welding of copper plate with flux AN26* (no composition given) but with some weld porosity. In a later paper, Korenyuk et al[43] discuss metal slag reactions in submerged arc welding of copper using fluxes AN5, AN10, AN20, and AN348A; the compositions may be found in Table 2. Flux AN20 was originally developed for steel.[61]

Orszagh[53, 54, 62] has developed 2 fluxes VUZ3Cu and VUZ4Cu (compositions Table 2) for submerged arc welding of copper and copper alloys. These formulations are among the very few that were strictly developed for use with alloys of copper. Flux VUZ4Cu is specifically formulated to prevent elemental transfer from flux to weld metal.[62]

2.3.3.2. Fluxes for surfacing and joining copper to steel with wire electrodes

Ilyushenko et al.[47] use flux AN26 to join copper to thick steel (not cladding). The composition of the flux is still not reported and no mention is made of the existence of porosity as previously reported using this flux.[44]

Ilyushenko and Sedov[17] report that adding a mixture of 4 parts marble and 1 part aluminum powder in a quantity of 15-20% to flux AN20 permits successful welding using aluminum bronze wire electrodes (USSR designations but compositions not given).

Recent work at the Ohio State University[21] investigated more than 100 combinations of fluxes. The optimum formulation, experimental flux "# 37" (composition, Table 2), allowed porosity free deposits of

*Fluxes with prefixes AN are available under these designations in USSR.

TABLE 2. COMPOSITIONS (WEIGHT PERCENT) OF WELDING FLUXES FOR COPPER AND COPPER ALLOYS

Flux*	A50[72]	VUZ3Cu[72]	VUZ4Cu[72]	AN5[43]	AN10[43]	AN20[43]	AN348A[43]	#=37[21]
Source	BOC (Murex) Ltd. Waltham Cross, Herts.	Polytechna Bratislava, Czechoslovakia.		Paton Institute, Kiev, Ukraine, U.S.S.R.				Dept. of Welding Eng: Ohio State University U.S.A.
SiO_2	38.81	38.59	18.64	53.2	23.9	20.9	45.3	36.0
MnO	40.90	44.18	21.15	-	26.8	-	36.9	10.55
Al_2O_3	4.54	6.77	2.09	2.2	19.4	30.8	3.4	11.4
CaO	6.01	2.11	44.25	24.2	9.8	12.7	6.9	19.65
MgO	1.96	1.09	7.50	14.8	1.4	11.9	-	10.6
BaO	1.11	0.98	-	-	-	-	-	-
TiO_2	0.21	0.18	0.19	-	-	-	-	-
ZnO_2	-	0.50	<0.04	-	-	-	-	-
PbO	-	<0.05	<0.01	-	-	-	-	-
FeO	-	0.56	-	-	-	-	-	-
Fe_2O_3	1.61	-	1.18	-	-	-	-	0.2
MnO_2	0.39	-	0.12	-	-	-	-	-
C	-	0.02	0.02	-	-	-	-	-
S	-	0.04	0.02	-	-	-	-	-
CaF_2	4.50	4.50	4.50	5.2	17.0	21.4	7.0	9.75
K_2O	-	-	-	-	0.53	2.80	0.97	-
Unidentified	-	-	-	-	-	-	-	1.85
Total	100.04	99.54	99.68	99.6	98.8	100.5	100.5	100.0

*Source of composition is reference superscripted on flux designation.

aluminum bronze of up to 6 layers on steel, but the penetration from the initial pass was excessive.

Shekhter[36] obtained similar 6 layer deposits using flux AN60, a steel welding flux,[63] with aluminum bronze wire electrodes.* The welds required slow cooling in sand. He makes no mention of porosity.

Ershov[18] uses two 3 mm copper electrodes and one 2.7 mm aluminum electrode and a ceramic flux of CaF_2, Na_2SiF_6, and Na_3AlF_6 with an addition of 10% Ni powder; after 3 passes the resultant weld composition deposited on steel is 9.90% Al, 3.93% Fe, 4.95% Ni, 0.76% Si, remainder copper which is within the desired range. This is the most elaborate flux and wire combination reported.

2.3.3.3. Fluxes for cladding with strip electrodes of copper and copper alloys

Shadrin et al[35] report successfully cladding with aluminum bronze electrode* using the steel welding fluxes AN20[61] and AN60[63]

Shekhter's[36] results with strip electrodes, again with flux AN60 were similar to those he achieved with wire electrodes (previous subsection). No composition for fluxes AN26 or AN60 is reported in any of the literature reviewed nor is any source of these compositions specified.

Wilson,[23] using the combination of 25-50% AB Unionmelt, remainder Unionmelt Type 50 flux, previously mentioned in section 2.3.3.1., achieved preliminary success with copper strip electrodes of 19.0 mm x 0.8 mm but these are substantially narrower than those typically used in practice (50 - 60 mm).

*USSR designations BrAMts 9-2: Cu, 9% Al, 2% Mn,
BrOF 6.5-0.15: Cu, 6½% Sn, 0.15% P.

Orszagh[62] states that flux VUZ4Cu would be unsuitable for use with strip electrodes because it is susceptible to voltage fluctuations which are inherent in strip electrodes; he feels that flux VUZ3Cu is suitable for use with strip electrodes.

2.3.4. Flux related phenomena

2.3.4.1. Electrode melting rate

Drayton[64] reports evidence from a statistically designed experiment that flux can have a differential influence on melting rate, whereas Mantel[65] reports that the electrode melting rate is generally higher in the presence of MnO.

Semenova[66] derives from first principles that effective ionization potential is determined not by the principal component or arithmetical mean but by the component with the lowest ionization potential. This may be interpreted to mean that melting rate would be increased by eliminating from a flux combination the component of lowest ionization potential rather than altering the relative amounts of the flux components.

2.3.4.2. Metallurgical aspects

Dzhevaga reports that for fluxes based on FeO, SiO_2 and MnO, manganese alone transfers to the weld metal.[67] Elsewhere he cites evidence that for multipass submerged arc welding of copper and its alloys porosity decreases with increasing particle sizes of the flux, where the optimum size is > 1 mm.[49] This is reputedly due to the relatively larger amounts of hydrogen adsorbed onto the surface of the flux, but the form of the hydrogen as H_2O or H_2 is not clearly indicated. The observation that the particle size relates to porosity has been confirmed by Waring;[68] he has not suggested a mechanism.

If a fine grain flux is required, the addition of potassium permanganate is recommended to eliminate porosity.[49] Aluminum bronze is cited as being particularly susceptible to hydrogen porosity due to the large decrease in solubility of hydrogen from the liquid state, to the solid state.

Nelson[21] and Flenner et al[56] neglect the effect of particle size on porosity of multilayer deposits of aluminum bronze. If the effect is as marked as that indicated by Dzhevaga the choice of satisfactory fluxes may be extended beyond those found satisfactory by Nelson[21] and Flenner et al.[56]

Ilyushenko and Sedov[17] attribute the lack of porosity in aluminum bronze deposits, (section 2.3.3.2.) to the dilution of the atmosphere around the arc which reduces the partial pressure of hydrogen. This is achieved by using a marble additive to flux AN20, to produce CO_2.

2.4. Process Variables using Strip Electrode

Many conflicting data have been presented and generalizations made as to the effects of welding parameters on the process. These arise largely from a poor fundamental understanding of the process and from incorrect application of empirical relationships, particularly those borrowed from wire electrode technology.

The fundamental arc behavior is now largely known, due to the very fine work of the Germans Eichhorn and Lohrmann,[38] and Kretschmann[39] who used the techniques of X-ray flash photography, glass window viewing and argon shielding in their investigations. The results of this have been reviewed elsewhere in section 2.1.2.

Belov[61,63] in the Soviet Union has contributed the most reliable and thorough information on the effect of the welding parameters on the weld bead.

Of the following observations of the effects of parameters on the strip cladding process only Wilson,[23] using electrodes of deoxidized copper 19 mm x 0.8 mm, has results for alloys containing copper as the major constituent. In the remaining investigations electrodes were carbon steel[61,63] or stainless steel.[19,25-33]

In reviewing the effects of the parameters on the resultant welds, many claims are made with regard to the effect on dilution as a particular parameter is varied, e.g. in a very recent review of the literature the following contradictions are noted:"... However, increase of current is reported by Belov[61] and Bush and Colvin[33] to increase dilution, but van Bemst et al. quote the opposite effect.[16] Voltage increase is found to decrease dilution by Belov[61] and Gifford and Smith[69] and to have no effect by Bush and Colvin.[33]...."

The reason for the confusion is that dilution is not directly dependent on parametric variation, but results from the relative amounts of electrode and base metal that are melted and it is these quantities that are true dependent variables. For instance, if an increase in a particular parameter increases both the electrode melting rate and the amount of base metal melted, it is not until the relative amounts of these increases are quantitatively determined, that an intelligent observation can be made as to the resultant magnitude and sign of the change in dilution.

In order to avoid clouding the issue in this manner it is proposed not to report the effect of independent variables on dilution.

2.4.1. Power source

In cladding with the submerged arc process, two types of power source have been reported as used, those with a) a drooping characteristic or b) a flat characteristic.

Van Bemst et al[16] favor a drooping characteristic for more reproducible results to control bead composition. They suggest that arc voltage is regulated by adjusting the electrode feed speed with small variations in current; but a flat characteristic, having greater fluctuations in current, would lead to a wide variation of the melting rate.

In the verbal discussion of this paper[70] Gifford, Hazzard and Horsfield dispute the authors' conclusions. The summary of their remarks is:

a. The differences are simply a function of strip-flux combination.

b. The mass of the weld pool with strip electrodes damps the effect of rapid current fluctuation with a flat characteristic power source.

Eichhorn and Lohrmann[38] further state from evidence of experimental observation that although a power source may have internal automatic regulation, the self-regulating effect is overwhelmed by the melting characteristics of strip electrodes. During O.1s, the current can change from 600 amperes to 100 amperes as a result of voltage increases from 25 volts to 35 volts caused by localized melting of the strip electrode and corresponding arc lengthening. The local melting speed at this time is greater than the electrode feed speed. The arc then jumps to another spot with the current returning to 600 amperes.

2.4.2. Arc voltage

In strip cladding there are two measurable values of the arc voltage, the instantaneous voltage and the time averaged voltage. This results from the arc wandering across the width of the strip as

described in the section on arc behavior.

The time averaged value of the arc voltage is the one that is monitored and controlled in a given set of welding conditions. In practice the arc voltage is normally measured between the copper contactors by which the current is introduced into the strip, and the ground (earth) return which is attached to the workpiece. The voltage measured is thus greater than the true arc voltage, but it is common practice to quote it as the arc voltage. The higher the conductivity of the strip electrode, the less important the difference between the measured and actual values, because of the diminished effect of resistance heating of the strip electrode.

Control of the average voltage is critical when alloying elements are added from the flux, as flux consumption is a function of voltage.[16,19]

The measured voltage includes the anode, cathode, and arc potential. The contribution of each of these is difficult to determine as the usual practice of making probe measurements has not been successfully applied to submerged welding.[21]

A first order approximation of the magnitude of these voltages can be made by comparing the electrode melting rate at a fixed current for electrode positive and electrode negative and assuming that the anode and cathode voltage drop ratio is proportional to the ratio of the two melting rates. The arc voltage contribution is determined by extrapolating a plot of voltage versus flux consumed, to the point of zero flux consumption.[21,71] This method relies on the usual acceptance that for wire electrodes the electrode melting rate is not a function of voltage.[21,45] However, Belov[63] reports that for wire

electrodes an increase in voltage may decrease the electrode melting rate.

The aforementioned method of apportioning the voltage components will not work for strip electrodes because, as reported by Belov[63] and indirectly substantiated by Marshall et al.,[9] increases in voltage have the effect of increasing the strip electrode melting rate.

An earlier paper by Belov[61] states that the voltage range for strip electrode cladding is 26 to 40 volts, voltage below 26 volts leading to short circuits and above 40 volts leading to electroslag conditions.

Belov[61] demonstrates that changes in bead dimension as a function of voltage are nonlinear, being insignificant in the range 26 to 34 volts; but above 34 volts the functional dependences increase.

In light of these observations, it is most interesting that other strip cladding investigations have been concerned with the range of 26-34 volts,[16,25,28,29,31,33] and thus this choice may be the reason for the negligible effect of voltage reported in these papers.

Belov[63] shows that above 34 volts the height and width of the weld bead increase with voltage and penetration decreases. These observations are confirmed by Sudasch,[19] Gifford and Smith,[70] and Wilson.[23]

Belov[63] states that if electrode positive polarity is used the melting factor is virtually unchanged as a function of voltage. This may be an additional factor confusing some of the voltage melting rate observations of other investigators, as there is not

a clear dichotomy of observation for electrodes positive and negative.

2.4.3. Electrode polarity

Belov[63] reports a higher electrode melting rate for electrode negative but at the expense of greater fluctuation. This is confirmed by other investigators,[27,29,32] but the opposite effect has been reported by van Bemst et al.[16]

Similarly electrode negative is reputed to give both greater[9] and less[16] penetration than with electrode positive.

The most reasonable conclusion is that the effect of polarity on the weld is dependent upon the flux, and melting rate can vary widely or remain essentially constant during a polarity change depending on the flux composition used. This viewpoint is supported by Jackson[72] and Gourd.[73]

2.4.4. Arc current

The welding current used depends mainly on the strip dimensions and flux. The calculated current density of the strip will appear to be lower than that for a similar wire electrode, because the arc behavior on strip electrodes gives a resultant current density at the effective part of the strip of 10 to 100 times the apparent current density.[63]

Electrode melting rate increases as current increases.[28] Belov[61] shows that an increase in current from 550 amperes to 950 amperes. with all other parameters held constant, increases the fusion depth by a factor of 2 to 2.5, whereby the thickness of the deposit doubles and the width slightly increases. Wilson[23] confirms these observations.

It is suggested that increasing current decreases fluctuations of the instantaneous voltage.[44]

2.4.5. Traverse speed

Welding speed in experimental work has been varied between 1.2 mm s^{-1} and 4.2 mm s^{-1} and in practice from 2.0 mm s^{-1} to 3.0 mm s^{-1}.

Increase in welding speed decreases the thickness of the deposit but at the same time the electrode melting rate is decreased because arc energy is increasingly consumed by the greater amount of flux being fused.[61] Width and height of the weld bead also decrease with increasing speed.[19,61]

At any set of welding parameters there is a threshold speed beyond which penetration begins increasing with increasing speed.[23,61,63] This is believed to be because of a thinner layer of liquid metal under the arc[61] or even arcing onto solid base metal. If speeds are too low, unsatisfactory beads are produced which are wide and have unfused seams at the edges.[28,29] Increasing weld speeds also increases surface roughness.[19]

2.4.6. Electrode angle

Nearly all work to date has been performed with the electrode feed perpendicular to the workpiece. Marshall[15] notes that in a communication with Head Wrightson Ltd., he was informed that a slight trailing angle decreases penetration, but in a subsequent set of experiments he maintains the electrode perpendicular.[9]

Wilson[23] found that inclinations up to $\pm 18^{\circ}$ gave no appreciable effect on either geometry or penetration. Inclinations of over 18° caused strip buckling.

2.4.7. Electrode extension (stick-out)

The electrode extension commonly referred to as "stick-out" is the

distance between the contactors, where current is applied to the consumable electrode, and the workpiece.

Gifford and Smith[69] found that increased electrode extensions from 13 mm to 38 mm decreased penetration by 33% with stainless steel electrodes.

Belov[61,63] reported that increased electrode extensions using low carbon steel electrodes increase melting rate, which he attributed to resistance heating of the strip.

Campbell and Johnson[29] consider the range of 31-51 mm optimum, stating that over 51 mm the stainless steel strip overheats and below 25 mm the contactor tips clog with spatter and slag; they found no variation over this range.

Kitler and Sinikov[45] found that with copper wire electrodes having extensions between 30 mm and 60 mm there is no change, owing to the high conductivity of the electrode.

2.4.8. Energy-per-unit-length ('energy input')

Adams et al., [74 - 77] working in the field of heat transfer in welding, have commented on the importance of arc energy-per-unit-length as a parameter as opposed to the independent use of current, voltage, and speed.

Energy per unit length is the quantity:

$$\frac{q}{S} = \frac{IV}{S}$$

where I = arc current

V = arc voltage

S = relative speed between electrode and workpiece.

There is no consensus concerning the use of this quantity as a major criterion in characterizing welding operations with opinion split between its merits,[8,74-78] and demerits.[72,79]

In strip cladding two authors briefly mention this quantity[16,28] and neither discusses its significance in detail.

Marshall et al.[9] have found that the shape of stainless steel welds was primarily a function of energy-per-unit-length and that typically 6.37 - 6.70 kJ mm^{-1} gave concave profiles, 8.8 - 11.56 kJ mm^{-1} gave flat profiles and 15.27 - 15.46 kJ mm^{-1} gave convex profiles. It would seem more than reasonable that observations of this type hold only for one flux and strip electrode combination.

2.4.9. Summary of the effect of welding parameters

In the previous sections the effect of welding parameters on bead dimensions has been discussed qualitatively. In the majority of papers quantitative data is noticably absent. The exception to this is the work of Belov[61] who presents graphically the effects of current, voltage, welding speed, and flux on bead width, bead height, and penetration. The discussion of these effects is presented in the pertinent sections, 2.4.2, 2.4.4, and 2.4.5. Using the nomenclature graphically depicted in Figure 1, Belov's findings are rendered in Figures 9a to 9c.

2.5. Metallurgical

2.5.1. Structure and composition

Vainerman[10] characterizes a copper to steel weld as having a well defined fusion boundary with a 10-20μ interlayer, through which the iron content is approximately uniform except near the fusion boundary. It is reported that the structure of the weld in a copper to steel junction

consisted of a solid solution fusion boundary of 10-30μ (hardness 580-620 DPN) with uniformly distributed αFe in a solid solution matrix of iron saturated copper.[46]

Woods and Milner[80] have demonstrated that motion caused by the Lorentz force, and secondarily by the plasma jet, contributes to the rapid homogenization of dissimilar metals in the weld pool. This motion is proportional to the square of the current. The homogenization proceeds most rapidly for metals of similar densities and melting points.

Kitler and Sinikov[45] report maximum composition gradients of 4% in cladding steel using copper wire electrodes.

Ekatova[81] states that copper diffuses along grain boundaries of steel in the case where copper is used as a braze for steel. Thus diffusion distance is reported to be 1.1 times the grain size at a temperature of 1165^{O} for 300 seconds for a mild steel. He also demonstrates that this diffusion distance decreases as the carbon content of the steel is increased toward 0.9%.

Timofeev and Isaev[53] state that penetration of steel grain boundaries by copper alloy is a function of the copper alloy, type of steel, stress conditions, and the time that the copper alloy remains molten. The penetration is a minimum in the absence of tin and zinc in the copper alloy and is most severe for tin containing alloys. Penetration may be accompanied by cracking (see section 2.5.2). Typical penetration depths for copper are reported as 0.6 to 0.9 mm.This penetration along grain boundaries can embrittle steels of high yield strength but does not affect ductility of steels of low yield strength.

2.5.2. Cracking

Apart from cracking in the weld bead, the cracking of steel when being joined to copper has frequently been reported. Podgaetskii and Dzhevaga[50] report that cracking will occur during submerged arc welding of copper if any of the following levels of impurity occur:

≥0.7% P, ≥2% Sb, ≥0.1% Pb, ≥0.1% Bi.

Syrovatkin[46] reports no cracking when welding steel to copper.

Jordan et al.[82] and Asnis et al.[51] report that cracking of steel occurs when depositing aluminum bronze onto stainless steel and copper onto steel respectively, and relate this to the Rehbinder effect (surface active elements "dynamically penetrating a metal by absorption migration"). The editor of Welding Production[83] in a footnote suggests that this could be related to the relative values of the diffusion coefficient in α and γ iron or the free energy of the grain boundaries.

Asnis et al.[51] further state that cracking can be diminished or completely eliminated when the steel contains ferrite, because copper does not wet ferrite grain boundaries.

It has been reported that intergranular cracking of low carbon steel to a maximum of 0.001 mm occurs when depositing 70/30 cupronickel[85] by an oscillating MIG process. It is further stated that higher alloy steels have a greater propensity to crack and a nickel plate barrier may be necessary to prevent this.

2.5.3. Porosity

Podgaetskii and Dzhevaga[50] warn that porosity occurs in submerged arc welding of copper if any of the following impurity levels exist:

≥1% Cr, ≥4% Mn, ≥0.8% Mo, ≥0.1% Mg ≥1.4% Pb

Ilyushenko and Sedov,[17] Teital et al.[44] and Dzhevaga[49] discuss the occurrence of porosity and its elimination as being flux dependent, and this is further detailed in Section 2.4.

Hennemann[84] gives evidence that cracking of the steel substrate depends on stress and the composition of the copper alloy, bronze being particularly bad.

2.5.4. Corrosion

Although it is recognized that applications of the submerged arc strip cladding process will be utilized in corrosive environments, no attempt has been made in this work to review the literature on corrosion performance of iron containing copper alloys.

However, the following information pertains directly to corrosion performance of weld deposited claddings:

Kitler and Sinikov[45] report no corrosion in a weld with greater than 80% copper that is subjected to vapor of a saturated saline solution. Below 80% copper the corrosion increases as the iron content increases.

Newcombe[85] reports that copper alloys deposited by weld overlaying on steel and containing 3.5% Fe exhibit only surface roughening when immersed in seawater for 12 months. He suggests that it is incorrect to use corrosion data developed from wrought alloys since the weld deposited alloys are far from being equilibrium structures.

2.6. Summary of the Literature Reviewed

From the previous sections we can see that the following broad patterns emerge:

Submerged arc welding for cladding is limited by the deep penetration characteristic of the process. Several process modifications exist to produce weld beads with a lower dilution by decreasing the penetration or by compensating for the dilution resulting from the deep penetration.

The use of strip electrodes with or without a barrier layer produces characteristic weld beads which are very desirable for cladding operations. A considerable number of ad hoc investigations has been conducted by manufacturers of equipment and reported in the literature in the U.S.A., U.K. and Europe, citing the suitability of the strip cladding process using stainless steel electrodes.

The arc physics and material transfer characteristics for strip electrodes are such that many of the accepted rules governing submerged arc welding derived empirically from wire electrodes are not true, very suspect, or inapplicable.

The state of the art of submerged arc welding is well developed in the U.S.S.R. The Soviet literature provides the best characterization of the effect of parameters upon weld bead dimensions (and consequently upon composition); this, however, was determined for two similar fluxes and steel electrodes and steel substrates. It is not known under what sets of fluxes and material selections these guidelines apply.

The Soviet literature also contains the majority of work published on all types of submerged arc welding of copper. The fluxes developed are largely developed from existing steel welding fluxes.

Two welding fluxes VUZ3Cu and VUZ4Cu, exclusively for the welding of copper and copper alloys have been developed in Czechoslovakia.

The technology for submerged arc welding of copper and copper alloys, and fluxes for the same, are virtually nonexistent in the U.S.A., U.K., and Europe in spite of several attempts dating back to 1950.

The derivation demonstrating that ionization potential is controlled by the constituent with the lowest ionization potential

may provide an understanding of the varying electrode melting rates which were previously unexplainable.

The morphology of the iron-copper weld beads resulting from the cladding of steels with copper is reasonably well understood. The Rehbinder effect has been suggested as a mechanism for the cracking of steel substrates sometimes observed in welding copper and copper alloys to steel. It appears to be a trend to cite this although no investigation reports an attempt to prove or disprove this mechanism. Although the existence or absence of cracks in the steel substrate is widely reported, the understanding of their occurrence is rather vague.

3. OBJECTIVES

Welding processes had long suffered from operative difficulties in that no practical means were available for predicting thermal events and the properties of the welds arising from these events. Instead the knowledge of welding was largely empirical. In recent years research on heat transfer and arc behavior has increased the knowledge of welding; however a great deal of work needs to be done before all events in welding are understood to the degree necessary for an accurate predictive model which is necessary for the precise application of the welding process.

The current state of welding science is that theory, although not developed to a predictive stage, enables investigators to narrow research areas into those most likely to result in useful information. Chalmers[86] has coined the term "enlightened empiricism" to describe this. Still, welding is considered by many to be art rather than science.

It has been emphasized in Section 2 that a clear understanding of the effect of the independent variables and consumables on the deposits produced in submerged arc strip cladding is not available. Virtually all relevant information on the use of strip electrodes for cladding is for ferrous alloys. Most research and development has been undertaken for specific applications; the majority of British and American papers have been presented by employees of firms manufacturing welding equipment and consumables. Because of this, comprehensive results are not available.

The objectives of this investigation were:

a. To establish relationships between the variables of submerged strip cladding (arc voltage, arc current,

travel speed, electrode extension, angle of incidence, polarity and flux) and the composition and dimensions of the weld bead.

b. To relate results to heat transfer theory, particularly arc energy-per-unit-length.

c. To produce satisfactory copper cladding using a single pass welding routine with strip electrodes.

4. EXPERIMENTAL PROCEDURE

4.1. Welding Equipment

The general layout of the welding equipment appears in Figure 6 and is detailed in section 4.1.1. ff.

4.1.1. Power source

The power source used was a three phase full wave rectifier, Type MRA 1200F (BOC Ltd) with a drooping characteristic and an open circuit voltage of 64 volts. Stepless current regulation is achieved by means of a magnetic amplifier. The maximum continuous rating is 1200 amperes. The rating was found to be conservative with 1400 amperes available for experimental runs.

The MRA 1200F provides an auxiliary supply of 60 volts d.c., to power the control panels and strip feed motor.

4.1.2. Controls

The control panel has facilities for controlling:

a. electrode feed speed,

b. arc voltage.

An additional switch for current control was placed adjacent to the instrumentation to facilitate correcting current while it is being monitored.

4.1.2.1. Voltage control

Voltage on the BOC equipment is controlled by maintaining a specific arc length related to the desired voltage value set on the control panel, and using variable electrode feed speed. If the electrode feed speed is too high the rate of strip melting is insufficient and the arc length is diminished below that necessary to maintain the desired value, thus resulting in a lower voltage.

In this case the drop in voltage is detected by a thyristor and a relay is excited, disengaging a clutch, which in turn stops the electrode feed rolls. The electrode melting extends the arc length to that necessary for achieving the desired voltage, and this relay then engages the clutch so that electrode feeding resumes. Since it is virtually impossible to set the feed speed exactly to that which matches the linear electrode melting rate, due to aberration inherent in the process from the arc behavior, the optimum feed speed is one that is just incrementally beyond the maximum instantaneous linear electrode feed speed, resulting in the fewest stops and starts and the maximum control of voltage available.

In the case that the electrode feed speed is inadequate and the voltage increases beyond the desired value, due to equipment design, the arc voltage must exceed the reference voltage selected by more than 5 volts before the speed is increased. The welding process is clearly out of control when this happens.

In practice accurate voltage control is obtained by setting the electrode feed speed just below the value at which the electrode feed stops, and then altering the voltage selection subtly to obtain the desired voltage on the recorder. It was found possible to obtain the desired voltage within 15 seconds of start up using this technique.

4.1.2.2. Current control

Before the start of welding, the power source control dial is set up to the desired current, and accurate control is then achieved by utilizing a triple position switch (increase, neutral, decrease) on the power supply or an identical switch adjacent to the recorder. It was found advisable to control current accurately, then voltage although an iteration of the procedure may be necessary. Total

control can be achieved in conjunction with the use of the voltage and electrode feed speeds oontrols within the 15 seconds mentioned.

4.1.2.3. Traverse speed control

Traverse speed is initially set by use of a rule and timer, adjusting the rheostat on the carriage to result in travelling the desired distance in 30 seconds. Actual traverse speed was determined for the stable welding conditions of the middle 200 mm of each weld. Deviations from the initial speed that is set occurs during welding, necessitating the determination of the actual speed of each weld.

4.1.3. Cladding unit

A cladding unit from an ESAB A6 machine was adapted for use with the conventional BOC submerged arc/fusarc wire feed equipment mounted at the end of the boom. The A-6 unit, Figure 7, consists of two bakelite strips (to prevent electrode buckling), contact plates, current pick up terminal and flux tubes. The wire feed rolls were replaced with a pair of serrated flat rolls.

4.1.4. Welding carriage

Relative motion between the electrode and the plate is achieved using a modified lathe with a platform 610 mm x 250 mm propelled along rails by a variable speed motor.

4.1.5. Instrumentation

Current and voltage were recorded using a Smith's Servoscribe dual trace recorder.

Current was determined by measuring the voltage across a shunt where 100 amperes = 75 millivolts and the recorder is scaled to read in amperes.

4.2. Consumables

4.2.1. Strip electrodes

The electrodes used were coils of phosphorus deoxidized copper (DHP)* strip, 62 mm x 0.5 mm in a half hard temper to facilitate feeding through the cladding head without buckling of the strip.

4.2.2. Underliners (barrier layers)

Underliners were lengths of deoxidized copper* 62 mm x 0.5 mm and 62 mm x 1.0 mm in a half hard temper. Underliners 62 mm x 2.0 mm were fabricated by oxyacetylene welding two 1.0 mm strips face to face and joining at several locations at the edges.

4.2.3. Weld plates

Weld plates were hot rolled mild steel+ flame cut to 250 mm x 500 mm and 25 mm or 50 mm thick. The surfaces were prepared by shot blasting.

4.2.4. Submerged arc welding fluxes

The fluxes used were Muraflux A50, a medium viscosity flux for welding steel recommended by BOC (Murex) Ltd., VUZ3Cu and VUZ4Cu the former recommended by Orszagh[62] of VUZ and the latter not recommended by him for use with strip electrodes; and experimental fluxes Cuproflux A and Cuproflux B† supplied by Metrode Ltd. The compositions of Muraflux A50, VUZ3Cu and VUZ4Cu are given in Table 2.

* DHP Copper - phosphorus deoxidized copper per BS 2870-62 of composition 99.85% Cu min. (Ag counts as Cu).

+ Mild steel - low carbon steel per BS 4360 Grade 43A (weldable) 0.25% C max.

† Refer to Appendix B.

4.3. Welding Procedure

4.3.1. Setting-up

Each steel test plate was degreased by swabbing with Inhibisol solvent to remove a protective film of light oil placed on the surface after the shotblasting operation. A 19 mm bolt was welded with a consumable stick electrode to the narrow end of a plate as an electrical terminal.

The test plate was elevated on three 100 mm x 100 mm x 50 mm refractory bricks to ensure identical heat flow conditions for each weld. Each plate was in a level position, ascertained by levelling the supporting bricks with a spirit level.

The strip electrode was cut obliquely to a point to facilitate initial arcing.

The current carrying cables were connected to the terminal bolt at the plate end and secured with a nut. If an underliner was to be used, a strip of the correct thickness was accurately located beneath the area to be welded and secured by a small clamp.

The electrode extension and angle were accurately set with a rule and protractor.

4.3.2. Welding

The current supply and control panel were warmed up for a minimum of 5 minutes. Current, voltage and speed were set to the desired values using the previously mentioned techniques. The electrode feed was switched on, with the contactor off, preventing electrode feeding. The contactor was turned on starting electrode feed and traverse simultaneously. As arcing commenced the electrode feed speed control cut in. The welding voltage and current were continuously recorded.

The welding speed was determined by timing the middle 200 mm of a 400 mm weld.

To terminate welding, the electrode feed was stopped for a few seconds before the contactor and traverse, in order to allow the electrode strip to burn back and thus facilitate removal of plate from the welding equipment.

After cooling of the plate, the unfused flux was removed and then the slag was removed from the weld deposit.

4.4. Data

4.4.1. Collection

Two transverse sections (four different cross sections) were cut from each test plate by means of a band saw. The sections were shaped, surface ground, and macro-etched with a 3% Nital to reveal the heat affected zone. The heat affected zone is defined by the fusion boundary corresponding to a peak temperature of 1510^{o} C and by a boundary separating steel which has undergone a solid state phase change from metal which has not been transformed. This latter boundary corresponds to a peak temperature, found by Adams et al.[75] of 703^{o} C. This was used to ascertain that each weld was conducted under thick plate conditions.

Three to five samples of the weld bead were drilled at various locations of each weld and analyzed for copper, iron and manganese by plating from solution to to platinum electrodes.

Each weld cross section was photographed adjacent to a millimeter scale. The areas were determined using an OTT conventional planimeter accurate to ± 5%, taking three consecutive circuits and dividing the total to find the mean.

Penetration and height were measured at 5 locations on each cross section, and the mean of each determined.

The quantities that can be readily identified on each weld cross section (Figure 1) are:

a) A_n - nugget area, total area of molten and resolidified base metal and electrode.

b) A_m - melt area, cross sectional area of molten and resolidified base metal.

c) A_r - reinforcement area, cross sectional area of molten and resolidified electrode.

d) A_z - heat affected zone area, area of base metal adjacent to the weld which has undergone a phase transformation due to heating above a critical temperature.

e) D_w - bead width.

f) D_p - penetration depth.

g) D_h - bead height.

In section 5, empirical equations are reported between the above weld dimensions and experimental variables. The experimental variables are represented by the following literal nomenclature:

a. I - amperage;

b. V - voltage;

c. q/S - energy-per-unit-length;

d. S - traverse speed;

e. D_e - stick out;

f. D_u - thickness, underliner;

g. α - angle of incidence of strip electrode upon base plate;

h. P - polarity.

Although important, the following variables were not investigated:

a) preheat;

b) electrode composition;

c) electrode width;

d) base metal composition;

e) multipass welding;

f) welding processes other than submerged arc.

4.4.2. Reporting dependent variables

As stated in the literature review, one of the prime criteria for cladding with copper alloys is to minimize dilution, i.e. to maximize the contribution to the weld bead from electrode melting as opposed to base metal melting. It is therefore desirable to estimate the composition of a weld from welding parameters. The first step is to calculate the volume fraction of electrode metal in the weld pool. In the case where the weld is made from a single component electrode and a single component base metal, and assuming no elemental loss or gain from the flux, the following relationship of the cross sectional area is: (Refer to Figure 1)

$$f_e = \frac{A_r}{A_n} \quad . \qquad \ldots\ldots \quad 4\text{-}1$$

But

$$A_n = A_m + A_r \qquad \ldots\ldots \quad 4\text{-}2$$

therefore any two of the three quantities A_r, A_m, and A_n are sufficient to calculate the volume fraction by equation 4-1.

If any two of these areas can be related to welding parameters the volume fraction can then be determined from the parameters.

This determination can be refined to take into account any elemental loss to, or gain from, the flux and also the effect of an underliner. It can further be expanded to allow for multicomponent systems.

To determine the weight fraction of electrode metal using the same assumptions as for equation 4-1, the following relationship is used:

$$C_e = \frac{\rho_e A_r}{\rho_e A_r + \rho_w (A_n - A_r)} \quad \ldots\ldots \quad 4\text{-}3$$

The two cross sectional areas chosen to be related to the welding parameters were weld nugget area and weld reinforcement area. The reasons for the choice of weld nugget area as one of the two experimental observations used to calculate weld composition are delineated in the next subsection. The choice of weld reinforcement as the other was because of its relationship to the electrode melting rate.

4.4.2.1. Weld nugget area

Nugget cross sectional area was chosen as one of the two areas used to characterize the weld and to estimate the weld composition; Jackson[71] had shown that weld nugget area was a function of welding parameters irrespective of the flux type, and that the weld nugget area was proportional to a given amount of heat energy input. A relationship was developed for steel wire electrodes.

Jackson et al.[55] recently tried to extend this relationship to aluminum bronze electrodes but neglected to correct for the enthalpy difference between aluminum bronze and steel. A suitable modification to take account of the dissimilar metal superheat is developed below.

The quantitative relationships for each weld are modified to become equivalent to a weld entirely of steel, with the same enthalpy as the original multicomponent weld. It is assumed that the temperature of the melted electrode reaches the melting point of the steel.

For the case where $T_w > T_e$, the equivalent volume of a weld entirely of base metal with the same enthalpy as the original two component weld is calculated as:

$$V_n^{eff} = V_n \left[\frac{f_e \left(h_{e,T_w} - h_{e,298} \right) - f_w \left(h_{w,T_w} - h_{w,298} \right)}{\left(h_{w,T_w} - h_{w,298} \right)} \right] \quad \ldots\ldots 4\text{-}4$$

Since the welding direction is perpendicular to the cross sectional plane in which areas are measured as welding observations, the respective cross sectional areas may be substituted into equation 4-4 for the volumes. This treatment can be extended to multicomponent systems.

This approach has been used to correct thermodynamically the results quoted by Jackson[55] in the case of the substitution of aluminum bronze wire electrodes for steel wire electrodes; this is described in Appendix A. Using this correction allows a major simplification in handling the data.

Therefore, the ultimate aim of a predictive estimate of the composition of a weld deposit is achieved as follows:

The enthalpy excess of A_n^{eff} compared to A_r determines A_m; thus with A_r and A_m equation 4-1 or 4-3 may be used to estimate the composition.

4.4.2.2. Weld reinforcement area

In those cases where no underliner is used to minimize dilution, all of the weld cross sectional areas above the original surface of the base plate is equivalent to the contribution from electrode melting to the weld nugget, Figure 1. This neglects any small amount of elemental gain from, or loss to, the flux. Similarly the cross sectional area of melted plate is equivalent to the contribution of the base metal to the weld nugget.

However, when an underliner is present during welding the contribution of the underliner to the weld nugget appears to be from electrode metal since the underliner rests on the surface of the base plate. Therefore, we define two quantities: apparent weld reinforcement cross section area (A_r) and actual weld reinforcement cross sectional area (A_r^{act}), Figure 18:

$$A_r^{act} = A_r - D_u W_u. \qquad \ldots\ldots 4\text{-}5$$

This subtracts out the contribution from the underliner, giving only the contribution from electrode melting. The apparent weld reinforcement area is the quantity reported in Tables 2, 4, 6, 8, 10, 12 and 13.

4.5. Experimental Design

The basic plan was to use a factorially designed series of welding experiments. In a factorially designed experiment, the nominal values of the independent variables have zero correlation between them. This was primarily intended to ensure that there would be no statistical bias to the results.

It was fully intended both to utilize the actual recorded values

of the independent variables and to analyze these results by multiple regression techniques. This proved particularly useful, since after the initial experiments had determined the broad patterns of the relations between dependent and independent variables, additional experiments were conducted, enabling the more exact nonlinear relations based upon theory to be found by multiple regression analysis.

Any three of the four variables: current, voltage, traverse speed, and energy-per-unit-length (energy input) are truly independent, the fourth being fixed by the other three:

$$\frac{q}{S} = \frac{IV}{S} \qquad \ldots\ldots 4\text{-}6$$

Since the review of the literature revealed a paucity of information on energy input as a parameter characterizing weld cladding, and because of the appeal of this quantity from a theoretical point of view; it was chosen to be an independent variable.

Therefore, in the factorially designed experiments values were chosen for current, voltage and energy input. The welding traverse speed was then calculated from its functional relation to the other three quantities.

4.5.1. Factorial series A.

The independent variables chosen for Factorial series A were current, voltage, energy input, underliner thickness, electrode extension and electrode angle. Muraflux A50 was used throughout. The nominal values of these variables are given in Table 3. Sixteen welds were made to yield a quarter replicate. The welds were made in a random sequence. The actual values of the independent variables and

TABLE 3. NOMINAL VALUES OF INDEPENDENT VARIABLES FOR SERIES A.

variable	nominal low	nominal high
arc current (a)	900	1100
arc voltage (v)	33	37
energy/length (kJ mm^{-1})	13.0	15.3
underliner thickness (mm)	0.0	0.5
electrode extension (mm)	38	50
electrode angle (rad)	1.40	1.72

TABLE 4. NOMINAL VALUES OF INDEPENDENT VARIABLES FOR SERIES B.

variable	nominal low	nominal high
arc current (a)	975	1175
arc voltage (v)	35	38
energy/length (kJ mm^{-1})	14.2	16.5
underliner thickness (mm)	0.5	1.0
plate thickness (mm)	25	50

the fixed variable (i.e. speed) are given in Table 5. The dependent variables as observed are reported in Table 6.

The results were examined by multiple regression. No statistical correlation was found between weld composition and either electrode extension or electrode angle. These two parameters were eliminated from all further experiments; all subsequent welds were produced with the electrode perpendicular to the workpiece surface and an extension of 44 mm.

The analysis yielded the following equation:

$$Cu(\%) = 3.2\ x(10)^{-6}\ I\ \frac{q}{S} + 7.3(10)^{-5}\ V\ \frac{q}{S} + 13.4\ D_u + 34.3 \quad \ldots\ldots\ 4\text{-}7$$

The statistical significance of the first three terms are 0.98, 0.93, and > 0.99 respectively.

This equation was used to design the next series of experiments, and no significance is given to it other than to characterize the copper in the weld deposits of this first series of welds.

4.5.2. Factorial series B.

Since one of the primary objectives of this work was to clad successfully with a single pass routine, the variables shown to be significant in determining the percentage of copper in the deposits were altered in order to increase the copper content of the subsequent welds.

The independent variables current, voltage, energy input and underliner thickness were maintained with their values altered as described. Muraflux A50 was again used throughout.

TABLE 5. INDEPENDENT VARIABLES, FACTORIAL SERIES A.

weld	current (a)	voltage (v)	traverse speed ($mm\text{-}s^{-1}$)	energy / length ($kJ\text{-}mm^{-1}$)	underliner thickness (mm)	electrode extension (mm)	electrode angle (rad)	electrode polarity	flux name
1	900	38.0	1.90	18.1	0.0	50	1.40	+	A50
2	900	38.6	2.72	12.9	0.5	50	1.40	+	A50
3	910	33.2	2.14	14.3	0.5	38	1.40	+	A50
4	910	38.6	2.46	14.3	0.5	38	1.72	+	A50
5	920	38.0	2.08	16.9	0.0	38	1.72	+	A50
6	930	33.7	2.14	14.7	0.5	50	1.72	+	A50
7	930	33.8	1.93	16.3	0.0	38	1.40	+	A50
8	940	33.8	1.88	16.9	0.0	50	1.72	+	A50
9	1120	33.4	2.18	17.3	0.5	38	1.40	+	A50
10	1120	33.4	2.36	15.9	0.5	50	1.72	+	A50
11	1120	37.2	2.48	16.8	0.5	50	1.40	+	A50
12	1120	37.2	2.48	16.8	0.5	38	1.72	+	A50
13	1130	33.0	2.85	13.2	0.0	38	1.40	+	A50
14	1150	33.4	2.76	14.0	0.0	50	1.72	+	A50
15	1150	37.2	3.32	12.9	0.0	38	1.72	+	A50
16	1150	37.8	3.32	13.4	0.0	50	1.40	+	A50

All plates 25 mm thick

TABLE 6. DEPENDENT VARIABLES, FACTORIAL SERIES A.

weld	copper %	iron %	manganese %	weld nugget area (mm^2)	weld reinforcement area (mm^2)	heat affected zone area (mm^2)	weld height (mm)	penetration depth (mm)	weld width (mm)
1	74.4	23.8	0.93	521	437	418	6.2	1.5	70.9
2	74.5	27.0	1.03	-	-	-	-	-	-
3	72.3	25.6	1.69	-	-	-	-	-	-
4	78.7	19.7	0.90	578	558	445	8.4	0.9	67.1
5	81.3	17.2	0.97	-	-	-	-	-	-
6	74.3	24.1	0.70	-	-	-	-	-	-
7	78.5	20.2	1.05	-	-	-	-	-	-
8	71.8	26.1	1.17	-	-	-	-	-	-
9	89.5	9.8	0.68	-	-	-	-	-	-
10	85.9	13.4	0.77	-	-	-	-	-	-
11	89.3	9.5	0.75	-	-	-	-	-	-
12	82.2	16.5	0.83	-	-	-	-	-	-
13	70.2	28.2	0.78	-	-	-	-	-	-
14	67.4	30.5	1.15	-	-	-	-	-	-
15	70.4	27.6	1.26	-	-	-	-	-	-
16	74.3	24.2	1.14	-	-	-	-	-	-

Plate thickness was added as a variable to ascertain whether semi-infinite heat flow conditions existed for all welds. Sixteen welds were made yielding, in this case, a half replicate. The welds were again made in a random sequence. The nominal values of the independent variables are given in Table 4. The actual values of the independent variables are given in Table 7. The dependent variables as observed are given in Table 8.

A multiple regression analysis showed that there was no correlation between plate thickness, over the range used, and any of the dependent variables corroborating the assumption that semi-infinite heat flow conditions existed with all plate thickness. This variable was eliminated from all further experiments.

4.5.3. Factorial series C.

A third factorial series of experiments was performed in an identical manner to that of Series B, with the exceptions that flux VUZ3Cu was used throughout and all plates had a thickness of 25 mm. Reference is given to Table 4 for nominal values of the variables except that plate thickness as a variable is to be ignored.

The actual values of the independent variables are given in Table 9. The dependent variables observed are in Table 10.

Flux VUZ3Cu produced more suitable welds for copper cladding as there was less penetration and better bead profiles than with flux A50. For these reasons the emphasis for further experimentation was placed on utilizing this flux.

4.5.4. Additional experiments - electrode positive, fluxes A50 and VUZ3Cu

Eighteen additional welds were made: five with flux A50 and thirteen with flux VUZ3Cu. These were made to fill in the range for the independent variables to detect any deviations from linearity. In

TABLE 7. INDEPENDENT VARIABLES, FACTORIAL SERIES B.

weld	current (a)	voltage (v)	traverse speed ($mm\text{-}s^{-1}$)	$\frac{energy}{length}$ ($kJ\text{-}mm^{-1}$)	underliner thickness (mm)	electrode extension (mm)	electrode angle (rad)	electrode polarity	flux name
17	941	38.4	2.18	16.6	0.5	44	1.72	+	A50
18*	969	37.6	2.26	16.1	1.0	44	1.72	+	A50
19*	969	37.8	2.64	13.9	0.5	44	1.72	+	A50
20	973	34.4	2.36	14.1	0.5	44	1.72	+	A50
21*	984	33.6	2.26	14.6	1.0	44	1.72	+	A50
22	1000	37.4	2.57	14.6	1.0	44	1.72	+	A50
23*	1010	34.2	1.90	18.2	0.5	44	1.72	+	A50
24	1018	34.5	1.90	18.6	1.0	44	1.72	+	A50
25	1141	36.8	2.23	18.9	1.0	44	1.72	+	A50
26	1170	38.4	3.06	14.7	0.5	44	1.72	+	A50
27*	1175	38.0	3.45	13.0	1.0	44	1.72	+	A50
28	1180	33.6	2.81	14.1	1.0	44	1.72	+	A50
29	1190	38.0	2.45	18.5	0.5	44	1.72	+	A50
30*	1196	34.5	2.46	16.7	1.0	44	1.72	+	A50
31	1198	34.6	2.45	16.9	0.5	44	1.72	+	A50
32*	1199	35.2	3.23	13.1	0.5	44	1.72	+	A50

welds with asterisk (*) plate thickness 50 mm; all others plate thickness 25 mm.

TABLE 8. DEPENDENT VARIABLES, FACTORIAL SERIES B.

weld	copper %	iron %	manganese %	weld nugget area (mm^2)	weld reinforcement area (mm^2)	heat affected zone area (mm^2)	weld height (mm)	penetration depth (mm)	weld width (mm)
17	74.6	22.3	1.23	420	348	576	5.0	1.6	68.1
18	79.7	16.2	0.65	566	470	428	6.4	1.2	71.6
19	83.1	14.6	0.91	458	400	558	6.0	1.0	68.8
20	76.8	21.0	0.86	524	387	599	5.7	1.5	70.6
21	79.1	18.0	0.80	475	352	468	5.0	1.3	70.4
22	75.7	20.5	1.11	528	419	661	5.9	1.4	73.2
23	73.8	23.7	1.03	551	449	653	6.4	2.2	73.4
24	76.6	20.7	1.01	634	514	721	7.7	1.8	73.7
25	75.8	22.0	1.05	666	490	937	6.7	2.5	76.2
26	67.9	28.6	1.14	534	348	626	5.8	1.7	73.9
27	74.2	23.2	0.82	447	332	555	5.2	1.9	71.4
28	80.8	16.6	1.15	502	403	592	5.7	2.3	73.2
29	82.0	16.5	0.91	554	460	794	6.0	1.8	74.2
30	78.3	19.8	0.86	566	467	549	6.6	2.1	74.1
31	73.6	20.0	1.06	554	441	629	6.4	1.4	73.9
32	73.2	24.5	0.98	472	354	508	5.2	1.9	73.9

TABLE 9. INDEPENDENT VARIABLES, FACTORIAL SERIES C.

weld	current (a)	voltage (v)	traverse speed ($mm\text{-}s^{-1}$)	energy / length ($kJ\text{-}mm^{-1}$)	underliner thickness (mm)	electrode extension (mm)	electrode angle (rad)	electrode polarity	flux name
33	930	39.0	2.01	18.0	1.0	44	1.72	+	VUZ3Cu
34	941	38.4	2.24	16.1	0.5	44	1.72	+	VUZ3Cu
35	973	34.4	2.41	13.9	0.5	44	1.72	+	VUZ3Cu
36	980	36.0	2.04	17.3	0.5	44	1.72	+	VUZ3Cu
37	982	36.6	2.52	14.0	1.0	44	1.72	+	VUZ3Cu
38	993	37.3	2.33	15.9	1.0	44	1.72	+	VUZ3Cu
39	1010	39.5	2.61	15.3	0.5	44	1.72	+	VUZ3CU
40	1021	34.6	1.90	18.5	1.0	44	1.72	+	VUZ3CU
41	1142	38.0	2.45	17.7	0.5	44	1.72	+	VUZ3Cu
42	1148	35.0	2.89	13.9	0.5	44	1.72	+	VUZ3CU
43	1177	38.0	3.00	14.9	1.0	44	1.72	+	VUZ3Cu
44	1178	36.0	2.57	16.5	1.0	44	1.72	+	VUZ3Cu
45	1180	33.6	2.81	14.1	1.0	44	1.72	+	VUZ3Cu
46	1186	38.4	3.06	14.9	0.5	44	1.72	+	VUZ3Cu
47	1198	34.6	2.49	16.6	0.5	44	1.72	+	VUZ3Cu
48	1216	35.8	2.66	16.3	1.0	44	1.72	+	VUZ3Cu

All plates 25 mm thick

TABLE 10. DEPENDENT VARIABLES, FACTORIAL SERIES C.

weld %	copper %	iron %	manganese %	weld nugget area (mm^2)	weld reinforcement area (mm^2)	heat affected zone area (mm^2)	weld height (mm)	penetration depth (mm)	weld width (mm)
33	88.0	10.0	1.41	503	454	676	8.3	0.2	74.2
34	94.6	4.3	1.25	541	511	557	8.4	0.2	66.3
35	87.2	10.5	1.23	483	438	416	6.4	0.7	72.9
36	90.1	8.4	0.96	528	488	515	6.3	1.2	71.6
37	88.7	9.9	0.81	423	392	510	6.3	0.6	73.4
38	93.6	5.3	1.11	526	479	621	7.2	0.5	70.6
39	85.8	12.6	1.06	514	439	684	6.4	0.4	74.2
40	95.7	3.1	1.07	676	627	844	8.3	0.1	75.7
41	87.8	10.4	1.17	506	444	667	6.7	0.6	73.7
42	90.7	7.6	1.16	544	511	441	7.1	0.7	70.5
43	81.3	16.4	1.69	517	430	630	5.8	1.2	77.5
44	88.1	10.6	0.77	512	461	577	6.2	0.8	74.7
45	91.7	7.3	1.15	368	337	361	5.0	0.9	66.5
46	90.6	7.5	1.22	496	434	441	6.7	0.5	68.6
47	79.3	18.1	1.57	585	454	678	6.0	1.8	80.8
48	93.3	4.8	1.13	494	457	548	7.4	0.2	66.8

the case of the welds conducted with flux VUZ3Cu the range of underliner thicknesses was extended to 0.0 and 2.0 mm and the range of current, voltage, and energy input varied in finer divisions. A similar but less extensive supplementation of independent variables was undertaken for flux A5O. The independent variables for these experiments are in Table 11. The dependent variables are as in Table 12.

4.5.5. Additional experiments - electrode negative

Seven additional welds were made with electrode negative polarity: five with flux VUZ3Cu and two with flux A5O. Neither flux proved to be suitable with electrode negative polarity as the bead profiles were extremely uneven, having irregular sides and extremely variable height.

The independent variables for electrode negative experiments are in Table 13. The dependent variables as observed are in Table 14.

4.5.6. Additional experiments - other fluxes

Additional experiments were conducted with fluxes VUZ4Cu, Cuproflux A and Cuproflux B.

These fluxes were totally unacceptable for welding with copper strip electrodes. Deposits with flux VUZ4Cu exhibited extreme porosity, with pores on the order of 0.5 mm to 1.0 mm, and some cracking. Cuproflux A and B produced deposits of erratic dimensions, extremely rough surface, and varying bead height.

Powdered Fe_2O_3 was added to flux VUZ3Cu so that the combination was 1.6% Fe_2O_3, 98.4% VUZ3Cu, by weight. This was done to test the hypothesis developed during the course of this work that the major difference between fluxes VUZ3Cu and A5O was the Fe_2O_3 in the A5O. This is discussed in greater depth in Sections 5 and 6. Two welds were deposited, one each with fluxes VUZ3Cu and A5O, with identical welding

TABLE 11. INDEPENDENT VARIABLES, NONFACTORIAL SERIES

weld	current (a)	voltage (v)	traverse speed ($mm\text{-}s^{-1}$)	$\frac{energy}{length}$ ($kJ\text{-}mm^{-1}$)	underliner thickness (mm)	electrode extension (mm)	electrode angle (rad)	electrode polarity	flux name
49	975	34.8	1.82	18.6	0.0	44	1.72	+	VUZ3Cu
50	975	34.8	1.92	17.7	0.0	44	1.72	+	VUZ3Cu
51	975	34.8	2.22	15.3	0.0	44	1.72	+	VUZ3Cu
52	1013	39.0	3.09	12.8	0.0	44	1.72	+	VUZ3Cu
53	1106	33.0	3.20	11.4	0.0	44	1.72	+	VUZ3Cu
54	1112	36.0	3.13	12.8	0.0	44	1.72	+	VUZ3Cu
55	1148	35.0	2.42	16.6	0.0	44	1.72	+	VUZ3Cu
56	1148	35.0	2.95	13.6	0.0	44	1.72	+	VUZ3Cu
57	1148	35.0	3.56	11.3	0.0	44	1.72	+	VUZ3Cu
58	1148	35.0	4.32	09.3	0.0	44	1.72	+	VUZ3Cu
59	1148	35.0	5.21	07.7	0.0	44	1.72	+	VUZ3Cu
60	1170	34.6	2.51	16.2	2.0	44	1.72	+	VUZ3Cu
61	1188	34.0	3.31	12.2	0.0	44	1.72	+	VUZ3Cu
62	975	35.0	2.32	14.7	0.5	44	1.72	+	A50
63	975	35.0	2.74	15.0	1.0	44	1.72	+	A50
64	1160	35.0	2.52	16.1	2.0	44	1.72	+	A50
65	1160	35.0	2.54	16.0	0.0	44	1.72	+	A50
66	1175	35.0	2.50	16.5	0.5	44	1.72	+	A50

All plates 25 mm thick

TABLE 12. DEPENDENT VARIABLES, NONFACTORIAL SERIES

weld	copper %	iron %	manganese %	weld nugget area (mm^2)	weld reinforcement area (mm^2)	heat affected zone are (mm^2)	weld height (mm)	penetration depth (mm)	weld width (mm)
49	86.4	11.3	1.69	570	515	665	7.2	1.3	73.7
50	86.2	12.5	0.82	559	482	721	7.4	1.3	69.3
51	72.8	25.2	1.34	422	372	450	5.0	1.4	73.4
52	88.6	9.0	1.69	371	324	-	5.5	1.0	62.5
53	84.4	13.8	1.17	406	329	-	3.7	2.6	67.3
54	89.2	9.0	1.22	370	332	-	4.9	1.4	64.8
55	86.7	11.5	1.25	533	450	-	6.3	1.3	72.6
56	84.4	13.7	1.29	422	361	-	5.8	1.2	69.1
57	78.0	20.2	1.29	353	283	-	4.6	1.1	66.5
58	76.0	19.5	1.69	303	237	-	4.1	0.9	65.8
59	73.6	24.2	1.57	181	130	-	3.3	2.0	67.0
60	91.4	7.5	0.68	510	447	-	6.4	1.5	70.1
61	88.6	11.3	0.67	396	345	-	5.0	1.2	65.3
62	77.8	20.7	0.86	458	354	563	5.5	1.9	71.1
63	75.2	22.6	0.90	512	407	548	6.2	1.2	73.7
64	81.0	17.5	0.96	604	465	-	7.3	2.0	67.8
65	66.4	31.1	0.96	489	318	-	4.7	3.2	68.6
66	70.2	27.0	1.01	545	386	626	5.4	2.9	75.7

TABLE 13. INDEPENDENT VARIABLES, REVERSE POLARITY EXPERIMENTS

weld	current (a)	voltage (v)	traverse speed ($mm\text{-}s^{-1}$)	energy length ($kJ\text{-}mm^{-1}$)	underliner thickness (mm)	electrode extension (mm)	electrode angle (rad)	electrode polarity	flux name
67	988	36.0	2.24	15.9	1.0	44	1.72	-	VUZ3Cu
68	1000	36.0	2.07	17.4	0.5	44	1.72	-	VUZ3Cu
69	1010	38.0	2.24	17.1	1.0	44	1.72	-	VUZ3Cu
70	1010	38.5	2.23	17.4	0.5	44	1.72	-	VUZ3Cu
71	1128	35.0	2.41	16.3	0.5	44	1.72	-	VUZ3Cu
72	969	37.8	2.64	13.9	0.5	44	1.72	-	A50
73	984	33.6	2.26	14.6	1.0	44	1.72	-	A50

TABLE 14. DEPENDENT VARIABLES, REVERSE POLARITY EXPERIMENTS

Weld	copper %	iron %	manganese %	weld nugget area (mm^2)	weld reinforcement area (mm^2)	heat affected zone area (mm^2)	weld height (mm)	penetration (mm)	weld width (mm)
67	91.5	6.7	1.21	590	495	471	7.5	0.8	69.6
68	91.9	6.6	0.90	489	439	595	6.6	0.5	71.9
69	93.0	5.7	0.69	457	405	502	6.5	~0.0	71.1
70	90.8	7.4	1.24	477	409	545	6.2	0.9	72.1
71	89.4	9.5	0.60	506	419	643	6.8	0.6	71.6
72	79.1	18.0	0.80	458	400	558	6.0	1.0	68.8
73	83.1	14.6	0.91	474	352	468	5.0	1.3	70.4

parameters. The independent and dependent variables for each are in Table 15.

TABLE 15. INDEPENDENT AND DEPENDENT VARIABLES, VUZ3Cu FLUX WITH Fe_2O_3 ADDITION

weld	current (a)	voltage (v)	traverse speed ($mm\text{-}s^{-1}$)	energy length ($10^4 J\text{-}mm^{-1}$)	underliner thickness (mm)	electrode extension (mm)	electrode polarity	flux
74	1000	35	1.93	1.82	0	44	+	VUZ3Cu
75	1000	35	1.94	1.80	0	44	+	(98.4% VUZ3Cu (1.6% Fe_2O_3

weld	copper %	iron %	manganese %	weld nugget area (mm^2)	weld reinforcement area (mm^2)	weld height (mm)	penetration depth (mm)	weld width (mm)
74	91.2	8.6	1.2	538	484	7.2	0.2	76.00
75	71.0	28.0	1.0	616	420	5.4	2.9	78.45

5. RESULTS

5.1. Metallographic

5.1.1. Composition and structure

The range of copper contents for all welds successfully deposited is 66.4% to 95.7% by wet chemical analysis, (Tables 6, 8, 10, 12, 14, 15). Five welds each, from both the subset of welds produced with flux VUZ 3Cu and the subset of welds produced with A50, were analyzed for silicon by wet chemistry. The samples were chosen to be evenly spread through the range of copper contents produced with each flux. In all cases the silicon content was 0.025% ± 0.005%. Although metallographic examinations were made for samples across the complete range of compositions and for each flux, it was possible to select four welds to illustrate fully all the metallographic features observed. The copper contents of these welds are: 94.6%, 90.6%, 80.8%, and 67.9%.

Several welds were selected and examined using a Cambridge Microscan 2 and a Cambridge Microscan 5 scanning electron microscope. Copper and iron X-ray photographs for the four samples chosen to illustrate the features observed are presented in Figures 10-13. Included in these figures are color optical photomicrographs of the areas identical to those analyzed by the microprobe.

All welds have an iron rich phase 20-40μ thick, measured perpendicular to the interface between the weld bead and the base plate. This phase has a hardness of ~ 420 D.P.N. The remaining volume of the weld bead is comprised of a network of dendrites of α-Fe supersaturated with copper and a matrix of α-Cu supersaturated with iron. Because of coring in the dendrites, maximum copper concentrations were measured using Cu Kα radiation. The copper concentration of the copper

rich matrix was determined by FeKα radiation. The quantitative results are presented in Table 16.

In the samples containing a network of iron rich dendrites the maximum copper contents of the dendrites are relatively uniform, having a maximum variation in any one sample of 2% Cu and a variation of 5.6% Cu across the whole range of samples measured. Similarly, in the matrix, the range of compositions is <4% Fe in any one sample. These observations are in agreement with Kitler and Sinikov.[45] At approximately 80% copper and above, the matrix composition increases in copper content as the bulk composition increases in copper content.

Both the observations of the dendrite and matrix composition as a function of the bulk composition are as to be expected from the equilibrium phase diagram, Figure 14, since for all bulk compositions the first iron rich nuclei precipitate at the same composition but due to the large negative slope of the liquidus starting at 80% Copper, the initial copper rich nuclei have increasing iron contents for increasing bulk iron content. Similarly, the limit of solid solubility of copper in iron at the nucleation temperatures is nearly constant for the range of bulk compositions in this investigation.

The relatively even composition of the matrix is due to the network of dendrites creating a complex system of diffusion gradients at short distances.

The relative amounts of the two phases are determined by the overall composition of the weld. Using MnKα radiation manganese was found to distribute in approximately the ratio 2.5 : 1 with the greater amount occurring in the copper rich matrix. Utilizing this, the major constituent of each phase can be determined by difference.

TABLE 16. COMPOSITIONS AS DETERMINED BY ELECTRON BEAM MICROPROBE

Weld 26 bulk composition 67.9% Cu

matrix - Fe FeKα V = 20 kv SC=0.100 μa

dendrites - Cu CuKα V = 20 kv SC=0.094 μa

location *	K_{Fe}	C_{Fe}	location	K_{Cu}	C_{Cu}
1	0.0730	0.0565	1	0.0960	0.1052
2	0.089	0.0640	2	0.1086	0.1298
3	0.0812	0.0642	3	0.1356	0.1475
4	0.0570	0.0450	4	0.1130	0.1223
5	0.0800	0.0632	5	0.0895	0.0979
6	0.0571	0.0445			
7	0.0573	0.0447			
8	0.0661	0.0517			
9	0.0571	0.0445			
10	0.0668	0.0521			

Weld 28 bulk composition 80.8% Cu

matrix - Fe FeKα V = 20 kv SC=0.100 μa

dendrites - Cu CuKα V = 20 kv SC=0.093 μa

location	K_{Fe}	C_{Fe}	location	K_{Cu}	C_{Cu}
1	0.0940	0.0747	1	0.1397	0.1520
2	0.0770	0.0610	2	0.1400	0.1522
3	0.0938	0.0746	3	0.1530	0.1664
4	0.0887	0.0704	4	0.1343	0.1461
5	0.0835	0.0660	5	0.1390	0 1512

Weld 46 bulk composition 90.6%

matrix - Fe FeKα V = 20 kv SC=0.100 μa

dendrites - Cu CuKα V = 15 kv SC=0.095 μa

location	K_{Fe}	C_{Fe}	location	K_{Cu}	C_{Cu}
1	0.0296	0.0228	1	0.1532	0.1631
2	0.0431	0.0334	2	0.1490	0.1589
3	0.0340	0.0261	3	0.1580	0.1682
4	0.0436	0.0337	others too small for accurate analysis		
5	0.0366	0.0284			

Weld 34 bulk composition 94.6% Cu

matrix - Fe FeKα V = 20 kv SC=0.116μa

location	K_{Fe}	C_{Fe}	
1	0.0517	0.0437	
2	0.0366	0.0308	
3	0.0340	0.0285	no dendritic matrix
4	0.0325	0.0273	
5	0.0265	0.0222	
6	0.0262	0.0219	
7	0.0246	0.0206	

* location - steps of approximately 0.1 mm from interface.

This uses the approximation that the manganese in the matrix is equal to the amount determined by wet chemistry and the manganese in the dendrites is the fraction of the bulk amount determined by the ratio given previously.

In certain welds the copper content is so high that a network of iron rich dendrites does not form, and there are at most only a few discrete volumes of the iron rich phase, Figure 13. The diffusion gradient, except in the proximity of the α-Fe, is initially the unmelted plate; here a classical two component diffusion couple exists and smooth unidirectional gradients result. The results of two such cases are plotted in Figure 15.

Diffusion of copper along grain boundaries in the steel substrate occurs at grain boundaries in the iron rich phase at the boundary between the weld bead and the steel substrate. This may be seen in Figure 13b. Diffusion does not proceed down the grain boundaries unless the boundaries of the substrate and iron rich phase are in proximity.

No welds exhibited cracking in either the weld or the substrate.

5.1.2. Structure related to mechanical properties

Bend test pieces were prepared of square cross section with an edge dimension of 6.0 mm. These were from welds representative of the whole range of composition. All tests were successfully completed without cracking. These were for both the transverse and longitudinal directions for all samples tested with a test radius of 18 mm (3t).

5.1.3. Macroscopic features

Figures 16a -16c show typical cross sections of the welds made in the course of experimentation.

All welds made with flux VUZ3Cu have less penetration that those made with the same welding parameters using flux A50. This may be seen

by comparing Figures 16a and 16b to Figure 16c.

All welds made with flux VUZ3Cu have a flat, smooth bead surface. Welds made with flux A50 are generally concave on the top, with an undulating rough surface; ripple lines of equal height are parabolic in shape and correspond to solidification isotherms. The concavity may be seen in Figure 16c.

Instances of deep penetration may be found at varying locations. This is demonstrated by comparing Figures 16a and 16b, which are different cross sections of the same weld. The most probable location for deep penetration is directly beneath the edge of the strip electrode as seen in Figure 16c. Deep penetration beneath the electrode edge is extreme in the case of flux A50.

A weld made with flux VUZ3Cu was progressively planed in a direction perpendicular to the original base metal surface. Machining was terminated when the machined surface was 0.4 mm below the original base metal surface. To a first order approximation the area of the copper rich zones remaining at this level are proportional to the degree of penetration. Figure 17 shows these areas of penetration. Hence, these zones depict the random manner in which the arc moves across the width of the weld pool as well as the time dwell at the various locations.

The weld deposited utilizing VUZ3Cu flux adulterated with 1.6% Fe_2O_3 exhibited all of the macroscopic features of welds deposited with flux A50, i.e. deep penetration, surface concavity, and surface roughness.

5.2. Quantitative

Empirical equations based upon theoretical considerations have been obtained. These equations fully characterize the extent and approximate shape of a weld bead. The summary of these results are presented in Table 17.

The derivation of the equations in Table 17 are delineated in this section. The significance of the results and a model for the submerged arc welding process are discussed in Section 6.

As stated in Section 4.5.1, over the range of parameters used, electrode extension and electrode angle did not have an effect on the dimensions of the welds. This will be further discussed in Section 6.

5.2.1. Weld reinforcement area

The actual weld reinforcement area, for each flux, is linear with respect to energy input (q/S) and by extrapolation of the relationship $A_n = 0$ when $q/S = 0$ for each flux. The relationship for flux VUZ3Cu is:

$$A_r^{act} = 2.65 \times (10)^{-2} (q/S) \quad \ldots\ldots 5\text{-}1V$$

and for flux A50:

$$A_r^{act} = 2.48 \times (10)^{-2} (q/S). \quad \ldots\ldots 5\text{-}1A$$

Since the melting rate in $mm^3\text{-}s^{-1}$ is

$$\frac{dw}{dt} = A_r^{act} S \quad \ldots\ldots 5\text{-}6$$

then for each welding flux, the strip electrode melting rate is directly proportional to q and thus IV. The melting rate for flux VUZ3Cu is 6.9% greater than for flux A50. This is unlike the case of welds using wire electrodes, where melting rate is generally accepted to be independent of voltage.

TABLE 17. EMPIRICAL EQUATIONS FOR WELD DIMENSIONS

FLUX VUZ3Cu	FLUX A5O
$A_r^{act} = 2.65x(10)^{-2} \frac{q}{S}$ (5-1V)	$A_r^{act} = 2.48x(10)^{-2} \frac{q}{S}$ (5-1A)
(0.877)* (>> 0.9999)	(0.868) (>> 0.9999)
$A_n^{eff} = 1.03x(10)^{-2} I^{1/6} \frac{q}{S} - 105$ (5-2V)	$A_n^{eff} = 1.79x(10)^{-3} I^{1/3} \frac{q}{S} + 40.4D_u + 123.6$
(0.886) (>>0.9999)	(0.848) (>>0.9999) (0.992) (5-2A)
$D_h = 3.16 (10)^{-4} \frac{q}{S} + C.801 D_u + 1.06$	$D_h = 2.44x(10)^{-4} \frac{q}{S} + 0.95D_u + 1.50$
(0.761) (>>0.9999) (>>0.9999) (5-3V)	(0.867) (>0.9999) (>0.9999) (5-3A)
$D_w = 1.10 \times (10)^{-3} \frac{q}{S} + 53.9$	$D_w = 3.32 \times (10)^{-4} \frac{q}{S} + 70.7$
(0.640) (>0.9995) (5-4V)	(0.283) (0.800) (5-4A)
$D_P = -0.129V - 0.769 D_u + 5.9$	$D_P = 2.99)10)^{-3} I-0.120V - 0.619 D_u^{1/2} + 3.4$
(0.774) (0.980) (0.998) (5-5V)	(0.716) (0.992) (0.975) (0.980) (5-5A)

*Figures in parentheses indicate a) the number beneath the left hand side of each equation is the multiple correlation. b) the number under each term at the right hand side excluding the constant is the probability that the correlation is real as opposed to occurring by chance.

The linear relationship between the actual weld reinforcement area and energy input is shown in Figures 19 and 20. Figure 21 shows the same linear relationship for welds deposited at a constant voltage and no underliner using flux VUZ3Cu.

During extensive analysis of the data, no additional terms or interactions were found to be statistically valid.

The effect of an underlineron apparent weld reinforcement area is shown in Figure 22.

5.2.2. Effective weld nugget area

All weld nugget cross sectional areas were converted to the thermodynamically equivalent weld nugget area of steel by utilizing equation 4-4.

It was shown in the graph of effective weld nugget area versus energy input, Figure 21, that larger nugget areas were created with higher currents. Delsol[78] found this effect when investigating heat utilization in submerged arc welding with wire electrodes, which he attributes to greater heat transfer efficiency due to increased stirring of the weld pool at higher currents; this aspect is discussed in detail in Section 6.

The empirical equation for effective weld nugget area is, for flux VUZ3Cu:

$$A_n^{eff} = 1.03 \times (10)^{-2} I^{1/6} (q/S) - 105 \quad \ldots\ldots 5\text{-}2V$$

and for flux A5O:

$$A_n^{eff} = 1.79 \times (10)^{-3} I^{1/3} (q/S) + 40.4\, D_u + 123.6 \quad \ldots\ldots 5\text{-}2A$$

Figures 23 and 24 graphically show the relation between the effective nugget area, calculated from equation 4-4, and the values predicted by equations 5-2V and 5-2A respectively.

Table 18 shows the values calculated for the effective weld nugget area for all combinations of the variables in Factorial Series B and Series C. In all cases the values for flux VUZ3Cu exceed those predicted for flux A5O, using a given set of values for the independent variables. This proves that energy utilization is, on the average, more efficient with flux VUZ3Cu over the range of the experiments conducted.

Equation 5-2A includes a term representing the effect of the underliner width, whereas equation 5-2V does not. Since the first effect of the presence of an underliner is to utilize a fraction of the input energy to melt the underliner as opposed to the base metal, this factor has already been taken into account when using equation 4-4. In the case of flux A5O, where deep penetration occurs, even with an underliner, the addition of copper from the underliner increases the rate of homogenization of the weld pool.[80] Both these occurrences increase the transfer of heat through the weld pool to the base plate and thus increase the volume of plate melted. In the case of flux VUZ3Cu, these effects are not significant as will be discussed in detail in Section 6.

The effect of an underliner on the actual weld nugget area is shown in Figure 22.

5.2.3. Weld height

Weld height is dependent upon energy input and the thickness of the underliner. The quantitative relationship in the case of flux VUZ3Cu is:

$$D_h = 3.16x(10)^{-4}\ q/S + 0.801\ D_u + 1.06 \quad \ldots\ldots 5\text{-}3V$$

TABLE 18. CALCULATED VALUES OF EFFECTIVE WELD NUGGET AREA

I (a)	q/s (kJ/mm)	A_n^{eff} (VUZ3Cu) (mm^2)	A_n^{eff} (A5O, D_u = 0.5mm) (mm^2)	A_n^{eff} (A5O, D_u =1.0 mm) (mm^2)
975	14.2	356	296	316
1175	14.2	361	312	352
975	16.5	422	377	356
1175	16.5	448	356	396

and in the case of flux A50:

$$D_h = 2.44x(10)^{-4} \; q/S + 0.95 \; D_u + 1.50 \qquad \ldots\ldots 5\text{-}3A$$

The coefficient of D_u in each case is related to the need to correct the actual underliner thickness to take account of the fact that the underliner width is less than the weld bead width and when melted only contributes a fraction of its original height to the weld bead.

The relationship of energy input to the height of the weld bead resultant from electrode melting is shown in Figures 25 and 26. The effect of underliner thickness on total height is shown in Figure 22.

5.2.4. Weld width

Weld width is dependent upon energy input. The quantitative relationship for flux VUZ3Cu is:

$$D_w = 1.10x(10)^{-3} \; q/S + 53.9 \qquad \ldots\ldots 5\text{-}4V$$

and for flux A50 is:

$$D_w = 3.32x(10)^{-4} \; q/S + 70.7 . \qquad \ldots\ldots 5\text{-}4A$$

The actual measured weld width is plotted versus energy input for flux VUZ3Cu in Figure 27.

Equation 5-4A only accounts for 28.3% of the observed values of width although no other statistically valid relationships were obtained. Since the arc has a high probability of discharging at the strip edge fluctuations in the instantaneous mass transfer from the time averaged value are largely accommodated by variations in width. For flux A50 arcing at the strip edge has a greater range of penetration and thus a more uneven instantaneous strip melting rate. It is believed that the width fluctuations arise from this effect.

5.2.5. Weld penetration

The depth of penetration for each flux, is dependent upon voltage and underliner thickness, and in the case of flux A50 only, is dependent also upon current.

The empirical equation for flux VUZ3Cu is:

$$D_P = -0.129\ V - 0.769\ D_u + 5.3 \qquad \ldots\ldots\ 5\text{-}5V$$

and for flux A50:

$$D_P = 2.99x(10)^{-3} I - 0.120\ V - 0.619\ D_u^{1/2} + 3.4 \qquad \ldots\ldots\ 5\text{-}5A$$

The relationships between the actual penetration and that predicted by the empirical equations 5-5V and 5-5A are shown in Figures 28 and 29 respectively.

These equations only hold for the range to 4.3 mm-s^{-1} and do not fully characterize the penetration since they do not include speed as a variable. Figure 30 shows that at the highest welding speed, the penetration changes from a gradual reduction with increasing speed, and markedly increases. This observation is in agreement with Belov[61] who reports the onset of deeper penetration at a speed of 4.2 mm-s^{-1}, Figure 9c.

Welding speed is not included in equations 5-5V and 5-5A because the bulk of experimentation was done at speeds up to the order of 3.0 mm-s^{-1}; as can be seen in Figures 9c and 30, the downward trend cannot be truly resolved over this range.

The multiple correlations for equations 5-5V and 5-5A. namely, 0.774 and 0.731, are lower than those for the other empirical equations with the exception of those for the width. This is to be expected,

since the penetration is related to the arc movement which is transient by its very nature (Section 2.1.2). The measurement of this quantity is somewhat difficult, as the locations adjacent to those selected for actual measurement, may be quite different in penetration, Figure 16.

The coefficient of the term containing D_u in equation 5-5V is 0.769, which is very close to the ratio of the enthalpies of like volume of copper and iron at the melting point of iron which is 0.766.

In equation 5-5A, the effect of the underliner is proportional to the square root of its thickness. This is because in the case of a large amount of base metal melting, as occurs with flux A50, the effect of the underliner is compound; it:

a. consumes heat that would otherwise melt base metal.

b. aids in heat transfer to the base metal by both increasing weld pool thermal diffusivity and increasing the heat transfer by convection.

Figure 22 shows the proportionality of penetration to $D_u^{1/2}$ for the range 0.0-1.0 mm underliner thickness for flux A50. It also shows that for an underliner thickness of 2.0mm the mechanicms increasing plate melting are controlling; (empirical equations are valid in all cases for underliner thicknesses of 0.0-1.0 mm).

5.2.6. Electrode polarity effects

Weld beads with electrode negative polarity were generally unacceptable as stated in Section 4.5.5. However, it was determined that a change of polarity did not alter the strip electrode melting rate for welds made with flux VUZ3Cu.

The erratically shaped weld beads with electrode negative welding are attributed to the electron flow negating the necessary chemical reactions for dissolution of the oxide film and surface contaminants.

6. DISCUSSION OF RESULTS

The ultimate goal of the study of heat flow in fusion welding is to describe the heat source in useful mathematical terms such that it be possible to predict thermal events. It may be necessary to define shape, intensity and direction. The first attempts at giving fusion welding heat sources a mathematical interpretation, considered them as continuous point or line sources, and applied 'classical' heat flow theory. For the welding situation, of necessity, assumptions and approximations were numerous and often sweeping. However, under certain conditions, empirical equations based upon these concepts were found to be reliable, but under other conditions, considerably less reliable. When applied to the submerged arc process, only wire electrodes were previously considered.

The melting rate for strip electrodes has been demonstrated here to be dependent on power, as indirectly indicated by previous work.[9,63] This makes the energy input as a quantity more useful in characterizing the features of the weld than it has been for welding with wire electrodes. This aspect will be discussed in greater detail after a theoretical model has been presented for submerged arc welding with strip electrodes.

6.1. Theoretical model

The following model is presented to describe the phenomena associated with submerged arc welding with strip electrodes:

The strip electrode is consumed at a rate proportional to the welding power ($q = IV$) and is transported to the base plate in drops by the mechanisms described in detail by Eichhorn and Lohrmann.[38] The rate at which the electrode melts is also dependent upon the flux being used. The transfer of molten metal from electrode to weld pool occurs with a certain amount of superheat, the degree of superheat also depends on the flux being used. After an initial transient stage, the

welding process reaches stable conditions and the molten metal from the electrode carries a fraction of the superheat to the weld pool that is dependent upon the path that each drop takes. This assumes that the metal transfer is to a molten pool rather than directly to the still solid base metal plate. The experimental evidence here and that presented by Belov[61] indicates that at speeds below 4.3 $mm.s^{-1}$, the transfer is into a molten weld pool, but at higher speeds drops from the electrode may reach the base plate ahead of the weld pool.

There may or may not be base metal melting due to energy liberated at the anode or cathode spot, depending upon electrode polarity, at the base metal side of the arc. This is unclear from the experimental evidence.

The surface of the base metal is melted by the superheated droplets from the melted electrode. The amount of base metal melted is not related in a linear manner with the degree of superheat available from the metal transfered, but is mainly controlled by the copper content of the molten weld pool and the current. These effects are due to the following reasons:

a. Stirring and thus heat transfer efficiency increases with increasing current.[78,80]

b. Increased copper content of weld pool increases the thermal diffusivity and thus increases heat transfer efficiency.

c. Increased copper content of weld decreases the difference between the density of the weld pool and the impinging electrode metal droplets thus increasing mixing; this results in increased heat transfer efficiency.[80]

6.1.1. Effect of speed

The weld bead dimensions are largely determined by welding speed. Since energy is being supplied by the source at a given rate, the welding speed determines the longitudinal distribution of this energy and also the mode of dissipation of the heat into the base plate, i.e. through a molten weld pool or, beyond a certain speed, directly onto the base plate.

At a given welding power, as speed is increased, both the height and penetration decrease until the molten metal transfered from the electrode, starts to move off the leading edge of the weld pool, and directly impinges upon the base metal. Since the heat transfer to the base metal is now direct, the penetration increases drastically. Assuming that the electrode melting rate is sufficient to maintain a continuum of transfer, the speed could be increased until the transfer of molten electrode metal was entirely on the base metal. At this point the weld penetration would again begin to diminish. A graphical representation of this hypothetical welding situation is shown in Figure 31.

6.1.2. Effect of electrode angle

A change from perpendicular to a trailing electrode angle may slightly raise the speed at which the metal transfer begins to move directly onto the base plate. Conversely, a leading angle would lower the speed where the metal transfer moves off the weld pool. This has been confirmed by Barclay,[87] and may be the reason for the remarks made by Marshall[15] with regard to electrode angle.

Practically a trailing electrode angle may be of use for two reasons:

a. Deposition speed may be increased.

b. Thinner claddings may be deposited, without detrimental increase in dilution.

6.1.3. Effect of electrode extension

In the case of strip electrodes of high resistivity, melting rate would be related to the extent of resistance heating, I^2R. The greater the electrode extension the larger the effect. This aspect has been successfully accounted for in the case of wire steel electrodes.[71,78]

Resistance heating of the electrode clearly does not enter into the calculations for copper strip, over the range of parameters utilized in this investigation.

6.1.4. Effect of an underliner

An underliner has the following effects:

a. Contributes desired constituents to the weld pool.

b. Consumes part of the thermal energy that would otherwise melt the base metal.

c. Alters the thermal diffusivity of the weld pool.

d. Alters the density of the weld pool.

Clearly mechanisms a and b lower the resultant dilution. However, mechanisms c and d may contribute to lowering the dilution or may have the opposite effect.

If the thermal diffusivity of the weld pool increases, the heat transfer efficiency increases. Thus the dilution decrease will not be as great as expected from a and b or may in fact eradicate the effect of a and b increasing the dilution (e.g. copper underliners and electrodes). If the thermal diffusivity decreases (e.g. stainless steel underliners

and electrodes) the net result is less dilution than expected from a and b.

If the density of the weld pool approaches more closely the density of the droplets being transferred from the electrodes, the rate at which homogenization of the weld pool occurs is increased;[80] this increased stirring rate will increase heat transfer efficiencies[78] melting more base metal. The net result will be as discussed for thermal diffusivity effects.

The compound nature of these effects can be seen clearly in Figure 22 and by equation 5-5A where the functional dependence is upon the square root of the underliner thickness.

6.2. Effective weld nugget area

Converting weld nugget areas of an alloy to a thermodynamic equivalent of a single metal, in this case iron, provides a useful means of greatly simplifying the handling of data and deriving quantitative relationships when welding with dissimilar electrodes and workpieces. The usefulness of this approach has been demonstrated by:

a. The improved accuracy of the empirical relationship to predict nugget area, derived by Jackson,[55,71] (Appendix A).

b. The high degree of statistical correlation when using this quantity for characterizing the strip electrode melting in this investigation, (Section 5.2.2.).

c. The close correspondence of the coefficient of the underliner term in equation 5-5V to the value predicted entirely by theoretical considerations.

In this investigation, since speed was not an independent variable but fixed, trying to choose a value other than unity for the exponent of speed only alters the exponent of current.

It may, therefore, be considered desirable to choose current, voltage and energy input as the independent variables. However, this is a difficult experimental approach, since voltage :

a) is the most difficult parameter to vary in the welding process,

b) has the least latitude available that produces satisfactory welds,

c) appears to have a threshhold of ~ 33 volts before it contributes to variations in weld bead dimensions.

6.3. Flux

It is evident from the comparison of welds made in Factorial Series B and C, that flux has the biggest single effect on electrode melting rate and penetration into the base plate. This is a very significant discovery relative to cladding operations of the type currently being discussed.

Since Fe_2O_3 was the main constitutional difference between the A50 and VUZ3Cu fluxes the experiments described in Section 4.5.6. were carried out. The introduction of a controlled amount of Fe_2O_3 into flux VUZ3Cu produced drastically increased penetration and a reduction in the electrode melting rate, thus resulting in performance similar to the A50 flux.

Since submerged arc welding fluxes are produced from naturally occuring minerals, oxides of iron will inevitably be a constituent unless special processing removes them as in the process to produce VUZ3Cu.[62] Furthermore, in many welding situations the flux is expected to remove rust or mill scale from the base plate as a matter of course.[78]

In light of this, remarks concerning the deep penetration characteristics of submerged arc welding may be fortuitious.

Possible mechanisms for the effect of Fe_2O_3 may be:

a. Surface reactions occur in the presence of Fe_2O_3 causing melting with a greater superheat.

b. Fe_2O_3 is the flux constituent that ionizes most easily; in its absence the ionization energy is higher and thus a higher melting rate occurs,[66,71] but at a lower superheat.

Other equally valid hypotheses will undoubtedly be proferred but

in their absence both a and b above are necessary to describe both the characteristics of electrode and base metal melting observed.

These are areas worth more fully investigating.

The chemical mechanisms by which these phenomena occur are even more difficult to predict since the nature of the ionized radicals and their relative amounts are not known and with the present state of the art are conjectural at best.

6.4. Energy input

Energy input has proven to be a useful quantity in describing events relating to strip electrode melting. This factor has been modified when considering effective nugget area to allow for greater heat transfer efficiency.

Jackson[55] states that:

$$A_n = \frac{I^{1.55}}{10^{3.95} S^{0.903}} \quad \ldots\ldots 6\text{-}1\ (A\text{-}1)$$

If we accept that voltage is a constant and cancels out of the equation, (this is questionable as only 8 out of 130 welds were in the range above 33 volts, which is where voltage is considered to be an important variable) we may view it as:

$$A_n = \frac{1}{10^{3.95}} \left(\frac{I^{0.55}}{S^{-0.097}} \right) \left(\frac{q}{S} \right) \quad \ldots\ldots 6\text{-}2$$

The factor $I^{0.55}$ represents the effect of current on stirring action, an increase of which gives increased heat transfer efficiency. The small dependency on speed $S^{-0.097}$ indicates the slight change in heat transfer efficiency as the translational speed is altered thus changing the thermal gradients in the base metal.

7. CONCLUSIONS

1) Copper strip may be deposited onto mild steel as a weld bead of satisfactory shape for cladding and containing > 95% copper.

2) Equating multicomponent welds to the thermodynamic equivalent of a single metal is a useful and accurate means for facilitating data handling and determinating quantitative relationships between welding variables and the resultant welds.

3) The melting rate for strip electrodes is dependent on flux composition, but for a given flux a linear function of current-voltage product.

4) The actual weld reinforcement area is a linear function of energy input.

5) Weld nugget area is dependent upon the combined effects of energy input and a stirring factor which is a function of current.

6) Weld bead height and width are functions of energy input.

7) Weld width varies to accommodate instantaneous changes in mass transfer due to irregular arc behavior.

8) Penetration is a function of voltage and is a function of current for flux A50 but is not a function of current for flux VUZ3Cu.

9) Electrode negative polarity produces unsatisfactory welds. The electrode melting rate is not dependent on polarity.

10) The inclusion of an underliner:

   a) contributed desired constituents to the weld pool.

   b) consumes energy that would otherwise melt base metal.

c) alters thermal diffusivity of weld pool (higher thermal diffusivities increase base metal melting).

d) alters density of weld pool (as the weld pool density approaches the density of droplets from the electrode, homogenization rate increases; the resultant stirring increases heat transfer efficiency and thus increases base metal melting.

The resultant of the effects in items a-d determines the overall effect of an underliner addition.

11) The composition of the weld bead may be estimated from the relationship:

$$C_e = \frac{\rho_e A_r}{\rho_e A_r + \rho_w (A_n - A_e)} \quad \ldots\ldots \quad 4\text{-}3$$

where A_r and A_m are determined from welding parameters.

12) The presence of Fe_2O_3 in a flux composition decreases the electrode melting rate and increases weld penetration into the workpiece.

13) Flux VUZ3Cu produces welds of low dilution and excellent surface quality. (This flux is produced by a technique which removes Fe_2O_3).

8. SUGGESTIONS FOR FURTHER WORK

1) Investigations utilizing steel electrodes and steel underliners eliminate altering thermal diffusivity and maintain a density for the weld pool and transfering droplets. This would allow separation of the thermodynamic contribution of an underliner as opposed to its heat transfer related contribution.

2) Experimentation with a range of Fe_2O_3 additions to flux of the VUZ3Cu type would more fully characterize its contribution to electrode melting rate and penetration.

3) The effect of Fe_2O_3 should be examined using steel electrodes.

4) An accurate means of determining the anode, cathode, and arc potential drops should be devised to enable the determination of the partition of energy in welding.

APPENDIX A.

Jackson[71] has shown that the weld nugget area for steel wire electrodes and steel substrates can be represented by the empirical relationship:

$$A_n = \frac{I^{1.55}}{10^{3.95}\, S^{0.903}} \quad * \qquad \ldots\ldots \text{A-1}$$

This relationship is claimed to achieve an accurate estimate of the weld nugget size and to be independent of polarity, flux and welding process.

Jackson et al.[55] attempted to apply this relationship to welding aluminum bronze electrodes onto steel stubstrates via the submerged arc process. This relationship is shown by the line AA' in Figure A-1.

The following thermodynamic correction was made by the author which equates all weld nuggets to a steel weld nugget with enthalpy the same as the two component weld nugget:

Assume aluminum bronze thermodynamically similar to copper - all calculations in ^{o}K - thermodynamic data from Kelley.[88]

For iron

$$H_{1812}(\ell) - H_{298} = 74.05 \text{kJ g-atom}^{-1} \qquad \ldots\ldots \text{A-2}$$

For copper

$$H_{1812}(\ell) - H_{298} = 56.82 \text{kJ g-atom}^{-1} \qquad \ldots\ldots \text{A-3}$$

* English units - I [=] a, S [=] in min^{-1}, A_n [=] in^2

Since nugget areas are measured at ambient, densities are at 298°K:

$$1\ mm^3\ Fe\ @\ 298^{\circ}K = 7.86\ mg \qquad \ldots\ldots A\text{-}4$$

$$\frac{7.86\ mg - mm^{-3}}{55.85g\ g\text{-}atom^{-1}} = 1.407 \times (10)^{-4}\ g\text{-}atom\ mm^{-3} \qquad \ldots\ldots A\text{-}5$$

$$1\ mm^3\ Cu\ @\ 298^{\circ}K = 8.92\ mg \qquad \ldots\ldots A\text{-}6$$

$$\frac{8.92\ mg\ mm^{-3}}{63.54\ g\ g\text{-}atom^{-1}} = 1.404 \times (10)^{-4}\ g\text{-}atom\ mm^{-3} \qquad \ldots\ldots A\text{-}7$$

for Fe $h_{1812} - h_{298} = 1.407 \times (10)^{-1}\ g\text{-}atom\ mm^{-3} \times 74.05\ kJ\ g\text{-}atom^{-1}$

$$= 10.03\ J\ mm^{-3} \qquad \ldots\ldots A\text{-}8$$

for Cu $h_{1812} - h_{298} = 1.404 \times (10)^{-4}\ g\text{-}atom\ mm^{-3} \times 56.82\ kJ\ g\text{-}atom^{-1}$

$$= 7.976\ J\ mm^{-3} \qquad \ldots\ldots A\text{-}9$$

Assume nugget of iron 1 mm long and 1 mm^2 in area this requires 10.03 J heat input to produce.

In 52 welds[55] the Fe composition is 37.4% maximum, 33.30% minimum and 35.84% mean. For simplicity a representative weld is assumed to be 65% Cu 35% Fe, therefore the enthalpy is divided as follows:

$$10.03\ J\ mm^{-3} \times 0.35 \times V + 7.976\ J\ mm^{-3} \times 0.65 \times V = 10.03\ J \qquad A\text{-}10$$

$$V = 1.18\ mm^3 \qquad \ldots\ldots A\text{-}11$$

or an areal increase of 18%. Similarly, this can be calculated for any iron-copper ratio.

From equating these weld nugget areas the area of steel nugget predicted by Jackson's equation can then be converted into the appropriate weld nugget area of the two component weld. This is represented by the line BB' in Figure A1 which is a substantially better representation of the data.

All data from the experimental work of Jackson et al.[55] were analyzed by statistical techniques, but each nugget area was converted for the exact copper composition using the following equation:

$$A_n^{eff} = A_n \left[\frac{f_{Cu}\ 7.976\ J\ mm^{-3} + (1 - f_{Cu})\ 10.03\ J\ mm^{-3}}{10.03\ J\ mm^{-3}} \right] \quad \ldots\ldots\ A\text{-}11$$

Equation A1 predicts the nugget area corrected to a thermodynamic equivalent of steel with a correlation of 0.91, and the single term has a confidence of > 0.9995.

APPENDIX B.

A flux for submerged arc welding of aluminum bronzes has been formulated and marketed by Siderothermica, Milan, Italy. The flux is designated as SIDERFLUX BRAL/S.

The composition of two sample quantities, arbitrarily designated as samples A and B, were analyzed by the Department of Metallurgy, University of Queensland, Australia.[89] The compositions are given in Table B-1. The basic composition is formulated to liberate CO_2 and lower the partial pressure of hydrogen, similar to that described by Ilyushenko and Sedov.[17]

It is believed that Metrode experimental fluxes, Cuproflux A and Cuproflux B, were based upon these analyses.[89]

TABLE B.1. COMPOSITIONS OF WELDING FLUX SIDERFLUX BRAL/S.

Flux	SIDERFLUX BRAL/S	
Source	Siderothermica, Milan, Italy	
Sample	A	B
SiO_2	38.2	39.7
MnO	1.18	1.64
TiO_2	0.11	1.01
FeO	0.44	0.50
$CaCO_3$	34.4	33.6
$MgCO_3$	2.26	2.5
Na*	5.5	5.5
Al*	7.33	9.51
F *	11.2	11.0
Total	100.6	105.0

* X-ray diffraction shows these existing as

Na_3AlF_6 and Al.

Analysis by Dept. of Metallurgy, University of Queensland, Brisbane, Australia.

LIST OF SYMBOLS

A_m	-	weld melt area (definition section 4.4)	[mm^2]
A_n	-	weld nugget area (definition section 4.4)	[mm^2]
A_r	-	apparent weld reinforcement area (definition section 4.4)	[mm^2]
A_z	-	heat affected zone area (definition section 4.4)	[mm^2]
A_r^{act}	-	actual weld reinforcement area (definition section 4.4)	[mm^2]
A_n^{eff}	-	effective weld nugget area (definition section 4.4)	[mm^2]
C_i	-	weight fraction of component i	[$g\text{-}g^{-1}$]
D_e	-	electrode extension	[mm]
D_h	-	weld bead height	[mm]
D_p	-	weld penetration depth	[mm]
D_u	-	underliner thickness	[mm]
D_w	-	weld bead width	[mm]
f_e	-	volume fraction of electrode metal	[$mm^3\text{-}mm^{-3}$]
f_w	-	volume fraction of workpiece metal	[$mm^3\text{-}mm^{-3}$]
H_a	-	molar enthalpy at temperature a	[$kJ\ g\text{-}atom^{-1}$]
$h_{a,b}$	-	enthalpy of substance a at temperature b	[$J\text{-}mm^{-3}$]
I	-	current	[a]
K_i	-	ratio of peaks of element i, quantitative electron microscopy	
P	-	polarity	[+; -]
q	-	welding power (= IV)	[W]
q/S	-	energy-per-unit-length (energy input) (= IV/S)	[$kJ\text{-}mm^{-1}$]
S	-	welding speed	[$mm\text{-}S^{-1}$]
SC	-	specimen current	[μa]

T_e	-	fusion temperature of the electrode	[^oK]
T_w	-	fusion temperature of workpiece	[^oK]
V	-	voltage	[V]
V_n	-	weld nugget volume	[mm^3]
V_n	-	effective weld nugget volume	[mm^3]
W_u	-	underliner width	[mm]
α	-	electrode angle	[rad]
ρ_e	-	electrode density	[$g\text{-}mm^{-3}$]
ρ_w	-	workpiece density	[$g\text{-}mm^{-3}$]
dw/dt		melting rate	[$mm\ -S^{-1}$]

BIBLIOGRAPHY

1. L.W.Crane and P.Sexton, "The Submerged Arc Strip Cladding of Mild Steel with Copper and Copper Alloys", CDA-ASM Conference on Copper, 16-19 October 1972, Cleveland, Ohio, U.S.A.

2. H.G.Otto, "Aspects Relating to the Welding Mechanisms", High Energy Rate Working of Metals, 1966, (2), NATO Advanced Study Institute, Oslo, Norway, 472.

3. A.H.Holtzman, "Explosion Clads", ibid., 488.

4. M.Holmes, "An Economic Appraisal of Clad Pressure Vessel Manufacture" M.Sc. thesis, October 1972, University of Aston, Birmingham, England.

5. A.L.Phillips, (ed.), Welding Handbook, 6th Edition, section 2, American Welding Society, New York, New York, U.S.A.

6. C.M.Adams, Jr., University of Wisconsin, Milwaukee, Wisconsin, U.S.A., private communication.

7. B.T.Rubin, University of Aston, Birmingham, England. "Theoretical Model of the Submerged Arc Welding Process", to be published.

8. D.P.Parker, "Heat Flow in Welding Heavy Steel Plate", Sc.D. thesis, 1966, Massachusetts Institute of Technology, Cambridge, Mass, U.S.A.

9. A.B.Marshall, M.F.Jordan, and J.L.Aston, "Stainless Steel Strip Cladding", Welding and Metal Fabrication, August 1973, 292-301.

10. A.E.Vainerman, "Limiting the Iron Content in Copper and Copper Alloy Overlays on Steels", Welding Production, 1964, (2), 39-43.

11. A.R.Lytle, and E.L.Frost, "Welding with Multiple Electrodes in Series - a New Method of Unionment Welding", research report, 9 October 1950, Union Carbide Corporation, Niagara Falls, New York, U.S.A.

12. Yu.L.Krasulin, "Twin Arc Welding of Metals using Two Independent Arcs", Welding Production, 1960, (11), 60-62.

13. E.L.Frost, "Development of a Unionmelt Composition for Welding Copper Alloys", research report, 31 July 1950, Union Carbide Corporation, Niagara Falls, New York, U.S.A.

14. L.van Dyke, and G.Wittstock, "Submerged Arc Welding and Surfacing with Hot Wire Additions", Welding Journal, May 1972, 317-325.

15. A.B.Marshall, "An Investigation of Submerged Arc Strip Cladding using Highly Alloyed Fluxes", M.Sc. thesis, October 1969, University of Aston, Birmingham, England.

16. A. van Bemst, R.D. Daemen, and D.H.Young, "Practical and Metallurgical Comments on Recent Developments in Strip Cladding with Stainless Steels and Nickel-base Alloys", Metal Construction, 1969, (12s), 109-117.

17. V.M.Ilyushenko, and C.E.Sedov, "A Ceramic additive for Fluxes used for Deposition of Bronze". Automatic Welding, 1967, (12), 74-75.

18. S.A.Ershov, "Certain Special Features of the Submerged Arc Deposition of BrAZHN 10-4-4 Bronze on Steel", Welding Production, 1972, (5), 51-53.

19. E.Sudasch, "Heavy Pressure Vessel Overlaying", Welding Design Fabrication, May 1972, 46-48.

20. R.F.Arnoldy, "Bulk Welding in 1966", Welding Journal, February 1967, 117-122.

21. R.W.Nelson, "Submerged Arc Welding and Surfacing with Aluminium Bronze", M.S. thesis, 1973, The Ohio State University, Columbus, Ohio, U.S.A.

22. A.R.Taylor, "The Submerged Arc Strip Cladding of Mild Steel with Aluminium Bronze", M.Sc. thesis, November 1973, University of Aston, Birmingham, England.

23. J.L. Wilson, "The Use of Strip Electrodes for Surfacing by the Unionmelt Process". research report, 20 August 1973, Union Carbide Corporation, Niagara Falls, New York, U.S.A.

24. O.A. Bakshi, E.E.Belousov, G.P.Klebovkin, V.M.Solovskii, and T.V.Sumina, "Wear Resistance Hardfacing with a Powder-tape Electrode", Welding Production, 1960, (3), 30-33.

25. A.M.Horsfield, G.Almqvist, and C.H.Rosendahl. "Strip Cladding of Steel with Stainless and Nickel-based Alloys", British Welding Journal, 1966, 13, 315-325.

26. J.E.Norcross, "Strip Cladding Speeds Stainless Overlay", Welding Engineer, October 1965.

27. Anonymous, "Automatic Strip Cladding", Welding and Metal Fabrication. February 1966, 49-53.

28. R.D.Thomas, "Corrosion-resistant Weld Overlays by the Dual Strip Process", British Welding Journal, May 1966, 307-314.

29. H.C.Campbell and W.C.Johnson, "Cladding and Overlaying with Strip Electrode", Welding Journal, May 1966, 399-409.

30. H.C.Campbell, "Strip Electrodes for Overlay Welding", A.S.M. 1968 Materials Engineering Congress, 14-17 October 1968. Detroit, Michigan, U.S.A.

31. G.Almqvist and N.Egeman. "Stainless Steel Cladding with Strip Electrodes", Welding and Metal Fabrication, July 1963, 295-302.

32. J.Walburn and A.B.Marshall, "A New Look at Submerged Arc Welding", Welding and Metal Fabrication, 1969, 37, 268-274.

33. A.F.Bush and P.Colvin, "The Successful Application of the Strip Cladding Process with Austenitic Strips". Welding and Metal Fabrication, 1969, 37, 234-241.

34. A.J. Griffiths, "The Submerged Arc Cladding of Mild Steel with Cupro-Nickel". M.Sc. thesis. October 1972, University of Aston, Birmingham, England.

35. G.A.Shadrin, F.D. Kashchenko and A.L.Garyaev, "Clad Components Produced by Mechanical Deposition of Bronze on Steel", Automatic Welding, 1964, (5), 75-78.

36. S.Ya. Shekhter, "Spindle Coupling Steel Slide Blocks", Automatic Welding, 1960, (9), 73-75.

37. Yu.L.Krasulin, Dissertation 1963, Baikov Institute of Metallurgy, U.S.S.R. (from quote by Vainerman[10]).

38. F.Eichhorn, and G.R.Lohrmann, "Fundamentals of Arc Facing with Strip Electrode". Schweissen und Schneiden, August 1969, 311-315 (German).

39. G.Kretschmann, "Arc Formation in Strip Welding", Schweisstechnik, 1969, (2), 76-78 (German).

40. R.J.G.Dawson, private communication, Copper Development Association, Potters Bar, Hertfordshire, England.

41. N.A. Olshanskii, "Automatic Welding of Non-ferrous Metal Alloys", New Examinations of Welding Technique., Masshgiz, Moscow, U.S.S.R. 1952, quoted by Kitler et al.[45]

42. Yu.M.Korenyuk, "The Automatic Submerged Arc Welding of Plate Copper", Automatic Welding, 1962, (4), 22-27.

43. Yu.M.Korenyuk, G.P.Manzhelei, and D.M.Rabkin, "Interaction between the Metal and Slag when Submerged Arc Welding Copper". Automatic Welding, 1964, (5), 30-36.

44. I.L.Teitel, A.I.Plastinin, and Yu,M.Korenyuk, "The Submerged Arc Welding of Tubes made of Copper Plate", Automatic Welding, June, 1965, 74-77.

45. S.M.Kitler, and V.A.Sinikov, "Automatic Welding (Overlaying) of Steel with Copper Electrode Wire", Welding Production, 1960, (3), 4-8.

46. A.A.Syrovatkin, "Certain Features Involved on Welding Steel to Copper", Automatic Welding, 1964, (4), 69-71.

47. V.M.Ilyushenko, L.K.Bosak, and L.I.Grishkin, "Automatic Submerged Arc Welding of Copper to Thick Steel", Automatic Welding, 1966 (6), 84-85.

48. B.V.Grundinskii, I.A.Shlyamneva and G.A.Stepanov, "Interaction of Fused Copper with Steels during Building-up and Welding", Welding Production, 1970, (12) 18-20.

49. I.I.Dzhevaga, "Aspects of Pore Formation in Mechanised Submerged Arc Welding of Copper and its Alloys", Welding Production, 1968, (9), 1-6.

50. V.V.Podgaetskii and I.I.Dzhvega, "The Effects of Alloying Elements on the Submerged Arc Welding of Copper", Automatic Welding", 1962, (6), 47-55.

51. E.A.Asnis, V.M.Prokhorenko, and L.S.Shvindlerman, "Mechanism of Cracking during the Depositing of Copper onto Steel", Welding Production, 1965, (11), 15-20.

52. V.N.Timofeev and N.I.Isaev, "Deposition of Copper Alloys on Steel Surfaces", Automatic Welding, 1965, (4), 38-41.

53. V.Orszagh, "Some Problems of Welding Copper of Industrial Purity and their Partial Solution by Means of Submerged Arc Welding", Kovone Materialy, 1963, 134-150 (Slovak).

54. V.Orszagh, "Technology of Automatic Underlfux Welding of Copper", Zvaranie, February 1962, 39-43 (Slovak)

55. C.E.Jackson, P.D.Flenner, M.Killian, and R.Nelson, "Aluminum Bronze Overlays by the Submerged Arc Welding Process", research report, 1972, The Ohio State University, Columbus, Ohio, U.S.A.

56. P.D.Flenner, The Slag-Metal Relationship of a Copper Alloy Submerged Arc Weld", M.S. thesis, 1972, The Ohio State University, Columbus, Ohio, U.S.A.

57. C.E.Jackson, "Fluxes and Slags in Welding", first draft Welding Research Council Interpretive Report, July 1973, The Ohio State University, Columbus, Ohio, U.S.A., quoted by Nelson.[21]

58. E.M. Levi, C.R.Robbins, and H.F.McMurdie, Phase Diagrams for Ceramists, The American Ceramic Society, Columbus, Ohio, U.S.A., 1964.

59. A.P.Bennet, "How Sub-Arc Fluxes Are Made", Metal Construction and British Welding Journal, October 1969, 455-456.

60. L.McD.Schetky, private communication, International Copper Research Association, New York, U.S.A.

61. Yu.M.Belov, "Effect of Welding Conditions on the Bead Cross Section in Automatic Submerged Arc Surfacing Operations Using a Strip Electrode", Welding Production 1961, (12), 9-13.

62. V.Orszagh, private communication, Vyskumy Ustav Zvaracksy, (Welding Research Institute), Bratislava, Czechoslovakia.

63. Yu.M.Belov, "Characteristics of Electrode Metal and Flux Fusion in Automatic Surfacing Operations Using a Strip Electrode", Welding Production, 1964, (1), 19-23.

64. P.A.Drayton, "An Examination of the Influence of Process Parameters on Submerged Arc Welding", Welding Research International, 1972, (2), 1-19.

65. W.Mantel, "The Physics of the Welding Arc", Schweissen und Schneiden, 8, 286-287 (German).

66. O.P.Semenova, "On the Mechanisms of Arc Discharge", Comptes Rendres (Doklady) de l'Academie des Sciences de l'URSS, 1946, (9), 683-686, (English).

67. I.I.Dzhevaga, quoted without reference by Korenyuk et al.[43]

68. J.Waring, private communication, University of Queensland, Brisbane, Australia.

69. A.F.Gifford and N.Smith, Proceedings of the Second Commonwealth Welding Conference, 1965, 367-373, quoted by Marshall et al.[9]

70. A.F.Gifford, R.Hazzard, A.M.Horsfield and P.B.Fielding, Discussion of paper by van Bemst et al.[46] Metal Construction, 1969, (12s), 125-131.

71. C.E.Jackson, "The Science of Arc Welding", Welding Journal, 1966, 39, 129s-140s, 177s-190s, 225s-230s.

72. C.E.Jackson, private communication, The Ohio State University, Columbus, Ohio, U.S.A.

73. L.M.Gourd, "Electrode Burn-off Rates in Arc Welding", Metal Construction and British Welding Journal", March 1969, 150.

74. Z.Paley, J.M.Lynch, and C.M.Adams, Jr. "Heat Flow in Welding Heavy Steel Plate", Welding Journal, 1964, (2), 71s-79s.

75. J.M.Barry, Z.Paley and C.M.Adams, Jr., "Heat Conduction from Moving Arcs in Welding", Welding Journal, 1963, (3), 97s-104s.

76. C.M.Adams, Jr., W.G.Moffat, and P.Jhaveri, "The Effect of Plate Thickness and Radiation on Heat Flow in Welding and Cutting", Welding Journal, 1962, (1), 12s-16s.

77. C.M.Adams, Jr., "Cooling Rates and Peak Temperatures in Fusion Welding", Welding Journal,1958, (5), 210s-215s.

78. M.S.Delsol, "Heat Utilization in Submerged Arc Welding", Sc.D. thesis, 1968, Massachusetts Institute of Technology, Cambridge, Mass, U.S.A.

79. F.Eichhorn and K.Niederhoff, "Energy per Unit Length as a Unit Characterizing Heat Input of Automatic Welding", Schweissen und Schneiden, October 1972, 399-403, (German).

80. R.A.Woods, and D.R.Milner, "Motion in the Weld Pool in Arc Welding", Welding Journal, 1971, 163s-172s.

81. A.S.Ekatova, "Interaction of Copper with Iron and Steel during Soldering", Tsvet Metally, 1966, (1), 83-86, (Russian).

82. D.E.Jordan, A.J.Auchterlounie and D.J.Heath, "Cladding of Stainless Steel with Aluminum Bronze", Metal Construction, 1969, (12s), 11-12.

83. Unsigned editorial comment, Welding Production, 1965, (11), 20.

84. K.Henneman, "Welding Copper to Steel", Zeitschrift fur Metallkunde, 1968, (10), 762-769, (German).

85. G.Newcombe, "The Bimetal Concept", C.D.A. Conference on Plant Fabrication, November 1973, London, England.

86. B.Chalmers, Harvard University, Cambridge, Mass, U.S.A.

87. J.Barclay, unpublished research, Department of Supply, Ordnance Factory, Bendigo, Victoria, Australia.

88. K.K.Kelley, Contributions to the Data on Theoretical Metallurgy, Bulletin 584, 1960, Bureau of Mines, Department of the Interior, Washington, D.C., U.S.A.

89. A.M.Patton, personal communication, N.C.Ashton Ltd., Huddersfield, Yorks, England.

90. R.E.Johnson, Metals Handbook, Vol.8, American Society for Metals, Metals Park, Ohio, U.S.A., p.293.

BIOGRAPHICAL NOTE

The author was born in Quincy, Massachusetts, U.S.A., 29 April 1943. After graduating from Joseph Case High School, Swansea, Massachusetts, U.S.A., he entered the Massachusetts Institute of Technology, Cambridge, Massachusetts, from which he received the degree of Bachelor of Science in Materials Science in June 1965. From 1965 to 1966 he was American Brakeshoe (Abex) Research Fellow at the Massachusetts Institute of Technology.

In June 1966 the author entered the employment of Texas Instruments Inc., Attleboro, Massachusetts, U.S.A., as a materials engineer in the field of composite materials. In June 1971 he was granted an educational leave of absence to become a postgraduate research student at the University of Aston in Birmingham.

The author is a member of the American Society for Metals.

ILLUSTRATIONS

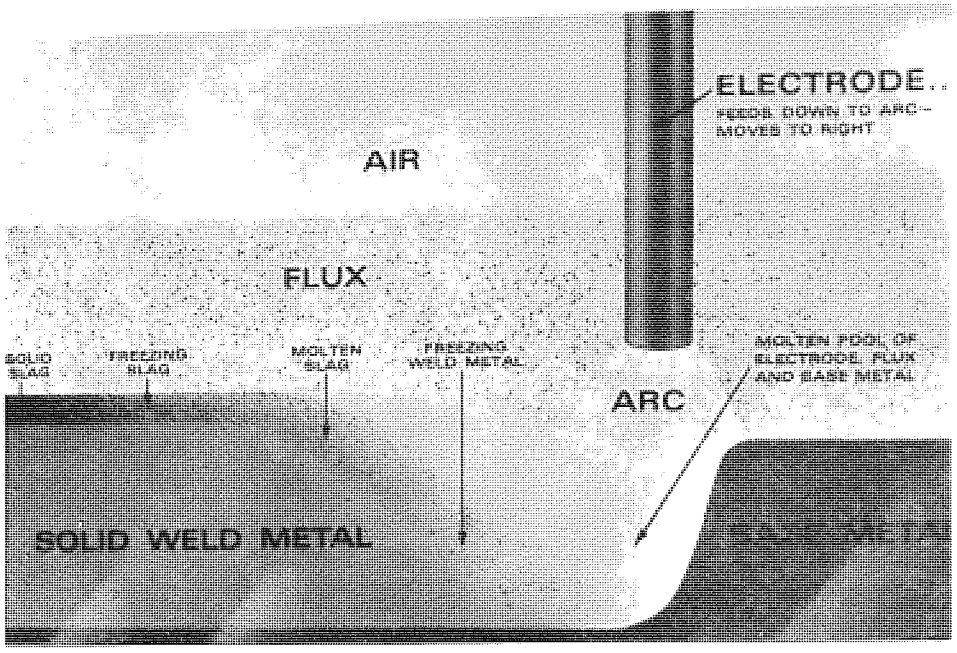

FIGURE 2. SUBMERGED ARC PROCESS, SCHEMATIC[5]

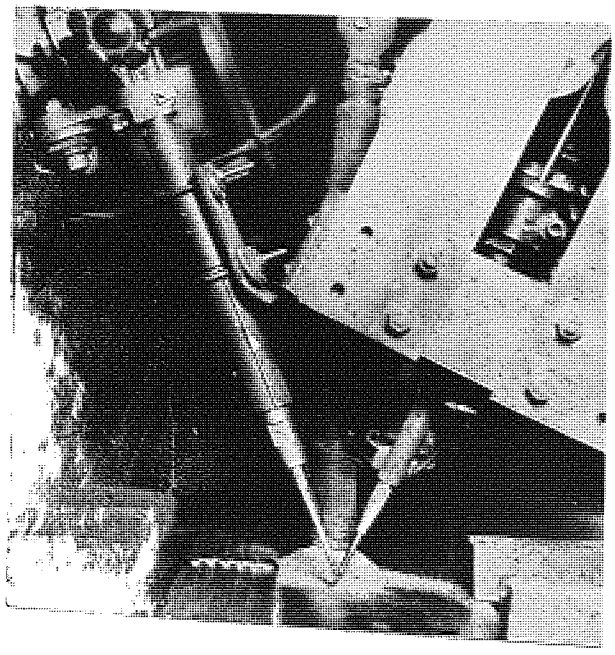

FIGURE 3. SERIES INDEPENDENT ARC PROCESS[11]

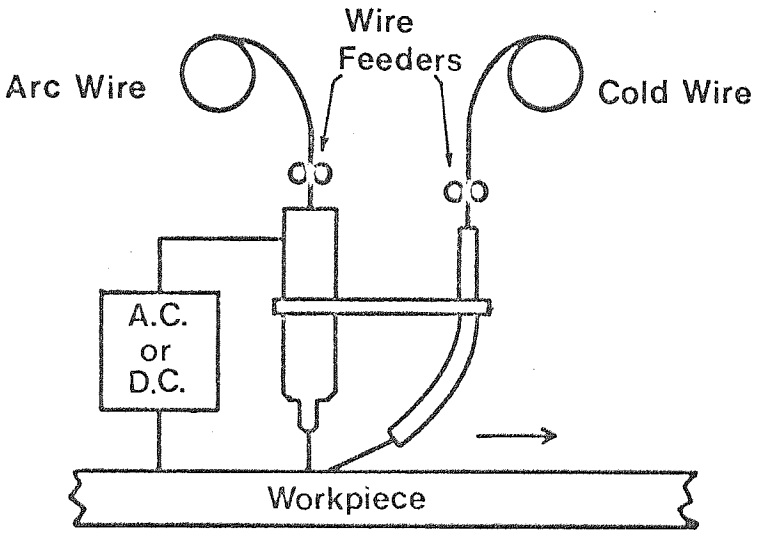

FIGURE 4. SUBMERGED ARC PROCESS, COLD WIRE ADDITION, APPARATUS SCHEMATIC

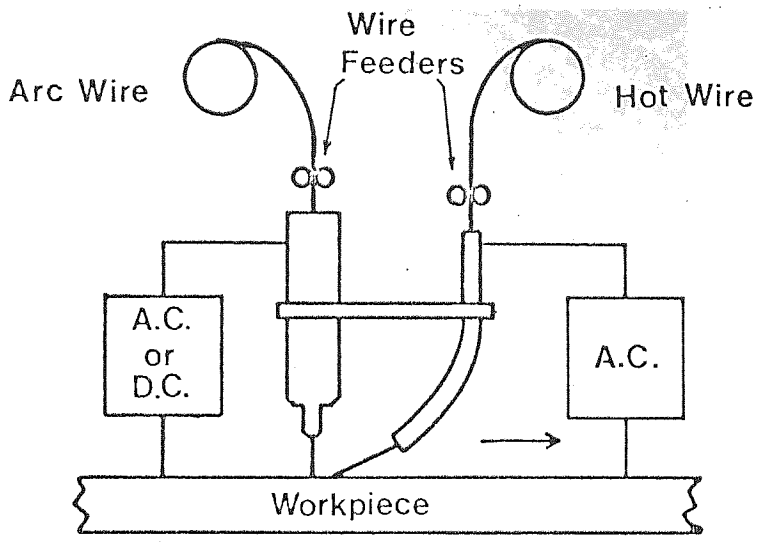

(a) APPARATUS

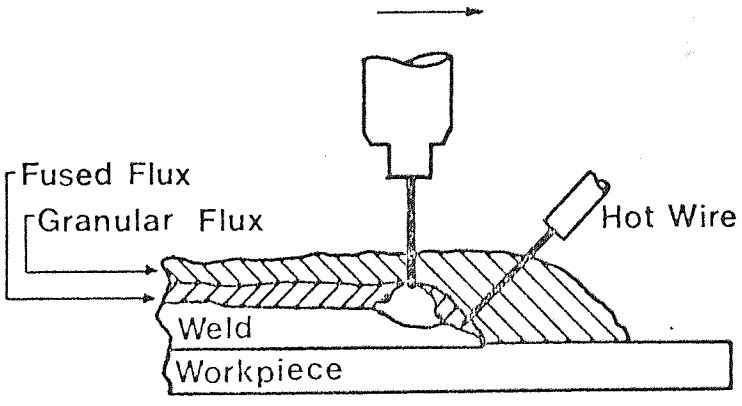

(b) PROCESS

FIGURE 5. SUBMERGED ARC PROCESS, HOT WIRE ADDITION, SCHEMATIC.[14]

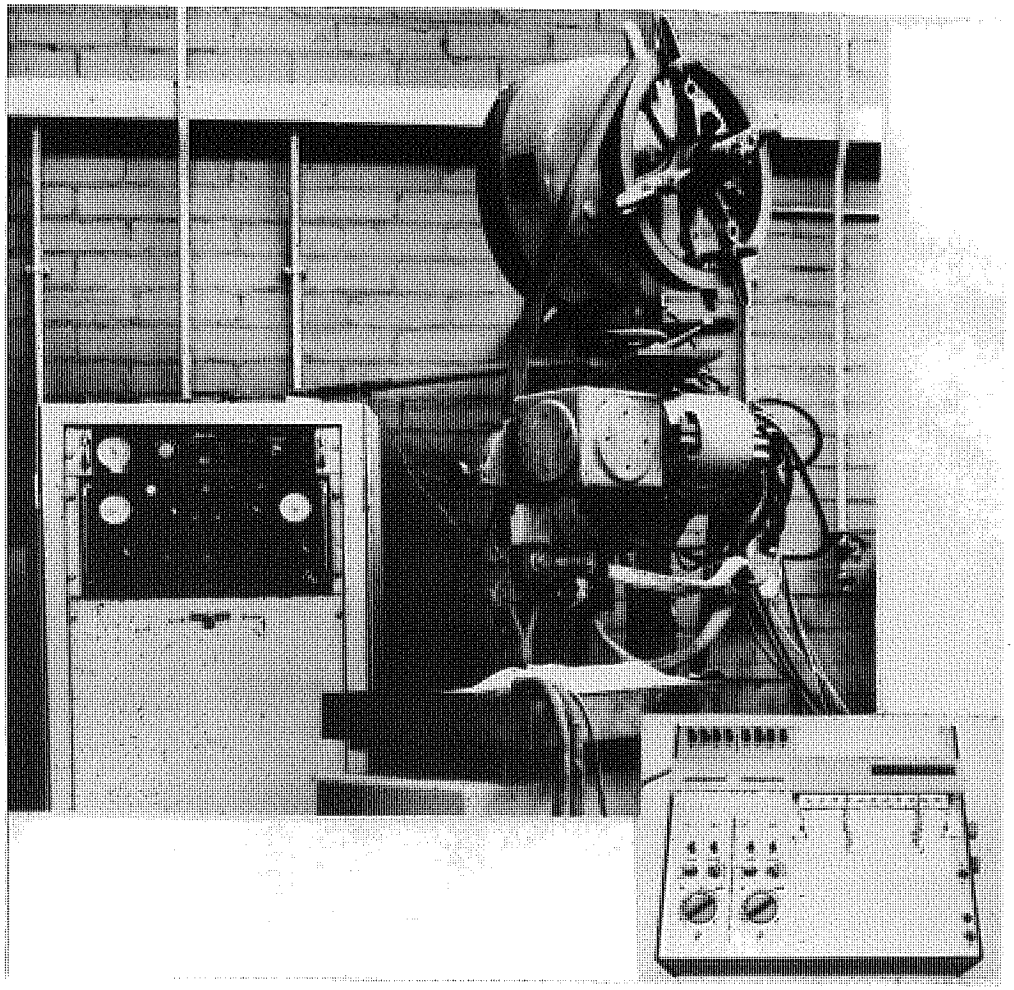

FIGURE 6. APPARATUS FOR CLADDING WITH SUBMERGED ARC PROCESS WITH STRIP ELECTRODES

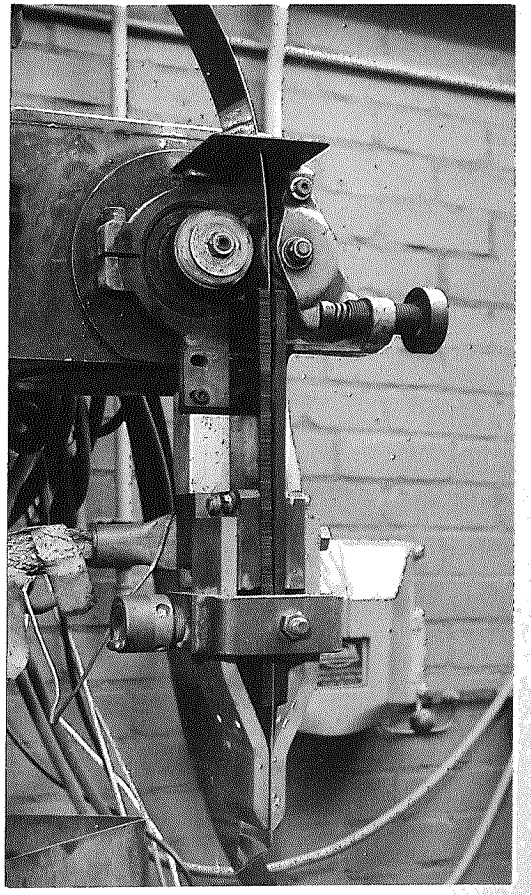

FIGURE 7. ESAB A6 HEAD FOR WELDING WITH STRIP ELECTRODES

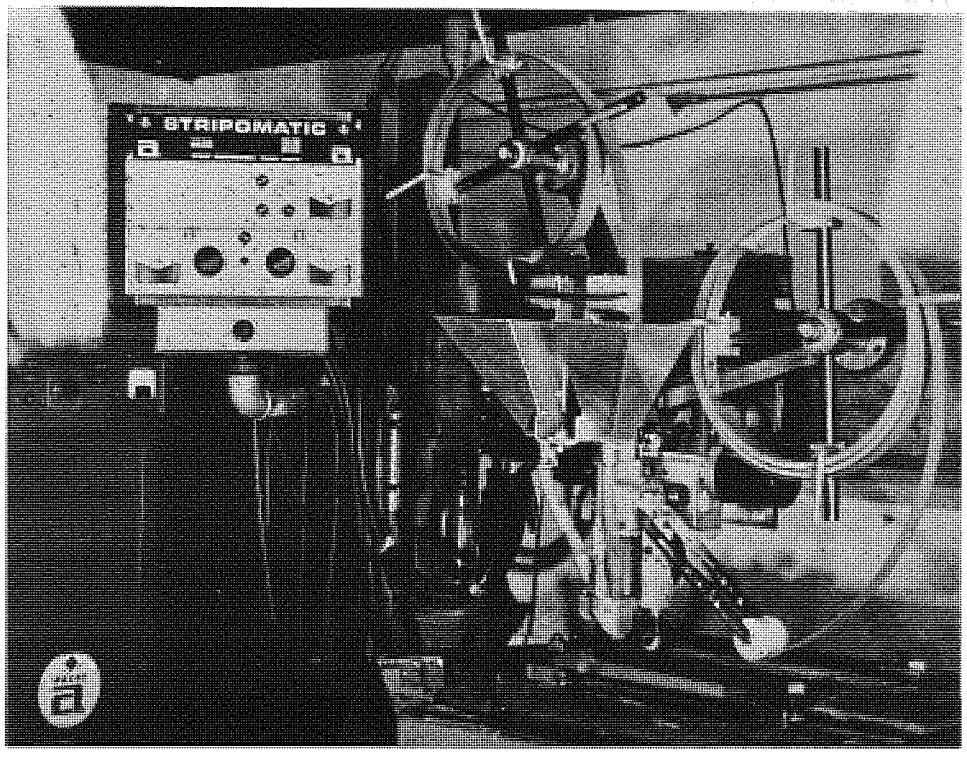

FIGURE 8. COMMERCIALLY AVAILABLE UNIT FOR CLADDING USING THE SUBMERGED ARC PROCESS WITH DUAL STRIP[28]

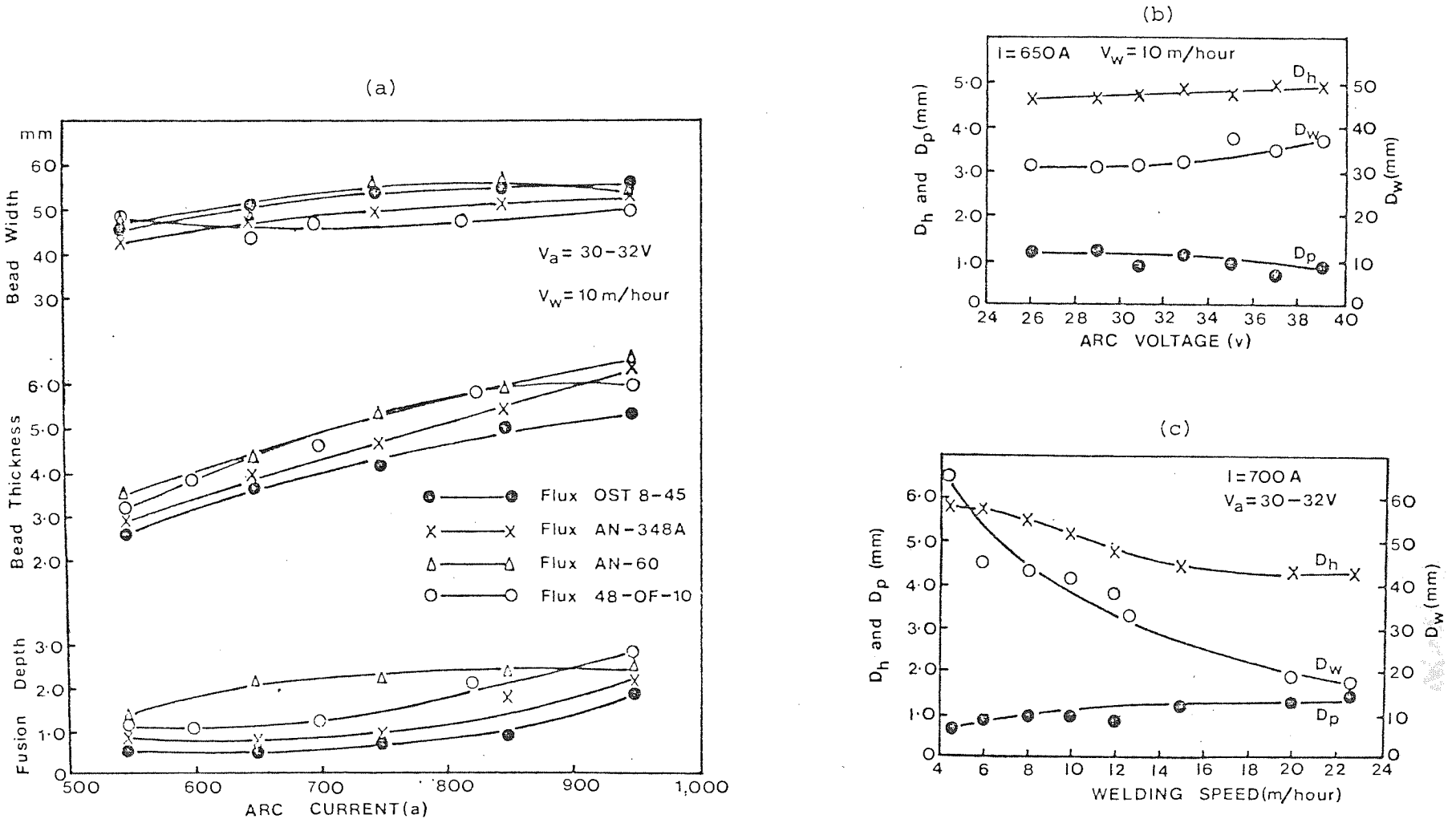

FIGURE 9. WELD BEAD DIMENSIONS VERSUS WELDING PARAMETERS, STEEL STRIP ELECTRODES[61]

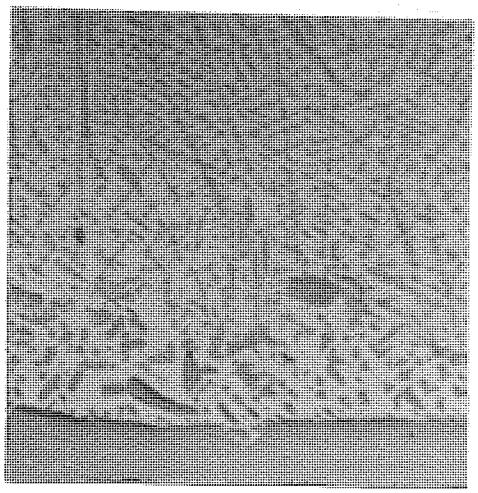

a. OPTICAL x 300

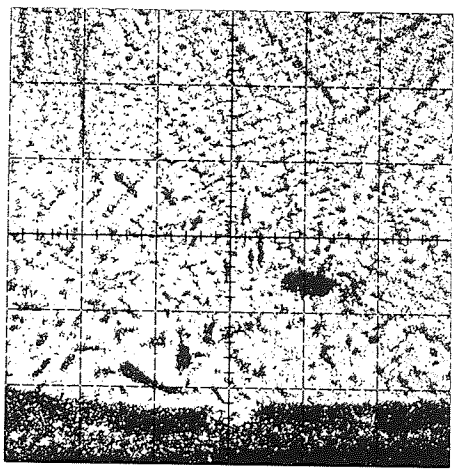

b. Cu Kα x 300

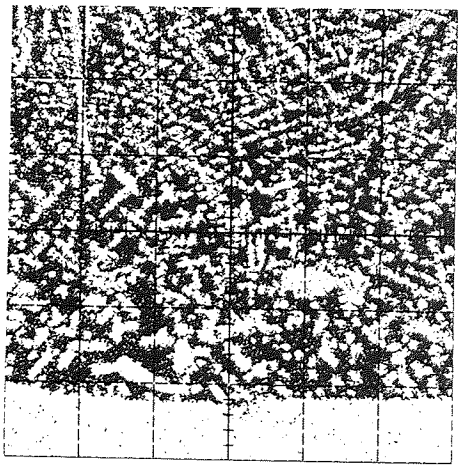

c. Fe Kα x 300

FIGURE 10. PHOTOMICROGRAPHS OF STRIP ELECTRODE WELD, BULK COMPOSITION 67.9%. (OPTICAL UNETCHED)

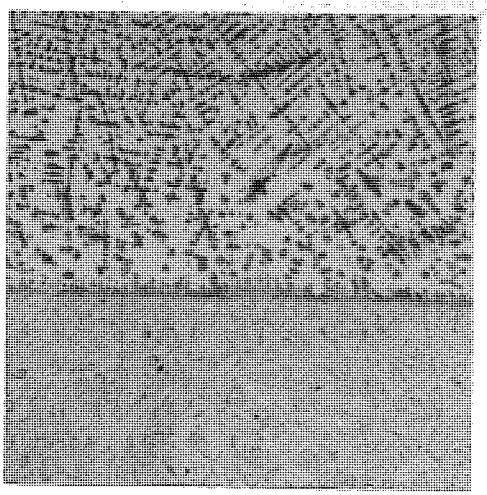

a. OPTICAL x 300

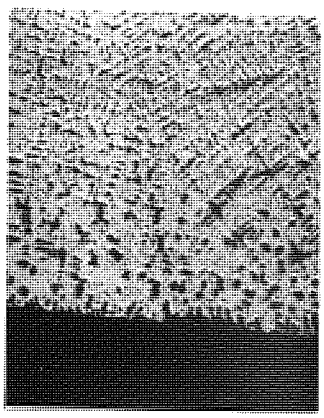

b. Cu Kα x 300

c. Fe Kα x 300

FIGURE 11. PHOTOMICROGRAPHS OF STRIP ELECTRODE WELD, BULK COMPOSITION 80.9%. (OPTICAL ETCHED FeCl

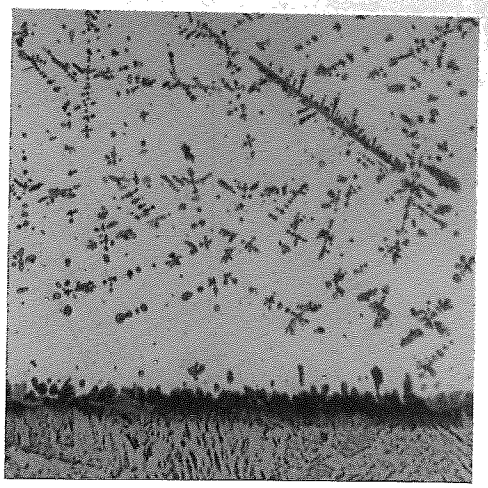

a. OPTICAL x 300

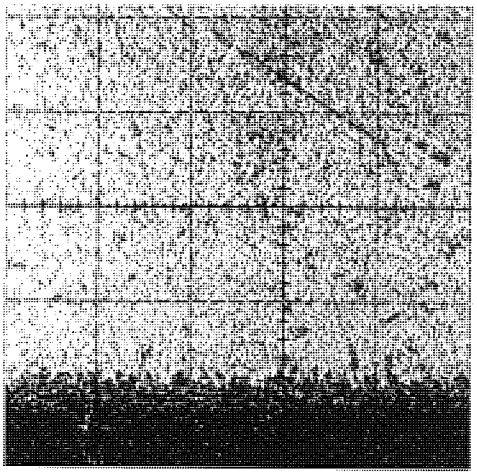

b. Cu Kα x 300

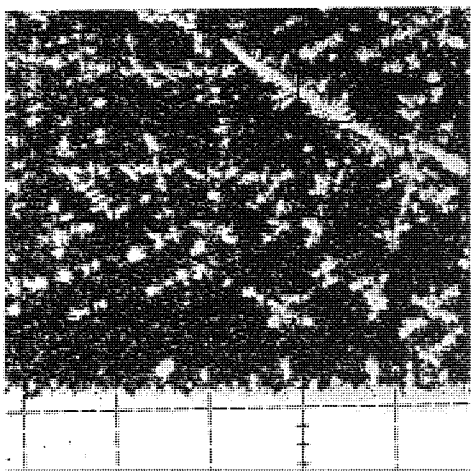

c. Fe Kα x 300

FIGURE 12. PHOTOMICROGRAPHS OF STRIP ELECTRODE WELD, BULK COMPOSITION 90.6%. (OPTICAL ETCHED FeCl

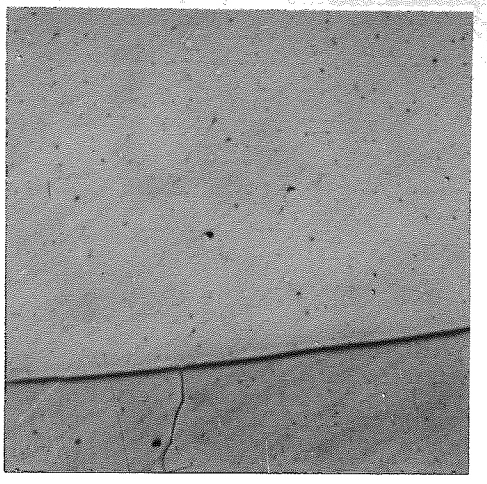

a. OPTICAL x 300

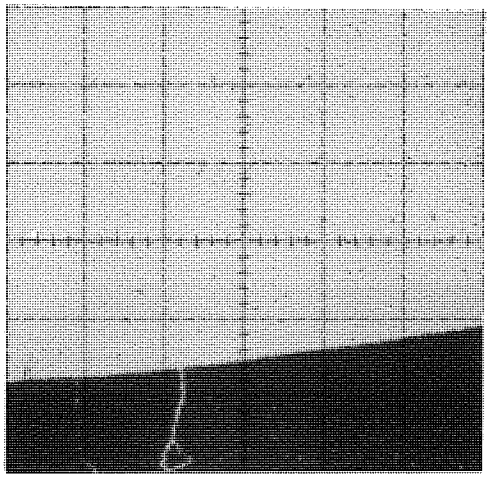

b. Cu Kα x 300

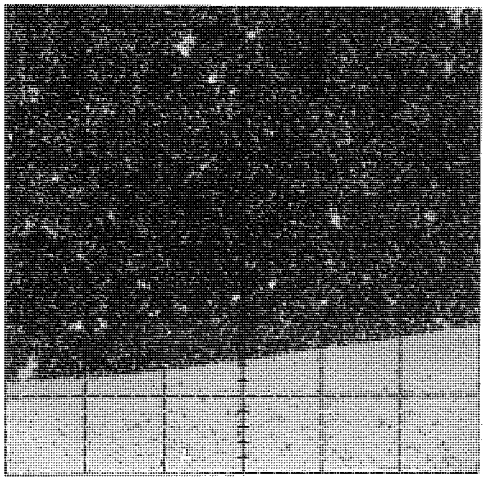

c. Fe Kα x 300

FIGURE 13. PHOTOMICROGRAPHS OF STRIP ELECTRODE WELD, BULK COMPOSITION 94.6%. (OPTICAL UNETCHED)

This page has been left intentionally blank

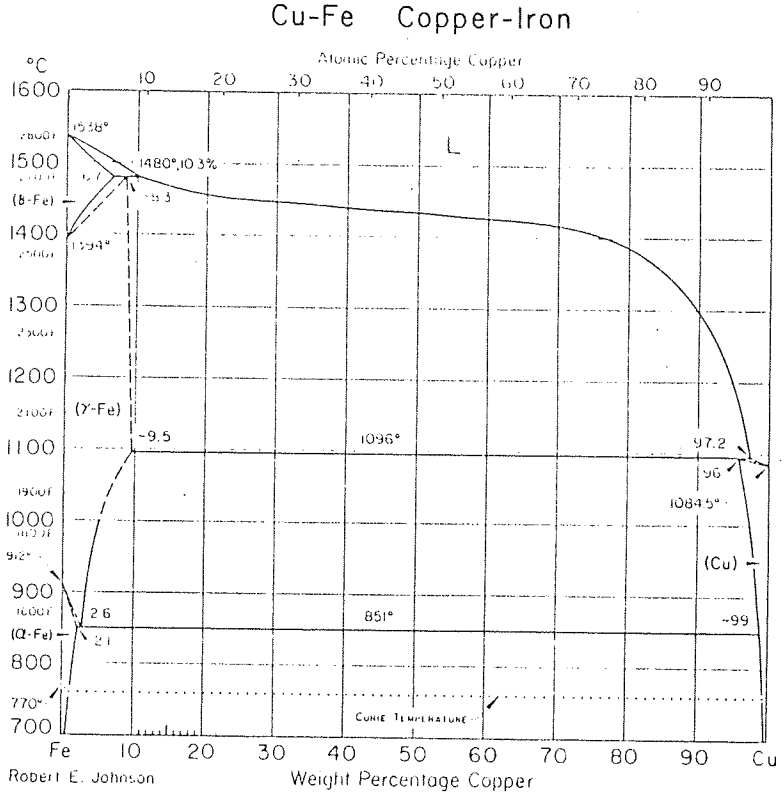

FIGURE 14. COPPER-IRON EQUILIBRIUM PHASE DIAGRAM.[90]

This page has been left intentionally blank

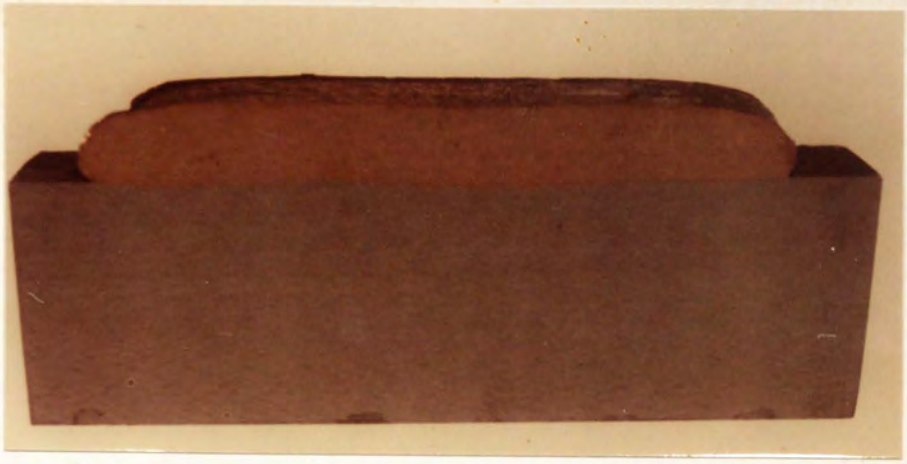

x 1.25

a. FLUX VUZ3Cu

x 1.25

b. SAME AS b,
DIFFERENT CROSS SECTION

x 1.25

c. FLUX A5O

FIGURE 16. WELD CROSS SECTIONS (UNETCHED)

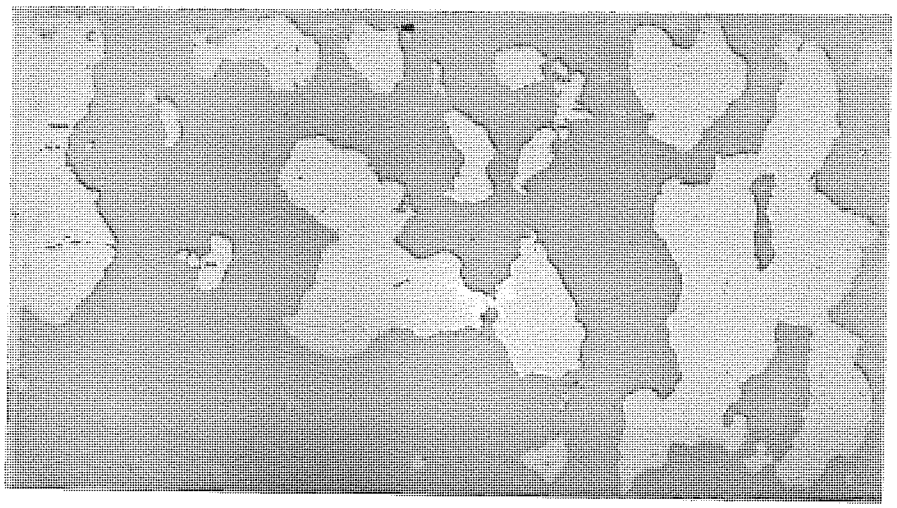

x 1

FIGURE 17. MACHINED WELD SHOWING AREAS OF PENETRATION GREATER THAN 0.4 mm (UNETCHED)

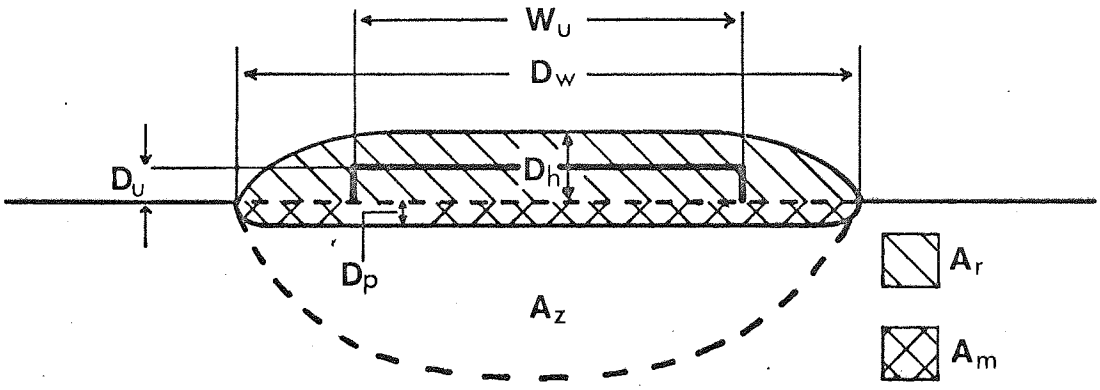

$$A_n = A_r + A_m$$
$$A_r^{act} = A_r + D_u W_u$$

FIGURE 18. WELD CROSS SECTION WITH UNDERLINER, SCHEMATIC

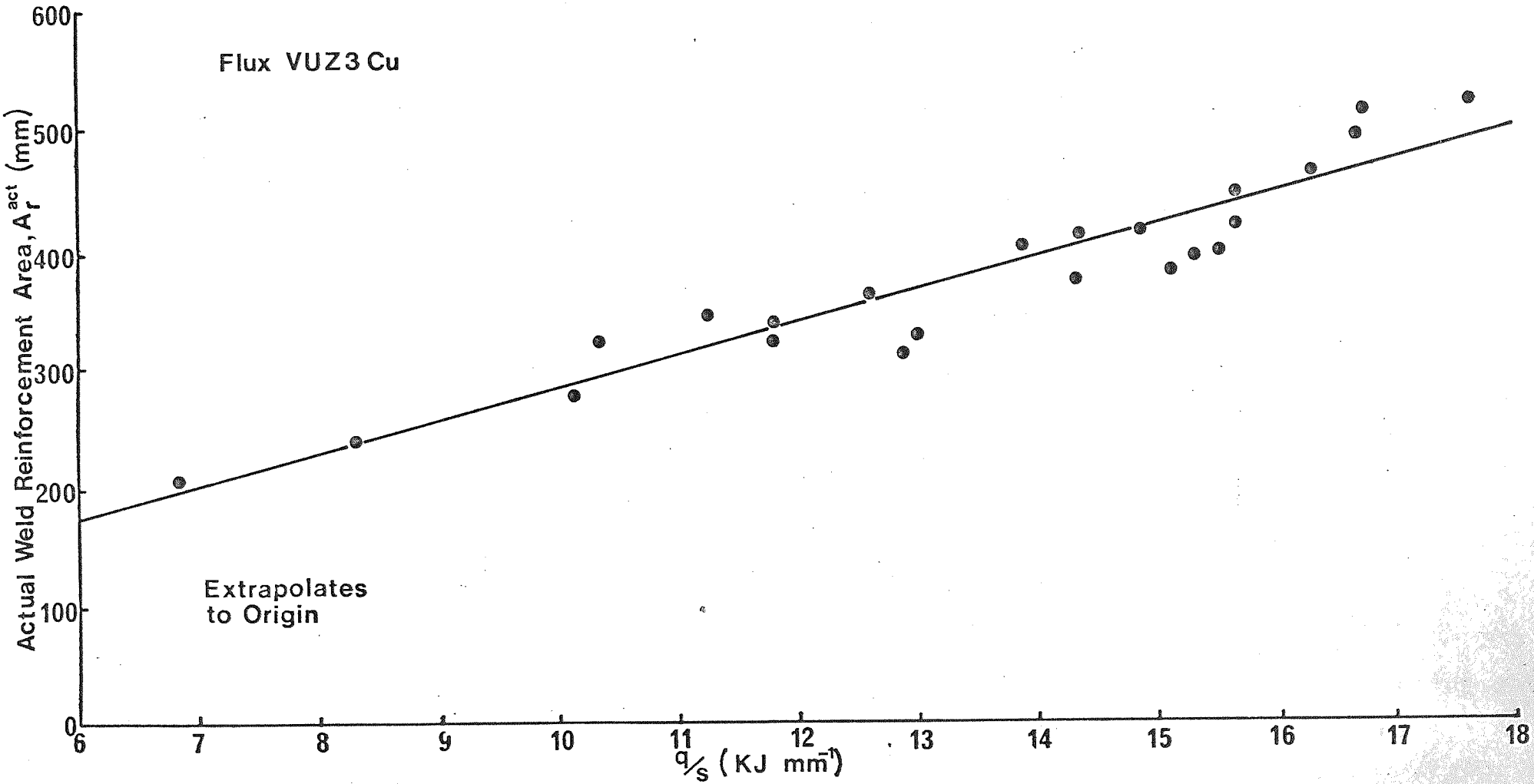

FIGURE 19. ACTUAL WELD REFINFORCEMENT AREA VERSUS ENERGY INPUT, FLUX VUZ3Cu

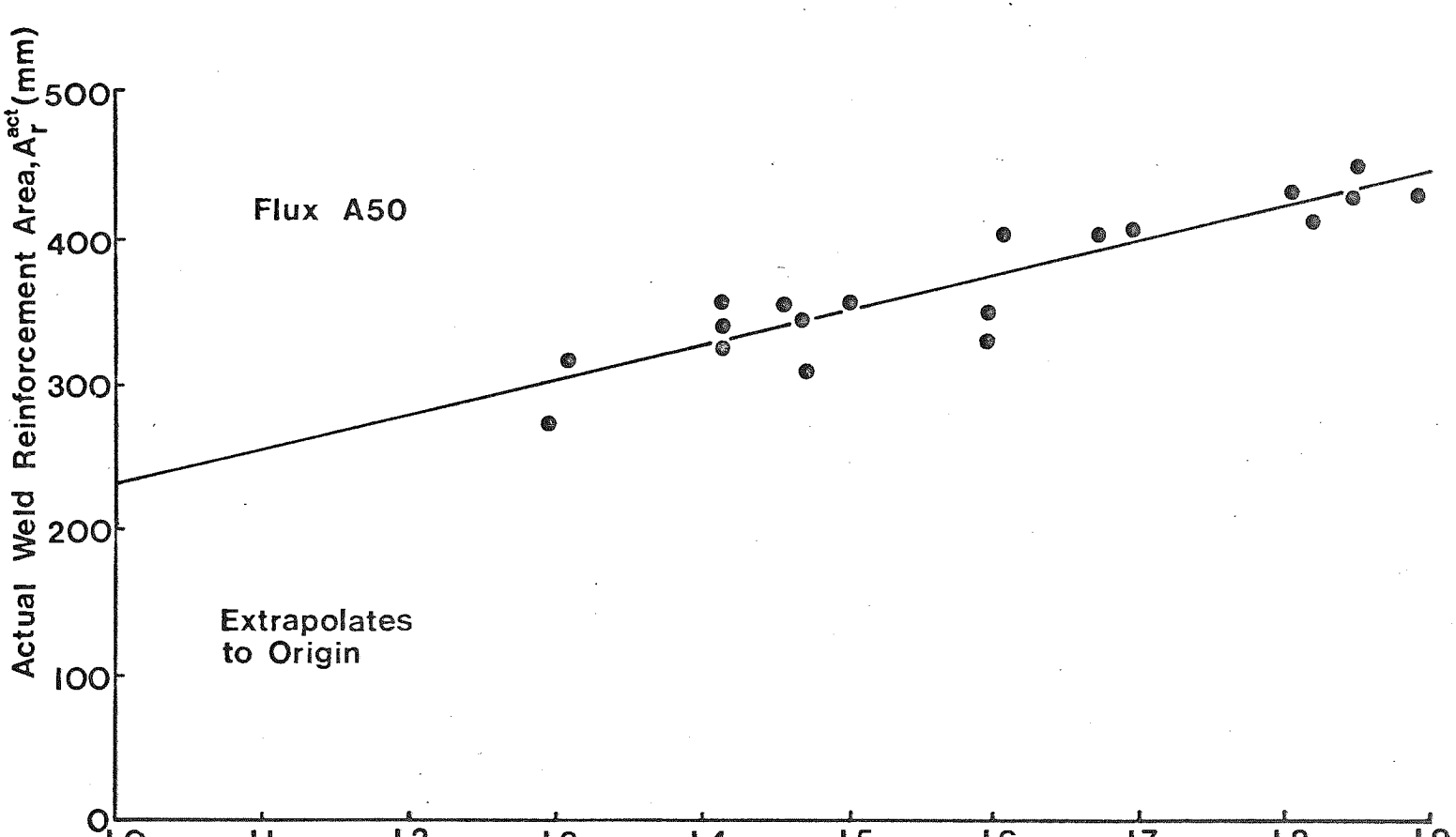

FIGURE 20. ACTUAL WELD REINFORCEMENT AREA VERSUS ENERGY INPUT, FLUX A50.

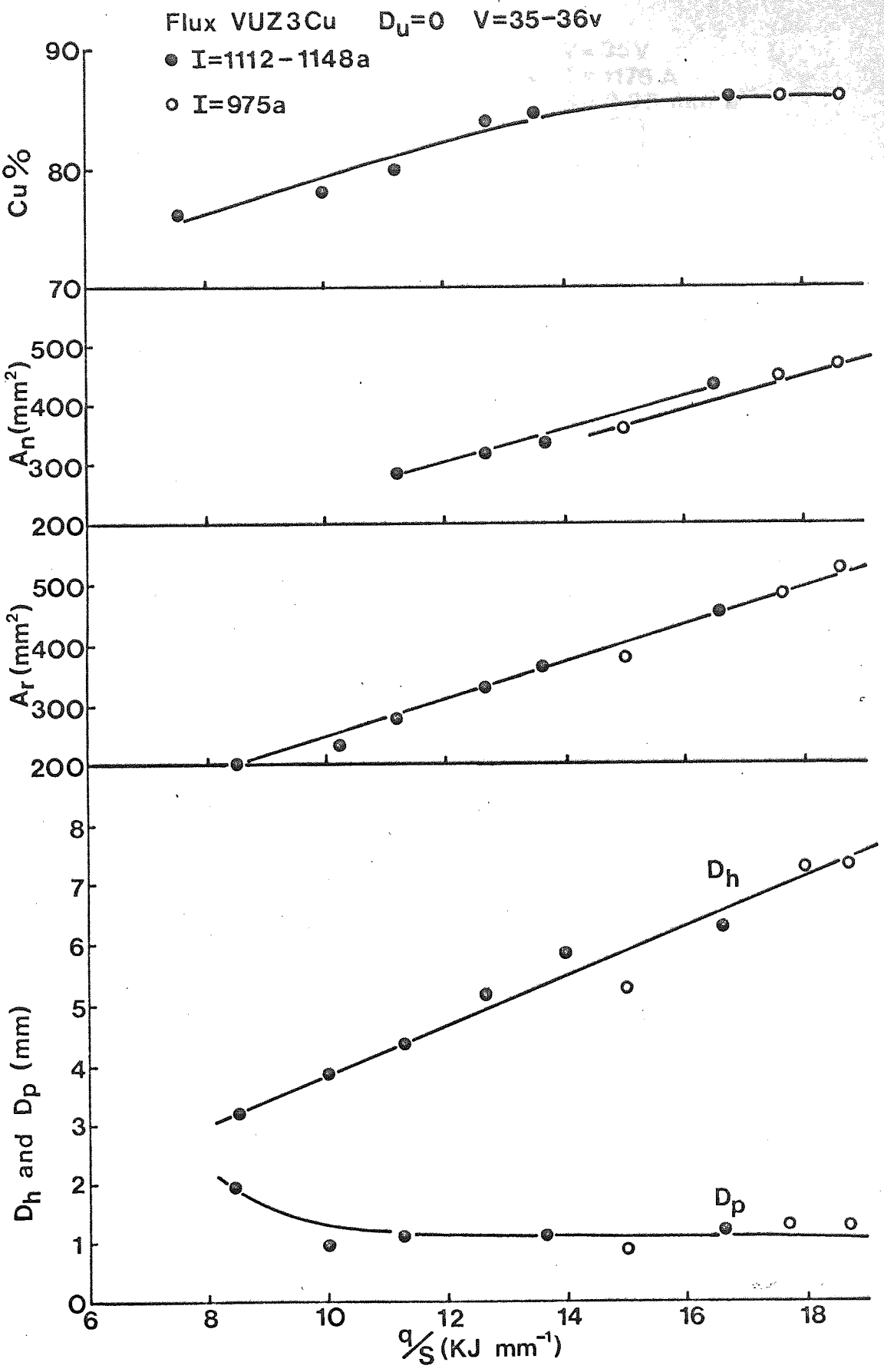

FIGURE 21. EFFECT OF ENERGY INPUT ON WELD DIMENSIONS AND COMPOSITION AT CONSTANT VOLTAGE AND NO UNDERLINER

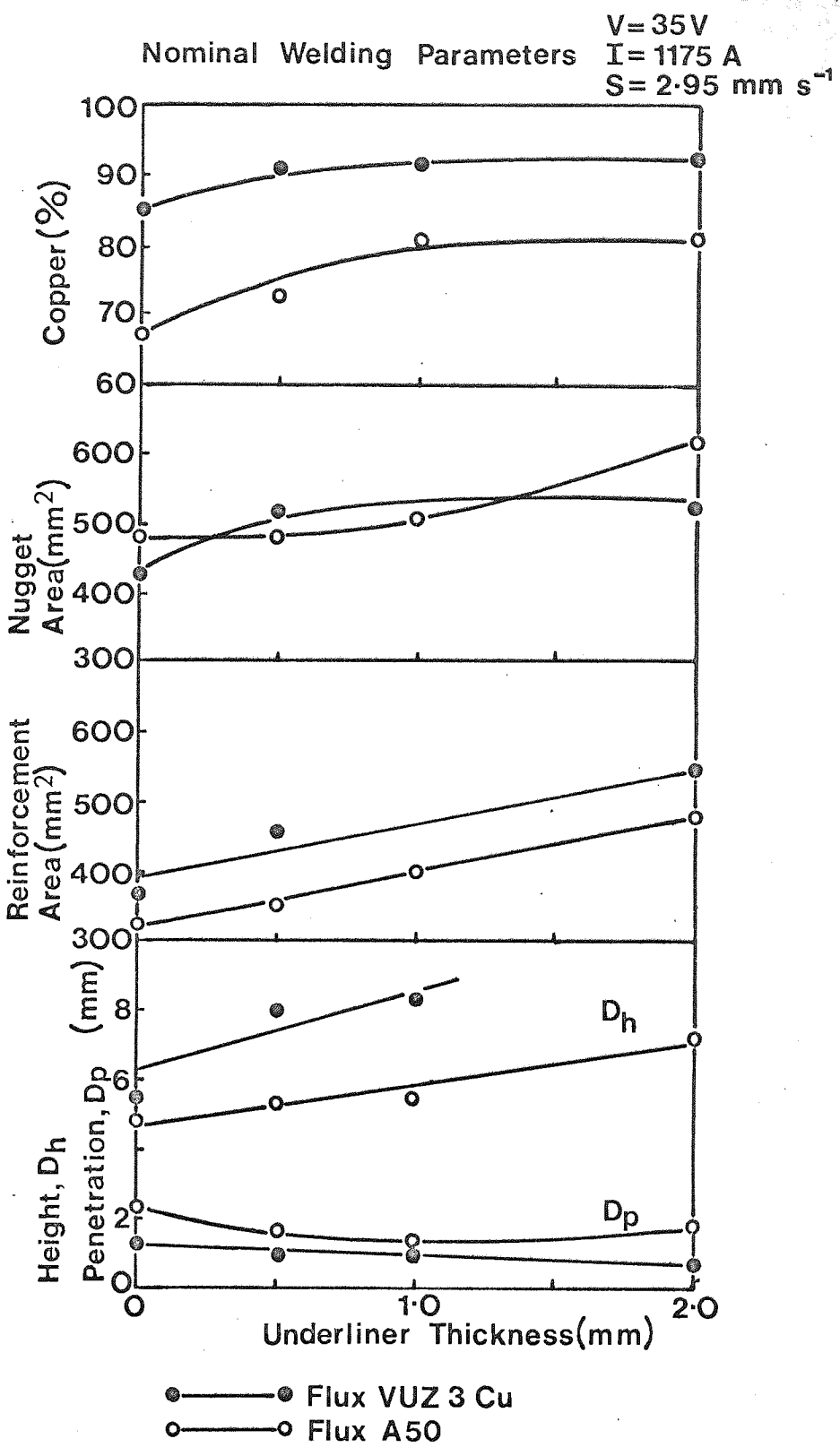

FIGURE 22. EFFECT OF UNDERLINER ON WELD DIMENSION AND COMPOSITION

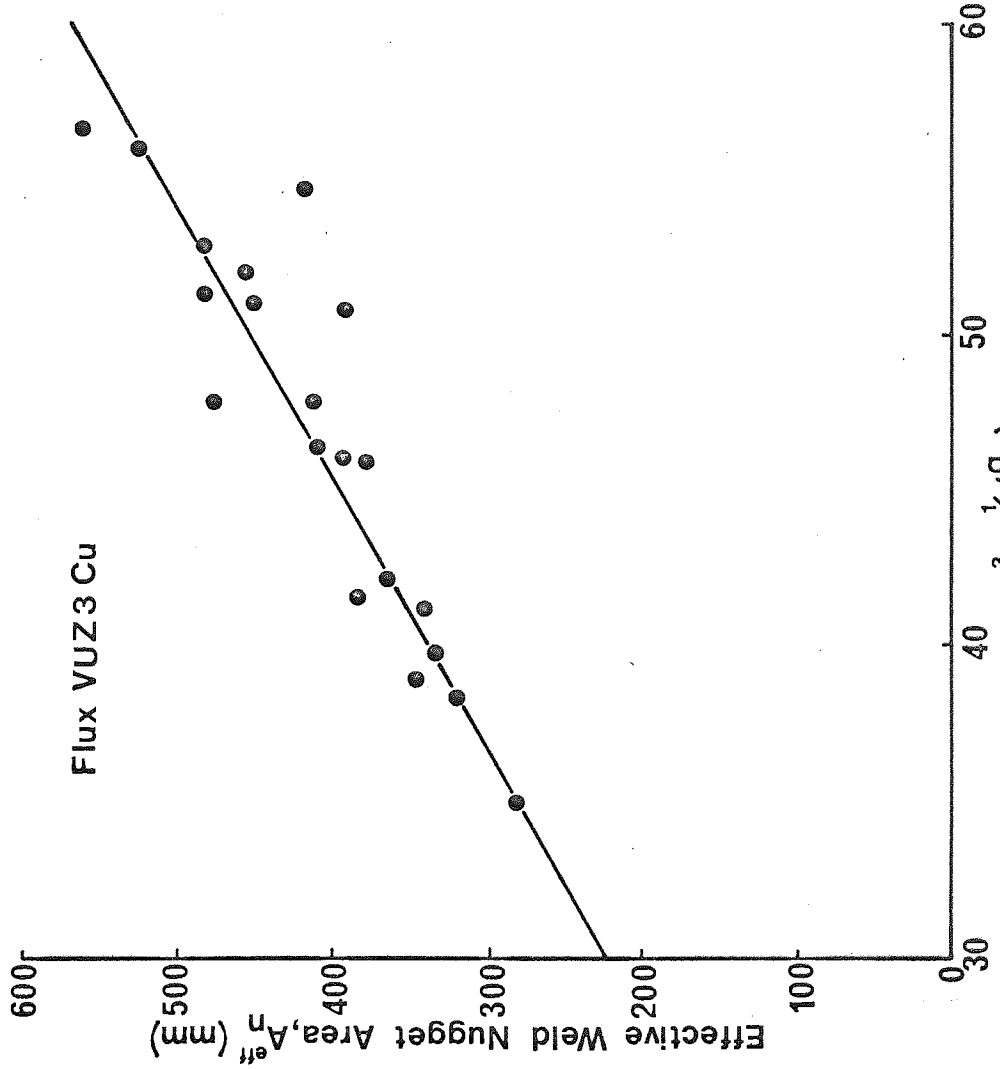

FIGURE 23. EMPIRICAL CHECK OF DERIVED EQUATION FOR EFFECTIVE WELD NUGGET AREA, FLUX VUZ3Cu

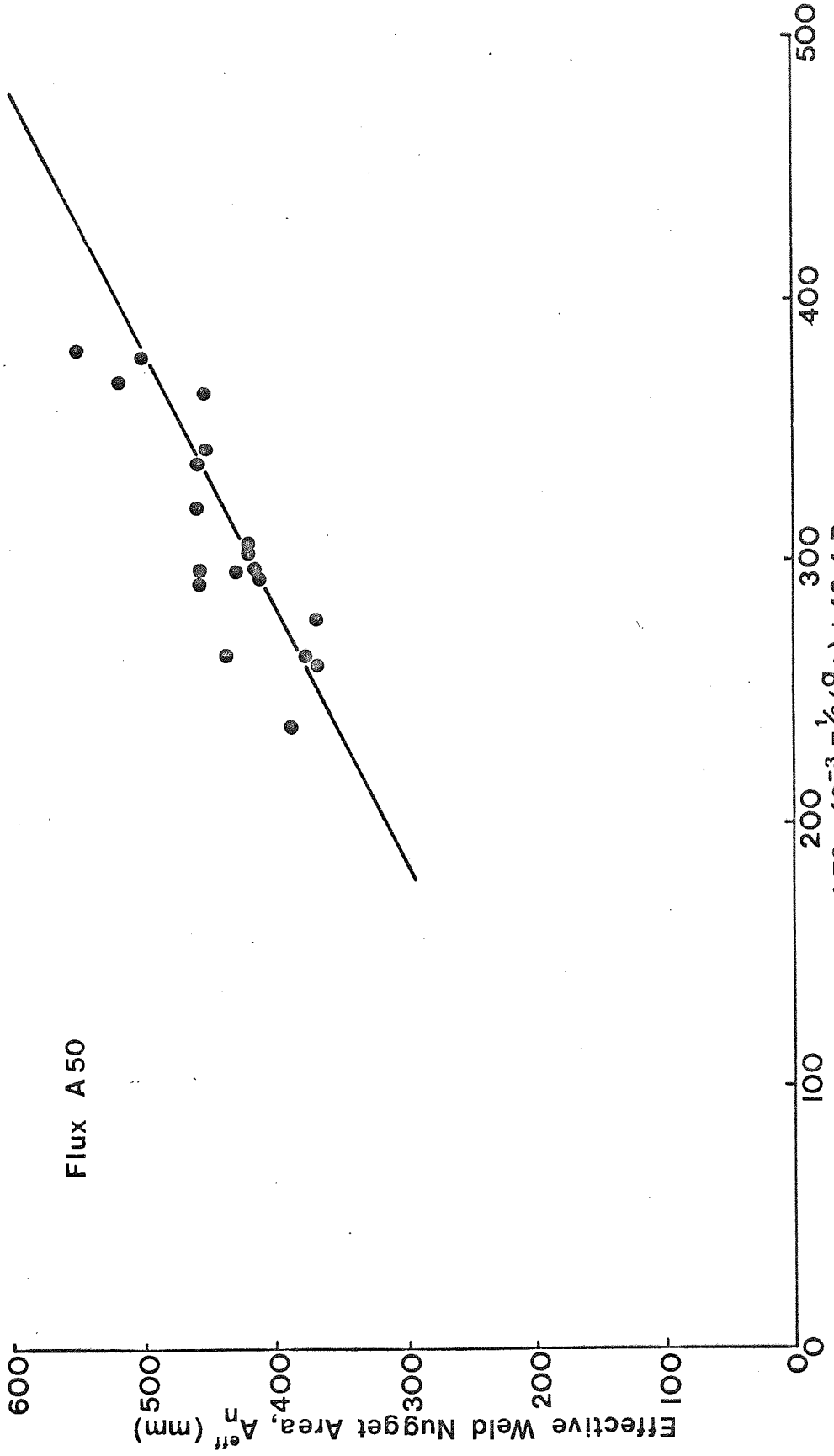

FIGURE 24. EMPIRICAL CHECK OF DERIVED EQUATION FOR EFFECTIVE WELD NUGGET AREA, FLUX A50

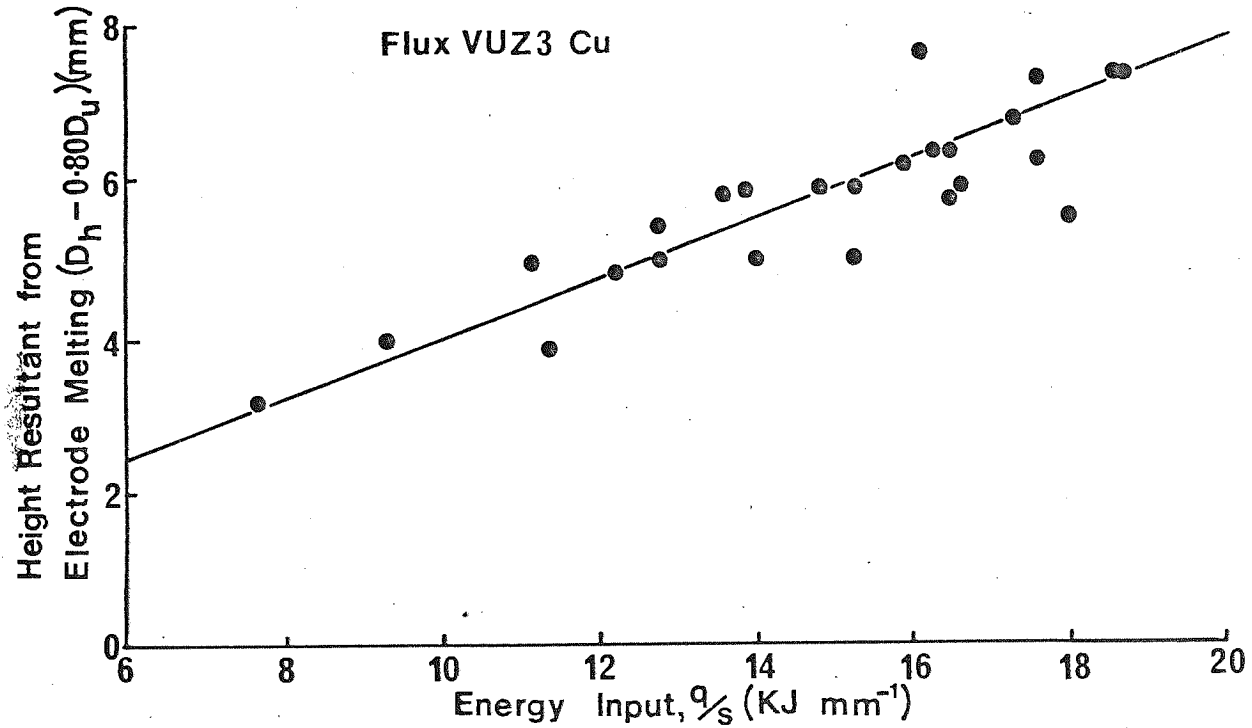

FIGURE 25. WELD BEAD HEIGHT RESULTANT FROM ELECTRODE MELTING VERSUS ENERGY INPUT, FLUX VUZ3Cu.

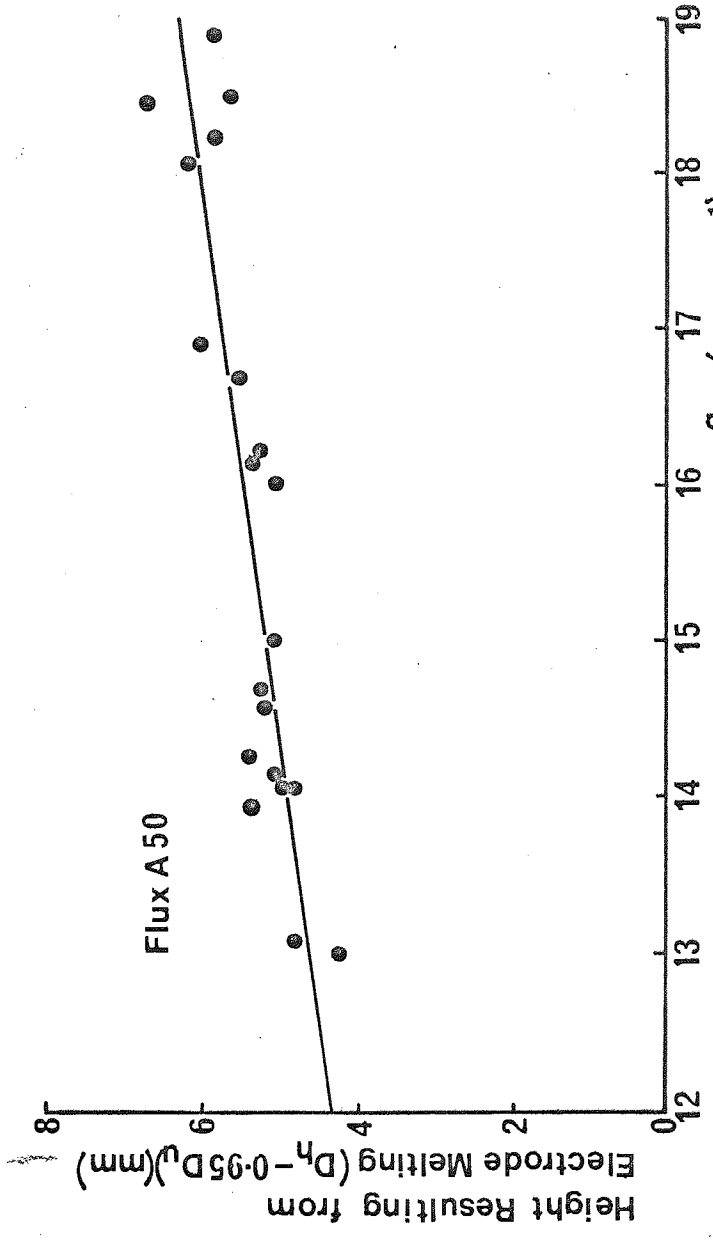

FIGURE 26. WELD BEAD HEIGHT RESULTANT FROM ELECTRODE MELTING VERSUS ENERGY INPUT, FLUX A50.

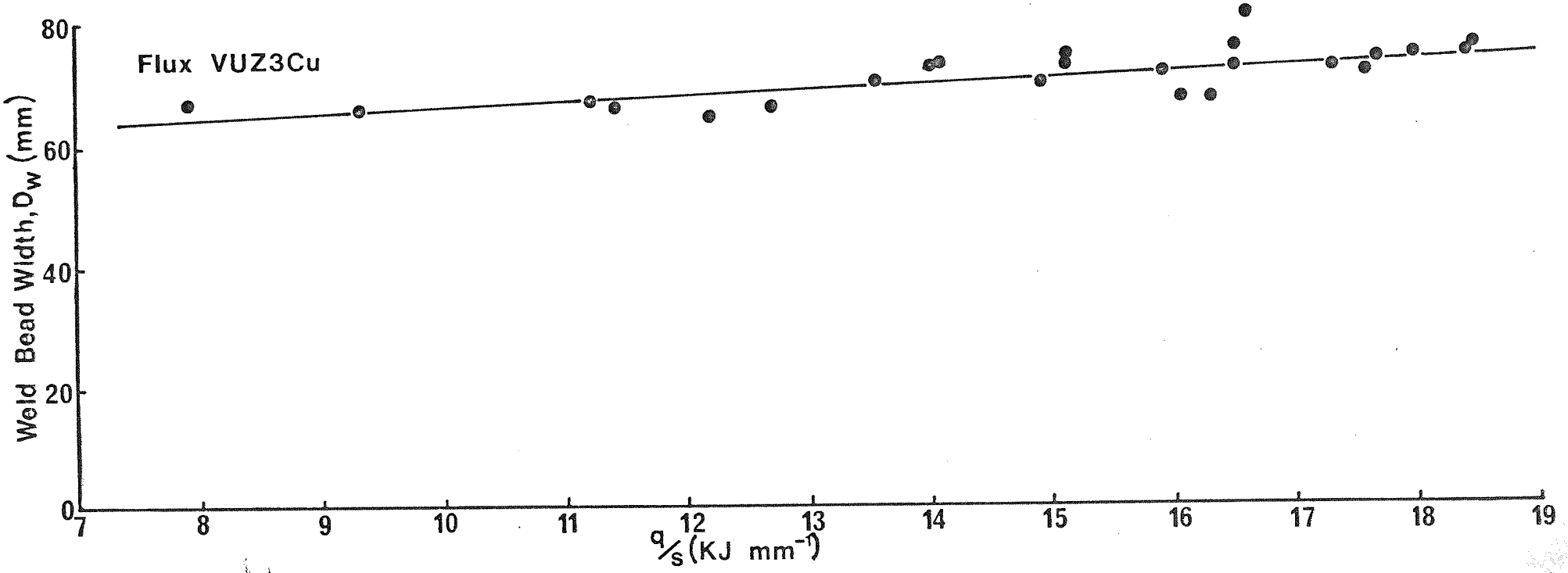

FIGURE 27. WELD BEAD WIDTH VERSUS ENERGY INPUT, FLUX VUZ3Cu

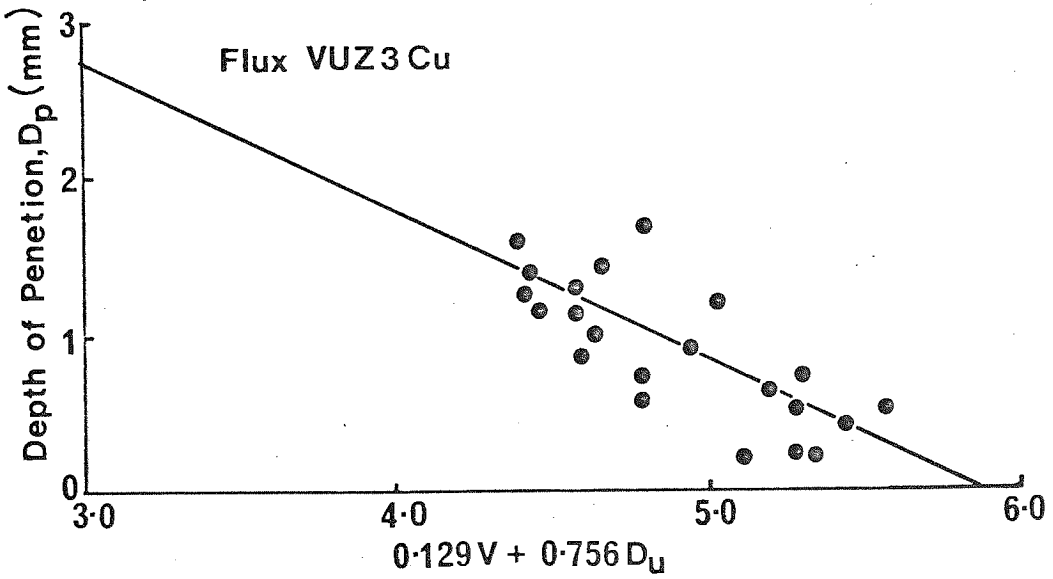

FIGURE 28. EMPIRICAL CHECK FOR THE DERIVED EQUATION FOR WELD PENETRATION, FLUX VUZ3Cu

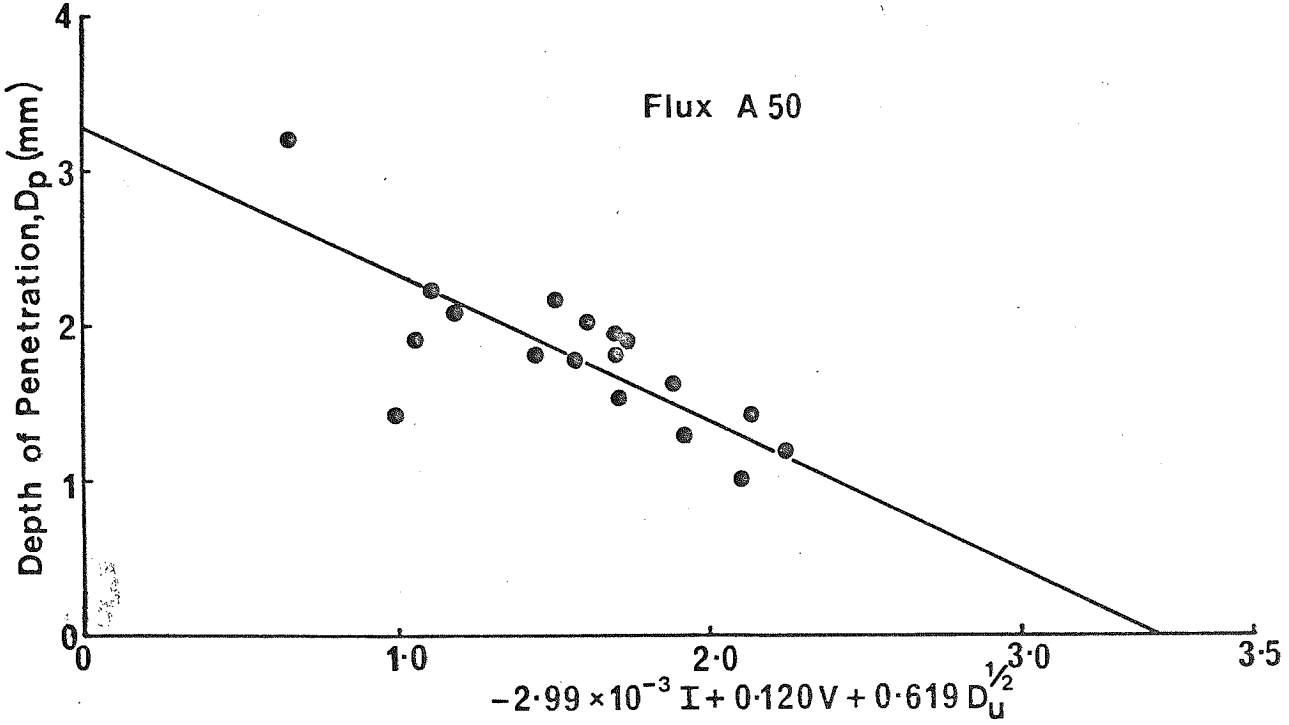

FIGURE 29. EMPIRICAL CHECK FOR THE DERIVED EQUATION FOR WELD PENETRATION FLUX A50

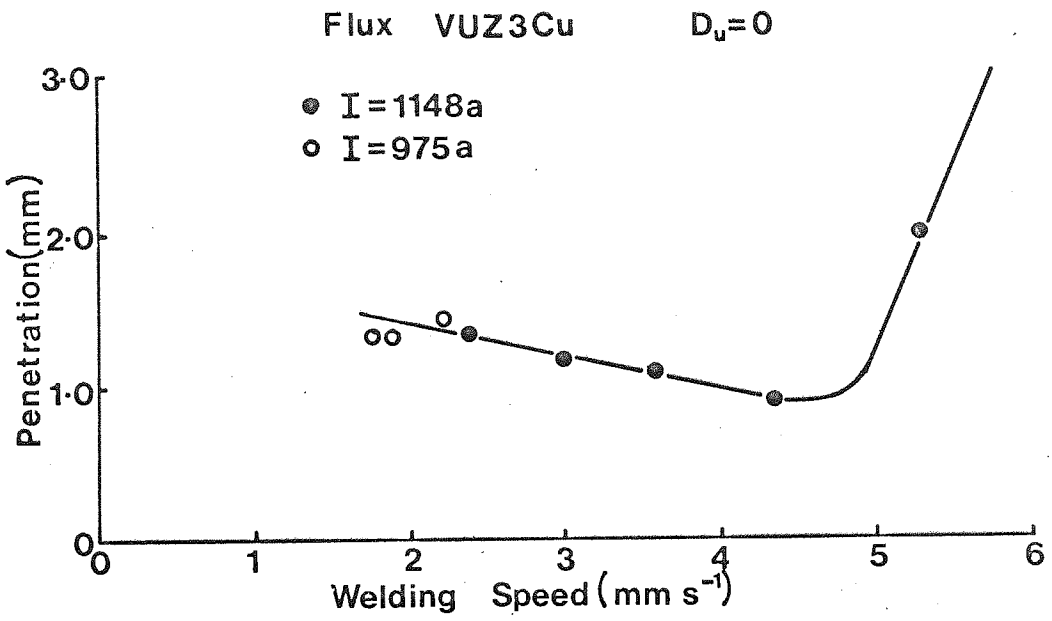

FIGURE 30. EFFECT OF SPEED ON WELD PENETRATION

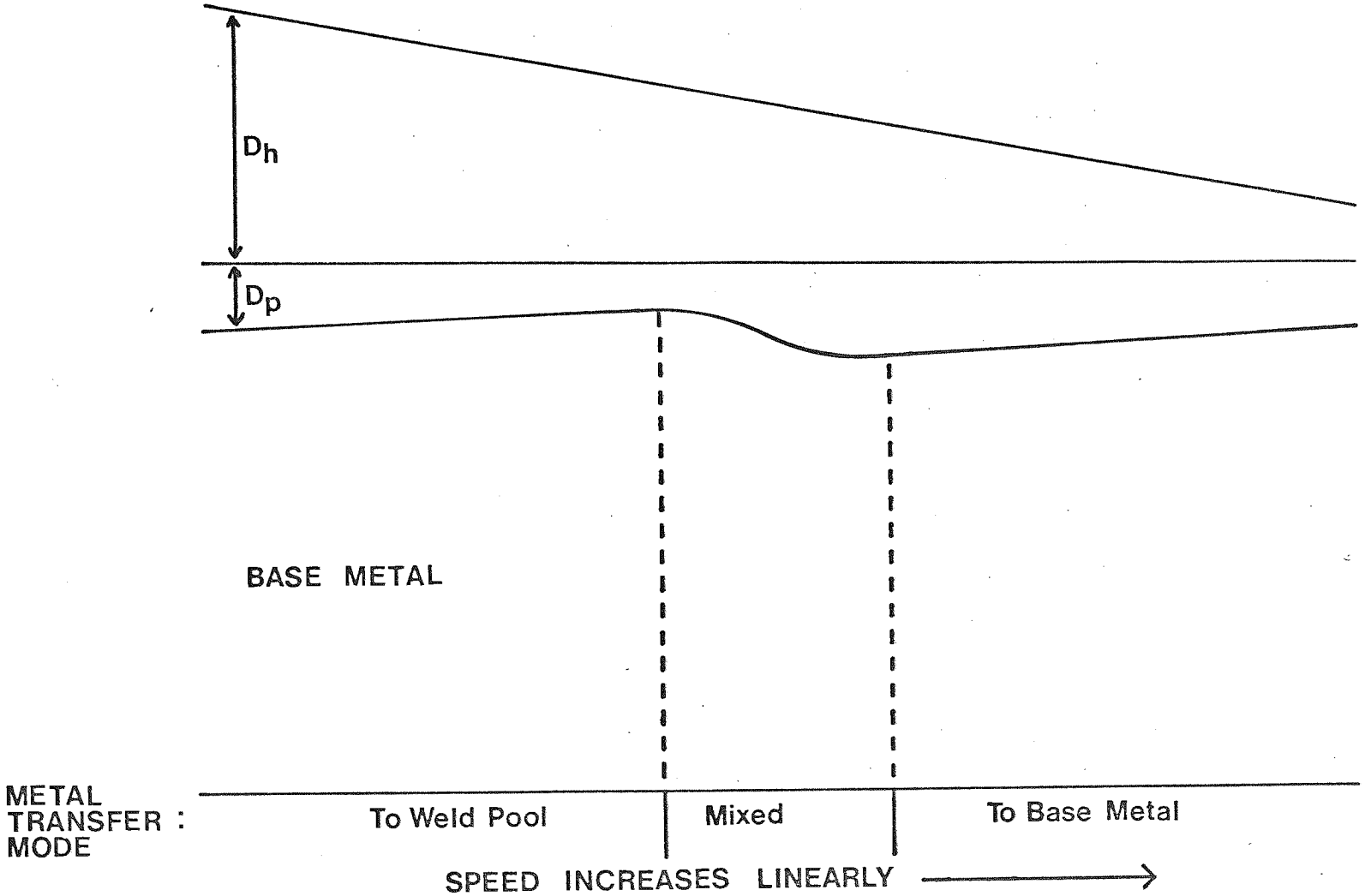

FIGURE 31. CROSS SECTION OF HYPOTHETICAL WELD MADE AT A LINEARLY INCREASING SPEED

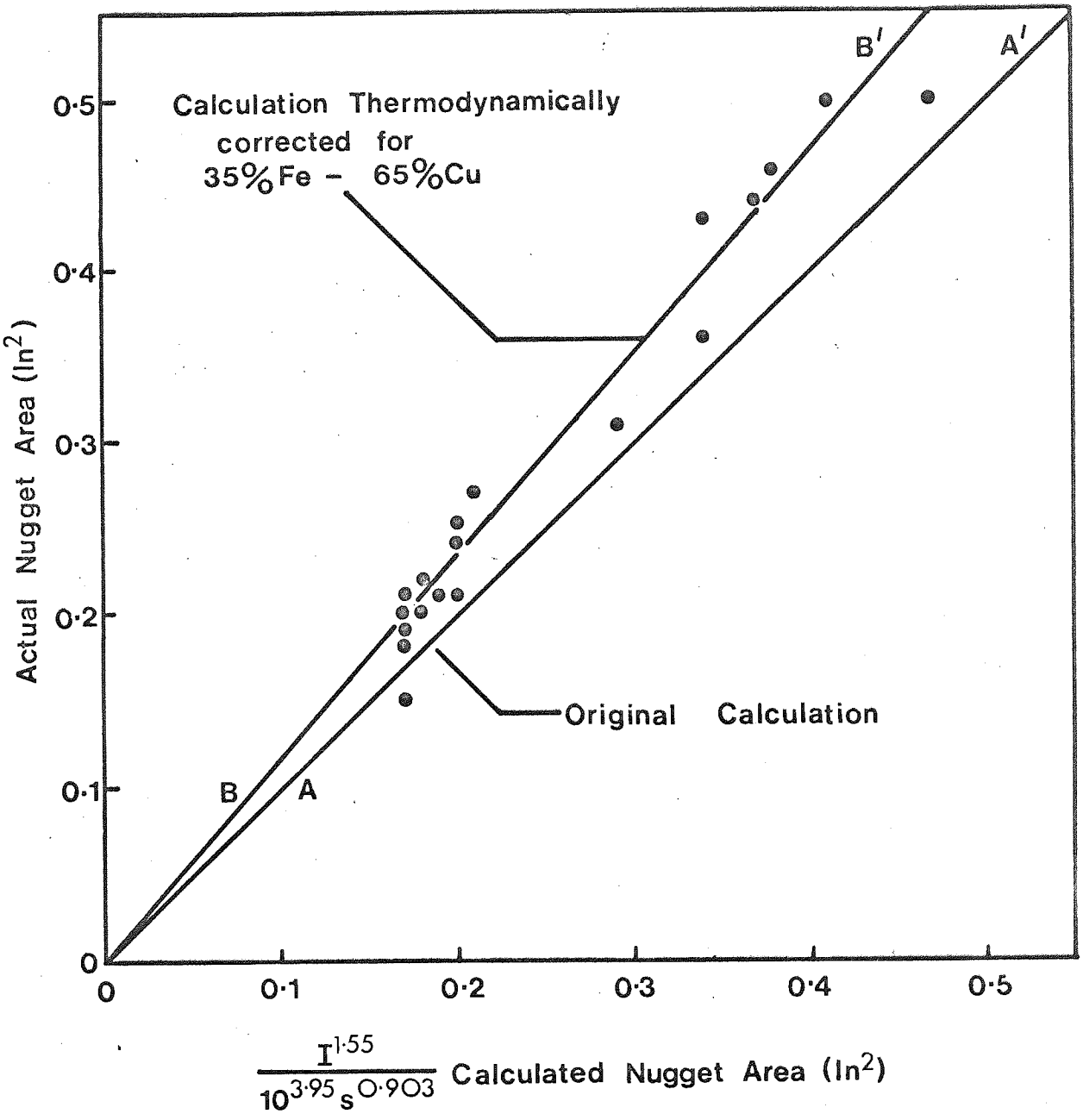

FIGURE A1. COMPARISON OF MEASURED VERSUS CALCULATED NUGGET AREA FOR SUBMERGED ARC WELDING: ALUMINUM BRONZE WIRE ELECTRODES, MILD STEEL BASE PLATE